



Strathclyde Institute of Pharmacy and Biomedical Sciences

PREPARATION AND ANALYSIS OF

NOVEL TUMOUR - TARGETED DELIVERY SYSTEMS

FOR PROSTATE CANCER THERAPY

Majed Al Robaian (201151609)

This thesis is the result of the author's original research. It has been composed by the author and has not been previously submitted for examination which has led to the award of a degree.

The copyright of this thesis belongs to the author under the terms of the United Kingdom Copyright Act as qualified by University of Strathclyde Regulation 3.50. Due acknowledgment must always be made to the use of any material contained in, or derived from, this thesis.

Signed:

Date:

Acknowledgments

First and foremost I would like to thank Allah (God) for given me the power to believe in myself and pursue my dreams. I could never have done this without the faith I have in you.

I would like to submit my sincere debt to the government of Saudi Arabia represented by Taif University and the Saudi Cultural Bureau in London for providing me with this great opportunity to undertake this rather challenging and inspiring project for which they provided the financial support.

I would like to express my sincere gratitude to my supervisor Dr. Christine Dufès for the patient guidance, encouragement and continuous support she has provided throughout my time as her student. Her guidance helped me in all the time of research and writing of this thesis. I have been extremely lucky to have a supervisor who cared so much about my work, and who was always responded to my questions and queries so promptly. I also would like to thank my second supervisor Dr RuAngelie.

I am thankful to my colleagues in our group; Sukrut Somani and my former colleague Dr. Hiba Al Dossari, for their contribution, advice and friendship.

Work on this thesis would not have been possible without encouragement and support from many people. Thanks to David Blatchford for his assistant with confocal microscope imaging. My deep thanks also go to my colleagues in the writing up room and all my friends in and outside SIBPS whose names are not

mentioned. Your friendship has been unswerving support and great comfort through thick and thin.

Finally, I would like to express my gratitude to my parents, my sister and my brother for their unconditional love. Without their blessing and encouragement, I would not have been able to finish this work. My deepest appreciation is expressed to my wife Sana for her continues support and love and to my three angels Rophia, Talia and Tiya for their love and patient and for giving me the courage to make it.

"Allah makes the way to Heaven easy for him who treads the path in search of knowledge." ~ Prophet Mohammad (PBUH)

Table of content

CHAPTER 1.INTRODUCTION AND AIMS OF THE STUDY	1
1.1. Prostate.....	2
1.1.1. Histology of the prostate	2
1.1.2. Pathology and treatment of the prostate	3
1.2. Prostate cancer	5
1.2.1. Incidence and prevalence	5
1.2.2. Types of prostate cancer	6
1.2.3. Symptoms of Prostate Cancer	8
1.2.4. Diagnostic Modalities for Prostate Cancer	9
1.2.5. Prostate Cancer stage	13
1.2.6. Grading of prostate cancer	17
1.2.7. Prostate Cancer Treatment	18
1.3. Gene Therapy.....	22
1.3.1. Overview.....	22
1.3.2. Viral Methods.....	30

1.3.3.	Non-viral methods	34
1.3.4.	Targeting Methods.....	48
1.4.	Aims and Objectives.....	63
CHAPTER 2.GENERAL MATERIAL AND METHODS.....		64
2.1.	Material.....	65
2.1.1.	Cell lines	67
2.1.1.1.	PC3.....	67
2.1.1.2.	DU145.....	68
2.1.1.3.	LNCaP	68
2.1.1.4.	B16-F10-luc-G5	69
2.1.1.5.	A431.....	69
2.1.1.6.	T98G.....	69
2.2.	Methods	70
2.2.1.	Nuclear Magnetic Resonance (NMR) spectroscopy.....	70
2.2.2.	Plasmid Deoxyribonucleic acid (DNA) preparation	73
2.2.3.	DNA complexation studies	76
2.2.4.	Fluorescence Spectrophotometry.....	79

2.2.5.	Transmission Electron Microscopy (TEM)	81
2.2.6.	Photon Correlation Spectroscopy (PCS).....	82
2.3.	Introduction to <i>In vitro</i> and <i>In vivo</i> studies.....	86
2.3.1.	<i>In vitro</i> studies.....	86
2.3.2.	<i>In vivo</i> studies	96
2.3.2.1.	Animal models	97
CHAPTER 3.THERAPEUTIC EFFICACY OF INTRAVENOUSLY ADMINISTRATED TRANSFERRIN TRANSFERRIN CONJUGATED DENDRIPLEXES ON PROSTATE CARCINOMAS.....		
		107
3.1.	Introduction.....	108
3.2.	Aims and Objectives.....	109
3.3.	Methods.....	109
3.3.1.	Preparation of the Tf-bearing polypropylenimine dendrimer	109
3.3.2.	Cell culture	110
3.3.3.	Cellular uptake of DNA.....	110
3.3.4.	<i>In vitro</i> transfection.....	111
3.3.5.	Anti -proliferative assay: MTT	111

3.3.6.	<i>In vivo</i> tumoricidal activity	112
3.3.7.	Statistical analysis.....	113
3.4.	Results	113
3.4.1.	<i>In vitro</i> studies.....	113
3.4.2.	<i>In vivo</i> study.....	119
3.5.	Discussion	128
CHAPTER 4. TUMOUR REGRESSION FOLLOWING INTRAVENOUS ADMINISTRATION OF LACTOFERRIN- AND LACTOFERRICIN-BEARING DENDRIPLEXES.....		
		135
4.1.	Introduction	136
4.2.	Aims and Objectives.....	138
4.3.	Methods	138
4.3.1.	Synthesis and characterization of lactoferrin- and lactoferricin-bearing DAB dendrimers	138
4.3.2.	<i>In vitro</i> biological characterization	141
4.3.3.	<i>In vivo</i> study.....	143
4.3.3.3.	Statistical Analysis	144

4.4. Results.....	144
4.4.1. Synthesis and characterization of lactoferrin- and lactoferricin-bearing DAB dendrimers	144
4.4.2. <i>In vitro</i> study	152
4.4.2.3. <i>In vitro</i> anti-proliferative activity	159
4.4.3. <i>In vivo</i> study.....	162
4.5. Discussion	170
CHAPTER 5.CONCLUSION AND FUTURE WORK	177
Appendix I: Publications.....	201

Table of Figures

Figure 1.1: Anatomy of the male reproductive and urinary system, showing the prostate (The University of Chicago Medical Centre, 2013).....	2
Figure 1.2: Microscopic image showing adenocarcinoma in Prostate (black arrow) (Adapted from Humphrey, 2007).....	7
Figure 1.3: Squamous cell carcinoma in the prostate (black arrow) (Adapted from Wang <i>et al.</i> , 2012).....	8
Figure 1.4: Metastatic prostate cancer. a) Primary prostate cancer adenocarcinoma. b) Large number of bone and lymph node metastases. c) Larger number of bone and lymph node metastases as compared to b or a. (Adapted from Kircher <i>et al.</i> , 2012).....	14
Figure 1.5: Gene in relation to a chromosome (Adapted from Cancer Research UK)	23
Figure 1.6: Geographical distribution of clinical trials for gene therapy (Adapted from Wiley, 2012)	29
Figure 1.7: Clinical trials for gene therapy (Adapted from Wiley, 2012).....	29
Figure 1.8: Viral vector Adapted from nano-life science (2009).....	31
Figure 1.9: General scheme of gene delivery using non-viral vectors (Adapted from Lungwitz <i>et al.</i> , 2005).	36

Figure 1.10: Non-viral vectors (Adapted from Dufès <i>et al.</i> , 2005).	36
Figure 1.11: Lipids formulation of liposomes (Adapted from Balazs and Godbey, 2011).....	38
Figure 1.12: Structure of cationic lipids and the helper lipid DOPE used in gene therapy (Adapted from Morille <i>et al.</i> , 2008).....	40
Figure 1.13: Structure of polymersomes (Adapted from Borman, 2010).	41
Figure 1.14: Linear and branched PEI	43
Figure 1.15: Transmission Electron Micrograph of dendrisomes with membranes from 6 to 10 nm thick (Adapted form Al-Jamal <i>et al.</i> , 2003).....	45
Figure 1.16: Dendrimer structure (Adapted from Brix, 2013).	46
Figure 1.17: Divergent and convergent growth (Adapted from Mukeshgohel, 2009).	47
Figure 1.18: Passive tumour targeting method	49
Figure 1.19: Cellular non-specific uptake strategies (Adapted from El-Andaloussi <i>et al.</i> , 2005)	51
Figure 1.20: Active tumour targeting method (Adapted from Park <i>et al.</i> , 2008).	52
Figure 1.21: Formulation strategies used for the delivery of drugs and nucleic acids to the tumour. (Adapted from Dufès <i>et al.</i> , 2013)	59

Figure 1.22: Schematic diagram of the bovine lactoferrin molecule. The N1 and N2 domains are colored in yellow and pink, respectively, while the C1 and C2 domains are colored in green and blue, respectively. The interconnecting helix between the lobes is colored in orange. The two iron atoms are shown as red spheres. (Adapted from Sharma <i>et al.</i> , 2013).....	62
Figure 2.1: The basis of NMR (Adapted from Hoffman & Ozery, 2013)	72
Figure 2.2: NMR Spectroscopy (Adapted from McGraw-Hill Education, 2013)72	
Figure 2.3: Plasmid DNA (Adapted from oregonstate.edu).....	74
Figure 2.4: Physical Methods in Chemistry and Nano Science. (Adapted from Barron, 2013).....	80
Figure 2.5: Diagram outlining the internal components of a basic TEM system (Adapted from Barrett Research Group).	82
Figure 2.6: Electrical double layer (adapted from Morfesis, 2010).	85
Figure 2.7: Miller Assay (Adapted from: http://www.sci.sdsu.edu/).	92
Figure 2.8: Confocal Laser Scanning Microscope (Adapted from Carl Zeiss, Inc.).	93
Figure 2.9: Transformation of Tetrazolium salt into formazan.....	95

Figure 2.10: Types and percentage of vertebrates used in animal studies in Europe in 2005 (Adapted from Commission of the European Communities, 2007). 98

Figure 3.1: (A) Confocal microscopy imaging of the cellular uptake of Cy3-labelled DNA (2.5 µg / well) either complexed with DAB-Tf, DAB or in solution, after incubation for 72 hours with PC-3 (top), DU145 (medium) and LNCaP cells (bottom) (Blue: nuclei stained).115

Figure 3.2: Transfection efficacy of DAB-Tf (“cplx DT”) and DAB dendriplexes (“cplx D”) in PC-3 (A), DU145 (B) and LNCaP cells (C). DAB-Tf and DAB dendriplexes were dosed at their optimal dendrimer: DNA ratio of 10:1 and 5:1 respectively. (Controls: DAB-Tf (“DT only”), DAB (“D only”) and naked DNA). Results are expressed as the mean ± SEM of three replicates (n=15). *: P <0.05 vs. the highest transfection ratio. Cplx D: Diaminobutyric dendriplex; cplx DT: Diaminobutyric polypropylenimine-transferrin dendriplex.117

Figure 3.3: (A) Tumour growth studies in a PC-3 xenograft model after intravenous administration of transferrin- bearing DAB dendriplex carrying plasmid DNA encoding TNFα (green), TRAIL (red), IL-12 (blue) (50 µg DNA / injection), uncomplexed DAB-Tf (brown), naked DNA encoding TNFα (pale green), naked DNA encoding TRAIL (orange), naked DNA encoding IL-12 (pale blue), untreated tumours (back) (n=10). (B) Variations of the animal body weight throughout the treatment (Colour coding as in A).....123

Figure 3.3 (continued): (C) Overall tumour response to treatments at the end of the study. (D) Time to disease progression. The Y axis gives the proportion of surviving animals over time. Animals were removed from the study once their tumour reached 12 mm diameter (Colour coding as in A).....124

Figure 3.4: (A) Tumour growth studies in a PC-3 xenograft model after intravenous administration of transferrin- bearing DAB dendriplex carrying plasmid DNA encoding TNF α (green), TRAIL (red), IL-12 (blue) (50 μ g DNA / injection), uncomplexed DAB-Tf (brown), naked DNA encoding TNF α (pale green), naked DNA encoding TRAIL (orange), naked DNA encoding IL-12 (pale blue), untreated tumours (back) (n=10). (B) Variations of the animal body weight throughout the treatment (Colour coding as in A).....125

Figure 3.4 (continued): (C) Overall tumour response to treatments at the end of the study. (D) Time to disease progression. The Y axis gives the proportion of surviving animals over time. Animals were removed from the study once their tumour reached 12 mm diameter (Colour coding as in A).....126

Figure 3.5: Bioluminescence imaging of the tumoricidal activity of transferrin - bearing DAB dendriplex carrying plasmid DNA encoding TNF α ("cplx DT-TNF"), TRAIL ("cplx DT-TRAIL"), IL-12 ("cplx DT-IL12") in a PC-3M-luc-C6 tumour model.....127

Figure 4.1: ¹HNMR spectra of DAB-Lf (A), DAB-Lfc (B).....146

Figure 4.2: DNA condensation of DAB-Lf and DAB-Lfc dendriplexes using PicoGreen® reagent at various durations and dendrimer: DNA weight ratios :

20:1 (■, black), 10:1 (●, red), 5:1 (▲, green), 2:1 (▼, blue), 1:1 (◆, cyan), 0.5:1 (◄, pink), DNA only (►, orange) (empty symbol, dark yellow : DAB-DNA, dendrimer: DNA weight ratio: 5:1) . Results are expressed as mean ± SEM (n=4).....148

Figure 4.3: Gel retardation assay of DAB-Lf and DAB-Lfc dendriplexes at various dendrimer: DNA weight ratios: 20:1, 10:1, 5:1, 2:1, 1:1, and DNA only.149

Figure 4.4: Transmission electron micrographs of a) DAB-Lf and b) DAB-Lfc dendriplexes (Bar: 100 nm).....149

Figure 4.5: Size (A) and Zeta Potential (B) of DAB-Lf and Lfc dendriplexes at various dendrimer: DNA weight ratios: 20:1, 10:1, 5:1, 2:1, 1:1, and 0.5:1. Result are expressed as mean± SEM (n=4).

Figure 4.6: Transfection efficacy of DAB-Lf and DAB-Lfc dendriplexes at various dendrimer: DNA weight ratios in A431 (A), B16-F10 (B) and T98G cells (C). DAB-DNA was dosed at its optimal polymer: DNA ratio of 5:1. Results are expressed as the mean ± SEM of three replicates (n=15). *: P <0.05 vs. the highest transfection ratio.....155

Figure 4.7: Transfection efficacy of DAB-Lf and DAB-Lfc dendriplexes in PC-3 (A), DU145 (B) and LNCaP cells (C). Results are expressed as the mean ± SEM of three replicates (n=15). *: P <0.05 vs. the highest transfection ratio.156

Figure 4.8: Confocal microscopy imaging of the cellular uptake of Cy3- labelled DNA (2.5 µg / well) either complexed with DAB-Lf, DAB-Lfc, DAB or in solution, after incubation for 24 hours with A431 (left) , B16-F10 (middle) and T98G cells (right) (Blue: nuclei stained with DAPI (excitation: 405 nm laser line, bandwidth: 415-491nm), green: Cy3-labeled DNA (excitation: 543 nm laser line. bandwidth: 550-620 nm) (Bar: 10 µm).158

Figure 4.9: Confocal microscopy imaging of the cellular uptake of Cy3- labelled DNA (2.5 µg / well) either complexed with DAB-Lf, DAB-Lfc, DAB or in solution, after incubation for 24 hours with PC-3 (right) , DU145 (middle) and LNCaP cells (left) (Blue: nuclei stained with DAPI (excitation: 405 nm laser line, bandwidth: 415-491nm), green: Cy3-labeled DNA (excitation: 543 nm laser line. bandwidth: 550-620 nm) (Bar: 10 µm).159

Figure 4.10: Biodistribution of gene expression after a single intravenous administration of DAB-Lf, DAB-Lfc and DAB dendriplexes (50 µg DNA administered). Results were expressed as milliunits β-galactosidase per organ (n=5). *: P <0.05 : highest gene expression treatment vs. other treatments for each organ.163

Figure 4.11: A) Tumour growth studies in a mouse A431 xenograft model after intravenous administration of DAB-Lf dendriplex carrying plasmid DNA encoding TNFα (50 µg/injection) (green), DAB-Lfc dendriplex (blue), DAB dendriplex (orange), naked DNA (red) and untreated tumours (back) (n=10). B)

Variations of the animal body weight throughout the treatment (Colour coding as in A).166

Figure 4.11 (continued): C) Overall tumour response to treatments at the end of the study. D) Time to disease progression. The Y axis gives the proportion of surviving animals over time. Animals were removed from the study once their tumour reached 11 mm diameter (Colour coding as in A).167

Figure 4.12: A) Tumour growth studies in a mouse B16-F10 model after intravenous administration of DAB-Lf dendriplex carrying plasmid DNA encoding TNF α (50 μ g/injection) (green), DAB-Lfc dendriplex (blue), DAB dendriplex (orange), naked DNA (red) and untreated tumours (back) (n=10). B) Variations of the animal body weight throughout the treatment (Colour coding as in A).168

Figure 4.12 (continued): C) Overall tumour response to treatments at the end of the study. D) Time to disease progression. The Y axis gives the proportion of surviving animals over time. Animals were removed from the study once their tumour reached 11 mm diameter (Colour coding as in A).169

List of Tables

Table 1.1: TNM classification used for Prostate cancer staging (Adapted from Clinical Practice Guidelines in Oncology: Prostate Cancer, 2013).	15
Table 1.2: Different viral vectors used in gene therapy (Adapted from Goverdhana <i>et al.</i> , 2005).....	33
Table 2.1: Advantages and Limitations of the Commonly Used Reporter Genes (from Schenborn and Groskreutz, 1999).....	101
Table 3.1: Anti-proliferative efficacy of TNF- α , TRAIL-and IL-12 encoding DNA complexed with Diaminobutyric polypropylenimine-transferrin and Diaminobutyric polypropylenimine in PC-3, DU-145 and LNCaP prostate cancer cells (reference).....	119
Table 4.1: Anti-proliferative efficacy of encoding DNA complexed with Diaminobutyric polypropylenimine-transferrin and Diaminobutyric polypropylenimine in A431, B16F10 and T98G skin cancer cells.....	161
Table 4.2: Anti-proliferative efficacy of encoding DNA complexed with DAB-Lf and DAB-Lfc in PC-3, DU145 and LNCaP prostate cancer cells.	162

Abbreviation

A431	Epidermoid carcinoma
AAV	Adeno associated virus
ADA	Adenosine deaminase
Arg	Arginine
AP	Alkaline phosphate
BPH	Benign Prostatic Hyperplasia
BGTC	Guanidinium-tren-cholesterol
B16-F10	Mouse melanoma cell lines
BRCA	Breast cancer
CAT	Chloramphenicol acetyltransferase
cCCD	Cooled, charge-coupled device
CLSM	Confocal Laser Scanning Microscopy
COA	Coenzyme A
CPPs	Cell-penetrating peptides
cDNA	Complementary DNA
CRPC	Castrate-resistant prostate cancer

D ₂ O	Deuterated water
DAB	Generation 3 diaminobutyric polypropylenimine
DAPI	4',6-diamidino-2-phenylindole
DDAO	7-hydroxy-9 <i>H</i> -(1,3-dichloro-9,9-dimethylacridin-2-one)
DDAO-G	9 <i>H</i> -(1,3-dichloro-9,9-dimethylacridin-2-one-7-yl)-D galactopyranoside
DMEM	Dulbecco's Modified Eagle Medium
DMSI	Dimethylsuberimidate di-hydrochloride
DMSO	Dimethyl sulfoxide
DNA	Deoxyribonucleic acid
DNA ses	DNA enzyme
Ds DNA	Double Stranded DNA
DOGS	Diocetylamidoglycylspermine
DOTAB	1,2-dioleyl-3-trimethylammonium-propane
DOTMA	N [1-(2, 3-diolelyoxy) propyl]-N, N, N-trimethylammonium chloride
DOPE	Dioleoylphosphatidylethanolamine

DRE	Digital Rectal Examination
E. coli	<i>Escherichia coli</i>
EDL	Electrical double layer
EIA	Enzyme immunoassays
EDTA	Ethylenediamine tetra acetate
EGFR	Epidermal growth factor receptor
EPR	Enhanced permeation and retention effect
FDA	Food drug administration
FLT1	Vascular endothelial growth factor receptor 1
FR	Folate receptor
GH	Growth Hormone
GFP	Green fluorescent protein
GLUT-1	Glucose transporter
GMP	Good manufacturing
GUS	β -Glucuronidase
HEPES	N-2-hydroxyethylpiperazine-N-2-ethane sulfonic acid

HSV-tk	Herpes simplex virus thymidine kinase gene
IC50	Growth inhibitory concentration
I.P	Intraperitoneal
KV	Kilo volt
Leu	Leucine
Lf	Lactoferrin
Lfc	Lactoferricin
LNCaP	Prostate cancer cell line
Lys	Lysine
MAPK	Mitogen-activated protein kinase
MEM	Minimum essential media
MTT	3-(4,5-dimethylthiazol-2-yl)-2,5- diphenyltetrazolium bromide
mRNA	Messenger Ribonucleic acid
NK	Natural killer cell
NMR	Nuclear Magnetic Resonance
ONPG	O-nitrophenyl- β -D-galactosidase

OTC	Ornithine transcarbamylase
PAMAM	Polyamidoamine
PBS	Phosphate buffered saline
pCMV β -Gal	Plasmid DNA encoding β -galactosidase
PCS	Photon correlation spectroscopy
pDNA	Plasmid DNA
PEG	Polyethylene glycol
PEI	Polyethylenimine
PIC	Protease Inhibitor Cocktail
PLB	Passive lysis buffer
PLL	Poly-L-lysine
PPI	Polypropylenimine
PSA	Prostate specific antigen
PSMA	Prostate specific membrane antigen
RNA	Ribonucleic acid
RPMI	Roswell Park Memorial Institute media
RECIST	Response evaluation criteria in solid tumour

SCID	Severe combined immunodeficiency
SDS	Sodium dodecyl sulphate
ssDNA	Single stranded DNA
SEM	Standard error of the mean
TBE	Tris-Borate-EDTA
TEM	Transmission electron microscopy
TLC	Thin-layer chromatography
TMS	Tetramethylsilane
TNF α	Tumour necrosis factor
TNM	Tumour Node Metastasis
Tf	Transferrin
TfR	Transferrin receptor
TRUS	Transrectal ultrasound-directed prostate

Summary

Cancer is a major public health problem worldwide. It is considered a major cause of death around the world. The World Health Organization estimates that 84 million people will die of cancer between 2005 and 2015, and the incidence is expected to increase continuously as the world population ages (Danhier *et al.*, 2010)

Prostate cancer is one of the most commonly diagnosed cancers in men and remains the second leading cause of cancer-related deaths in industrial countries. To date, there is still no efficacious treatment for patients with advanced prostate cancer with metastases. New treatments are therefore critically needed for these patients.

Gene therapy holds great promise for the intravenous treatment of prostate cancer. Non-viral gene delivery is emerging as potential safer alternative to the use of viral vectors for the treatment of various gene related diseases including cancer. Although non-viral vectors may not be as effective as the viral ones, the continuous research on rationally designing multifunctional non-viral polymeric gene delivery carriers resulted in improved delivery.

This study is carried out to prepare and evaluate the efficacy of tumour-targeted transferrin, lactoferrin and lactoferricin conjugated polypropylenimine dendrimer as a novel gene delivery system able to improve the delivery of the therapeutic gene to cancer cells, in a safe and targeted way.

We demonstrated that new tumour-targeted therapeutic systems recognizing receptors specifically overexpressed on prostate tumours, were able to improve the *in vitro* therapeutic efficacy on PC-3, DU145 and LNCaP prostate cancer cells when compared to the non-targeted delivery system, by up to 100-fold in LNCaP cells. *In vivo*, the intravenous administration of the tumour-targeted therapeutic system encoding Tumour Necrosis Factor (TNF) α resulted in tumour suppression for 60% of PC-3 and 50% of DU145 tumours.

The dendriplex encoding TRAIL led to tumour suppression of 10% of PC-3 tumours. IL-12 mediated gene therapy resulted in tumour regression of 20% of both types of prostate tumours. By contrast, all the tumours treated with DAB-Tf, naked DNA or left untreated were progressive for both tumour types. The treatment was well tolerated by the animals, with no apparent signs of toxicity.

The treatment of cancer cells with lactoferrin- and lactoferricin-bearing dendriplexes *in vitro*, led to an anti-proliferative activity enhanced by up to 5-fold for lactoferricin-bearing DAB in T98G cancer cells compared to the unmodified dendriplex. *In vivo*, the conjugation of lactoferrin and lactoferricin to the dendrimer significantly increased the gene expression in the tumour while decreasing the non-specific gene expression in the liver. Consequently, the intravenous administration of the targeted dendriplexes encoding TNF α led to the complete suppression of 60% of A431 tumours and up to 50% of B16-

F10 tumours over one month. The treatment was well tolerated by the animals, with no apparent signs of toxicity.

To our knowledge, it is the first time that an intravenously administered non-viral gene therapeutic system led to growth inhibition and even complete tumour suppression for prostate tumours.

In conclusion, these tumour-targeted therapeutic systems therefore hold great potential as a novel approach for the gene therapy of prostate cancer.

CHAPTER 1.

INTRODUCTION AND AIMS OF THE STUDY

1.1. Prostate

1.1.1. Histology of the prostate

The prostate is a part of the man's reproductive system. The normal prostate is a small gland about the size of a walnut, located immediately under the bladder and immediately in front of the rectum (Figure 1.1). Its main role is to produce some fluid which is included in sperm.

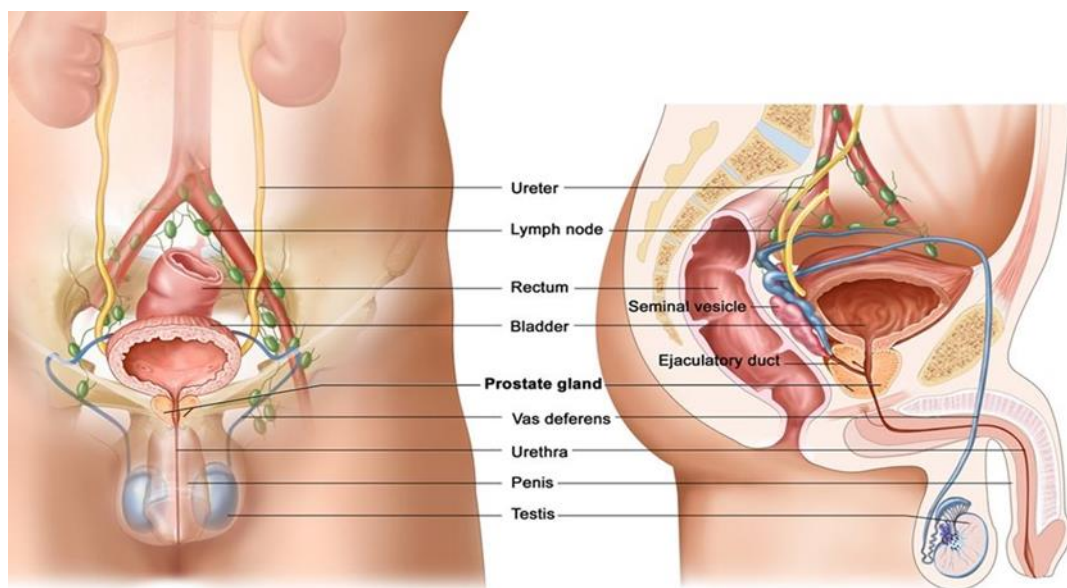


Figure 1.1: Anatomy of the male reproductive and urinary system, showing the prostate (The University of Chicago Medical Centre, 2013).

The anatomy of the prostate gland can be divided into three zones: the transitional, the central and the peripheral zones. These zones are classified depending on the function of the prostate tissue. Clinically, dividing the prostate anatomy into different zones is highly important as it allows knowing which areas of the gland are susceptible of developing cancer.

- The peripheral zone of the prostate gland is the outermost area located at the back of the prostate gland, closest to the rectum. This zone makes up 70% of prostate gland and is therefore the largest area that is susceptible to prostate cancer (McCall *et al.*, 2008).
- The central zone is constituted of non-glandular tissues which make up approximately 25% of the prostate gland. Around 5% of cancer cases start in this zone.
- The transitional zone of the prostate is the innermost zone, which makes up around 5% of the prostate gland. Both the transitional and the central zones continue to increase in size after the age of 40. In addition, this zone is the site of 10% of prostate cancer cases.

All the three zones of prostate gland are encapsulated in a fibromuscular layer called prostate capsule. As the prostate increases in size, this layer expands inwards, preventing the prostate from growing outwards. This thickening in this layer causes a blockage of the flow of urine (Zuckerman & Groome, 1937).

1.1.2. Pathology and treatment of the prostate

There are a number of conditions that can affect the prostate gland including prostatitis, prostate enlargement and prostate cancer.

Prostatitis is the inflammation of the prostate gland. Prostatitis is classified into four types, namely acute, chronic, asymptomatic inflammatory prostatitis and

chronic pelvic pain syndrome. Gram-negative bacteria, such as *Escherichia coli* and *Proteus* (Nickel, 1991), in the prostate causes a bacterial infection condition known as acute bacterial prostatitis. Chronic bacterial prostatitis is an occasional condition caused by bacterial infection in the prostate. Patients with chronic bacterial prostatitis usually have had recurring urinary tract infection. Asymptomatic inflammatory prostatitis and chronic pelvic pain syndrome are both non-bacterial prostatitis and the most common types of prostatitis (Habermacher *et al.*, 2006). The treatment is different for each type of prostatitis. Therefore, differentiating bacterial and non-bacterial types of prostatitis is essential for the treatment of this disease (Stevermer *et al.*, 2000).

The second prostate condition is the prostate enlargement, also known as benign prostatic hyperplasia (BPH), is a very common condition in older men. It involves an increase in the size of the prostate gland as a result of proliferation of epithelial cells without malignance presence (Thorpe *et al.*, 2003).

In contrast, prostate cancer is the malignant growth of the prostate gland. Although some of the signs of BPH and prostate cancer are the same, having BPH does not lead to cancer or increase the risk of prostate cancer. The malignant condition may be a threat to life and can spread to other parts of the body.

1.2. Prostate cancer

1.2.1. Incidence and prevalence

Prostate cancer is the most common malignancy in male population worldwide. It is the second leading cause of cancer death in men (Oberaigner *et al.*, 2006). In the UK, nearly a quarter of all cancer cases diagnosed in men are prostate cancer (www.prostate_research.org.uk, 2005). The probability of being diagnosed with prostate cancer is currently 1 in 10 men, and a new case of prostate cancer is diagnosed every 15 minutes. In the United States, around 190000 new cases are diagnosed in men each year, and it causes around 27,000 deaths annually (Taylor *et al.*, 2010).

The incidence rate of prostate cancer is strongly related to the age of the patient, with the highest incidence rates being observed in older men. It is of 500 per 100 000 men aged 55-59 and increases to 789 in patients aged 85 and older (www.prostate_research.org.uk, 2005).

Another factor that may increase the risk of developing prostate cancer is heredity. People under the age of 60 with a history of prostate cancer in one or more first-degree relatives are at increased risk. However, this factor is responsible for only 5-10 % of cases diagnosed with prostate cancer (Hunt, 2002).

In addition, a strong family history of breast cancer may increase the risk of prostate cancer. Previous studies showed an association between Breast Cancer 1 (BRCA1) and Breast Cancer 2 (BRCA2) mutation and the development

of prostate cancer in men. BRCA1 and BRCA2 are genes on chromosome 17 and 13 respectively, which normally help to suppress cell growth. A person who inherits certain mutations in these genes has a higher risk of getting breast, ovarian, prostate and other types of cancer. Men aged 65 and under, carrying BRCA2 gene, are seven times more at risk of developing prostate cancer than men from the same age group who are not carrying BRCA2. However, this rate is reduced to 4.5 times in older men (Gayther *et al.*, 2000).

The risk of prostate cancer may also be affected by ethnicity groups. In the United States, Black American men are at higher risk of being diagnosed of prostate cancer than White American men. On the other hand, this rate is lower in Asian American men when compared to White American men. Similar results have also been reported in the UK. An increasing risk of prostate cancer is shown in men moving from low-risk countries to high-risk countries, which suggests diet and lifestyle might be risk factors for prostate cancer (Cancer Research UK, 2009).

1.2.2. Types of prostate cancer

Prostate cancer is a cancer which develops from the abnormal proliferation of cells of the prostate gland resulting in the growth of the epithelial lining and eventual blockage of the urinary tract. Prostate cancer can take different forms in various parts of the prostate. The majority of prostate cancers are located in the epithelial tissues in the gland. The malignant form of the epithelium tissues is called adenocarcinoma (Figure 1.2). On the other hand, adenoma is a benign

tumour of epithelial tissues, which is not a cancerous condition (Dabbs & Silverman, 2001).

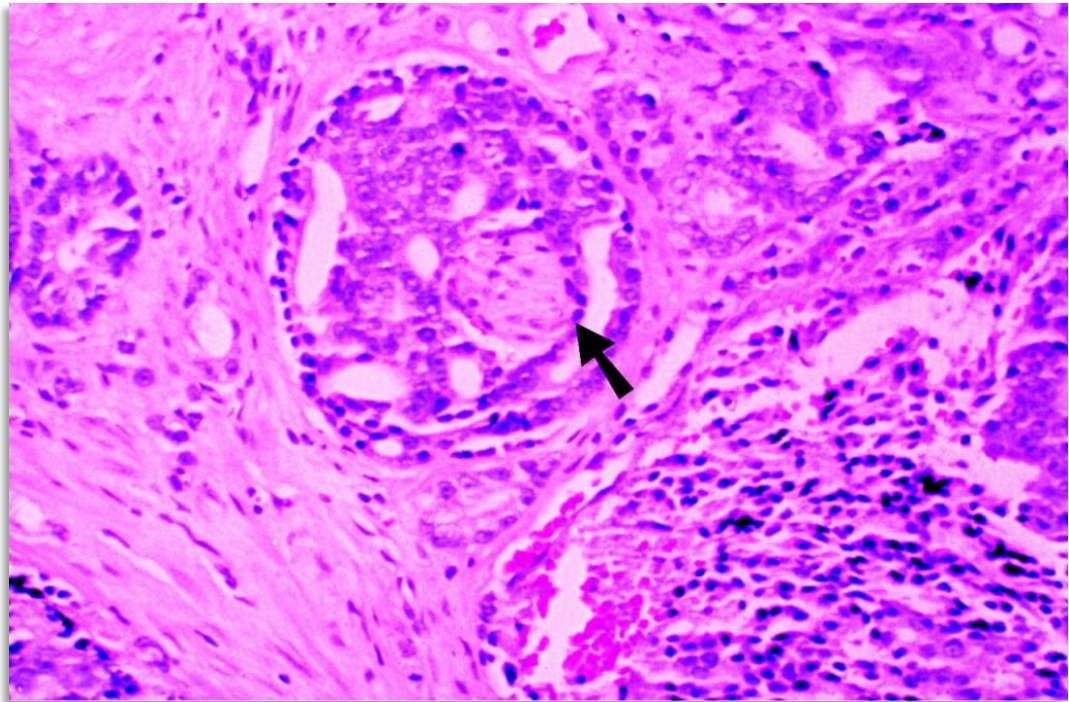


Figure 1.2: Microscopic image showing adenocarcinoma in Prostate (black arrow) (Adapted from Humphrey, 2007).

Another form of prostate cancer is the small cell carcinoma. This type of cancer is made up of round cancer cells and usually originates at nerve cells of the prostate gland. In contrast with adenocarcinoma, small cell cancer is very aggressive in nature and cannot be detected easily by prostate-specific antigen (PSA) test, as this type of cancer does not lead to an increase of the antigen levels while it progresses (Dixit *et al.*, 2012).

There is also a rare type of prostate cancer, known as squamous cell carcinoma (Munoz *et al.*, 2007) (Figure 1.3). It is a non-glandular cancer which

is characterised by its high degree of malignancy and its bone metastasis. Like small cell carcinoma, this type of prostate cancer is very aggressive in nature and does not show an increase in the PSA when it progresses.

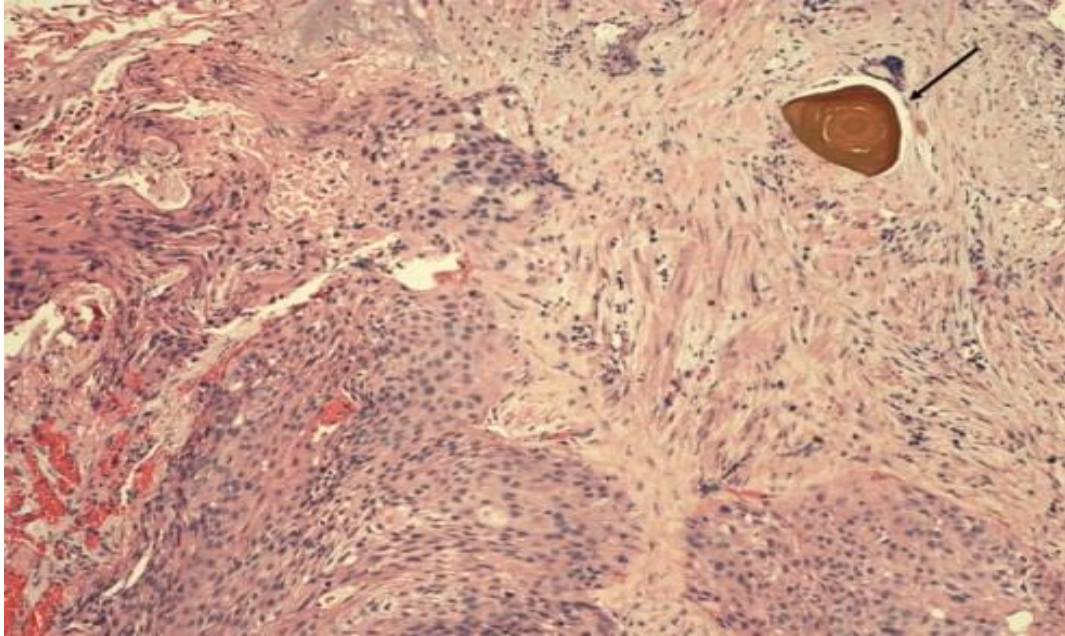


Figure 1.3: Squamous cell carcinoma in the prostate (black arrow) (Adapted from Wang *et al.*, 2012).

Other forms of prostate cancer exist, but are not very common. Examples of these types include sarcomas and transitional cell carcinoma. The latter does not originally develop in prostate but is rather derived from other tumours developed in the bladder or urethra (McCall *et al.*, 2008).

1.2.3. Symptoms of Prostate Cancer

Prostate cancer does not announce its presence while it progresses. Small confined prostate cancer may not show any symptoms and may not be detectable during routine medical check-up. However, as the cancer grows, one

or more symptoms may start to appear. These symptoms may include blood in semen or urine, difficulties in passing urine or not being able to urinate at all, necessity to frequently urinate particularly in the middle of the night, painful ejaculation, pain in the lower back, upper thighs or hips, weight loss, bone pain and swelling in both legs and feet.

It is important to note that these symptoms may not be indicators of prostate cancer, but the result of other prostate gland disorders such as prostatitis and Benign Prostatic Hyperplasia (BPH). However, for an early detection of prostate cancer, it is always recommended that men from the age of 40 should start annual prostate cancer tests such as Prostate Specific Antigen (PSA), Prostate Specific Membrane Antigen (PSMA), Digital Rectal Examination (DRE), Transrectal Ultrasonography (TRUS) and prostate biopsy.

1.2.4. Diagnostic Modalities for Prostate Cancer

1.2.4.1. Prostate Specific Antigen

One of the standard tests employed for the diagnosis of prostate cancer is the determination of the blood levels of the prostate-specific antigen (PSA) which is a substance produced by the prostate gland. Increased levels of PSA may indicate an abnormality in the prostate such as a prostate infection, an enlargement of the prostate gland or a prostate cancer (Brooks *et al.*, 2010).

PSA is a 34 KD glycoprotein serine protease enzyme which is a member of the kallikrein-related peptidase family. The gene encoding for PSA is located in the 19th chromosome in humans. PSA is produced by the epithelial cells of

the prostate gland and its role is to liquefy semen in the seminal coagulum so that the sperm can swim freely (Lilja, 2003).

PSA test measures the blood level of PSA. The level of PSA is measured in nanograms per millilitre (ng/ml). In healthy men, PSA is present in blood at very low levels. However, this level normally increases as the man ages. Normal PSA level for men aged 40 to 49 years is 0.0 to 2.5 ng/ml; for 50 to 59 years, up to 3.5 ng/ml; for 60 to 69 years, up to 4.5 ng/ml and for 70 to 79 years, up to 6.5 ng/ml (Oesterling *et al.*, 1993).

Increased level of PSA is a sensitive marker for detecting prostate cancer. Thus, higher level of PSA indicates higher prostate cancer risk (Thompson *et al.*, 2004). The raised PSA level in prostate cancer patients is not due to the increase of the activity of prostate cancer cells but to the abnormality in the growth of such cells. However, increased levels of PSA can be an indicator of other prostate disorders such as benign prostatic hyperplasia (enlargement of the prostate) or prostatic inflammation (Wever *et al.*, 2012). On the other hand, some factors such as obesity may reduce levels of PSA with the presence of prostate cancer (Bañez *et al.*, 2007).

1.2.4.2. Prostate Specific Membrane Antigen

Prostate Specific Membrane Antigen (PSMA) is another blood diagnostic marker for prostate cancer. PSMA is a 100-kd type II membrane glycoprotein which is expressed in all types of prostatic tissues, including cancerous forms of these tissues. The PSMA gene is located in the 11th chromosome in humans, in a

region that is not commonly deleted in prostate cancer (Chang, 2004). The function of PSMA enzymes on human prostate tissues and elsewhere remains unknown.

PSMA represents an excellent target for the diagnostic of prostate cancer. Moreover, it has been shown to be more effective than PSA in detecting prostate cancer cells. Serum levels of PSMA and PSA were evaluated clinically in 235 prostate cancer patients. The clinical data showed elevated levels of PSMA even in the presence of very low PSA levels. Thus, PSMA is a more sensitive marker for the detection of prostate cancer than PSA (Murphy, 1995).

In addition, PSMA levels have been found to be correlated with the aggressiveness of prostate cancer. PSMA levels were compared in different histopathologic categories in 450 patients diagnosed with prostate cancer (including 24 benign, 225 localized prostate cancer, and 201 metastases cases). The study showed that the highest PSMA levels were found in patients with metastasis prostate cancer. The lowest levels of PSMA were found in patients with benign prostate glands followed by localized prostate cancer (Perner *et al.*, 2007)

Moreover, PSMA is also used as an immunotherapy for targeting prostate cancer and other malignancies, and first-generation products have entered clinical testing (Chang, 2004).

1.2.4.3. Digital Rectal Examination

Serum-based test for prostate cancer should always be followed by Digital Rectal Examination (DRE). The procedure of DRE involves the insertion of a healthcare professional's lubricated-gloved finger into the rectum in order to check for abnormalities of the prostate gland. However, prostate cancer is not always detectable by DRE, especially if the tumour is too small to be detected or if it is positioned on the other side of the prostate gland which is inaccessible to the touch (Okotie *et al.*, 2007).

1.2.4.4. Trans Rectal Ultrasound-directed prostate biopsy

The Transrectal Ultrasound-directed prostate (TRUS) test involves the use of high-frequency sound waves to detect abnormalities in the prostate. This test is performed by the insertion of a small probe into the rectum, targeting it to the prostate and recording ultrasounds images. Any enlargement of the prostate or the presence of a tumour outside the prostate glandular capsule may be detected by TRUS. However, small tumours or tumours in other zones of the prostate gland are undetectable. In addition, TRUS may also be used as a guidance tool to guide biopsies needles (Lippman *et al.*, 1992).

1.2.4.5. Prostate biopsy

Any abnormal increase in PSA levels and abnormalities in DRE tests indicate the need for a biopsy examination for the prostate. Prostate biopsy is a surgical removal of a small amount of prostate gland tissues using a prostate biopsy

probe with a needle to retrieve a tissue sample to be examined under the microscope for the diagnosis of prostate cancer. The insertion of the needle can be done through the urethra, the perineum or through the rectum using ultrasound-guidance.

To minimize the discomfort during the biopsy, these procedures can be done under anaesthesia. The biopsy examination may cause bleeding in the rectum, the urine and the semen for several days. In addition, antibiotics are prescribed to patients prior and after the procedure to prevent infections.

The biopsy technique has shown success in the diagnosis of prostate cancer for several years. However, there is a concern that the biopsy may include only samples without cancer, although the cancer is present. Therefore, samples from different regions of the prostate may increase the diagnostic accuracy by this method (Eskew *et al.*, 1997).

1.2.5. Prostate Cancer stage

Clinically, prostate cancer is diagnosed based on the degree of spread of the cancer as non-metastatic disease or metastatic disease. A non-metastatic prostate cancer can be either a locally confined disease or a locally advanced disease which spreads outside the capsule of the prostate gland but has not spread to other organs.

The majority of prostate cancer cases occur in individuals over 60 years old and the development of progressive metastatic disease is slow in their

lifetime. Therefore, the majority of prostate cancer patients live with a locally confined disease which is not necessarily their cause of death in most of these cases (Okajima *et al.*, 2012). Locally confined disease diagnosed with low-risk may be treated with radiotherapy or radical surgery (Hull *et al.*, 2002).

On the other hand, metastatic prostate cancer spreads beyond the prostate capsule to the local tissue, the lymph nodes, bones, or other organs such as liver or lungs (Figure 1.4). In this type of prostate cancer, it may spread to other sites of the body even if the tumour is very small. This type of cancer is the most frequent cause of cancer death in men in the UK (McCall *et al.*, 2008).

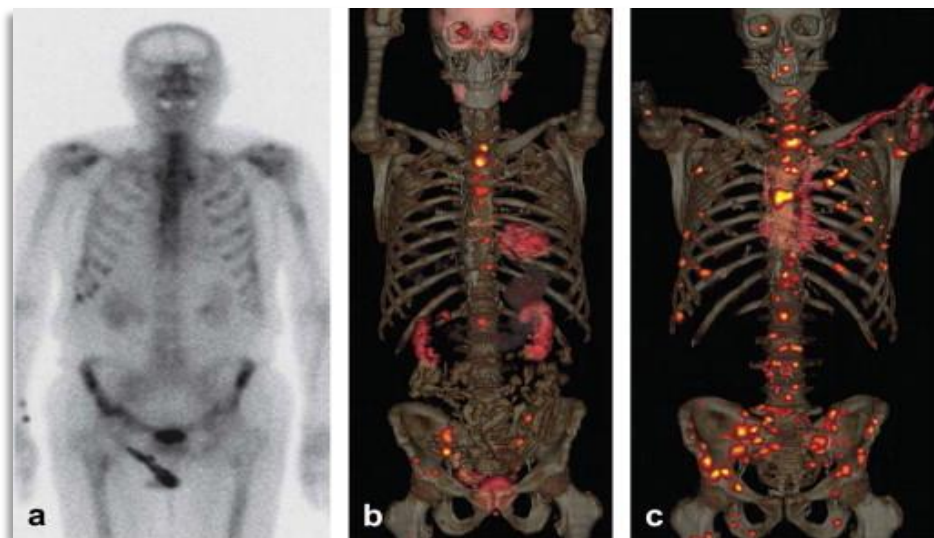


Figure 1.4: Metastatic prostate cancer. a) Primary prostate cancer adenocarcinoma. b) Large number of bone and lymph node metastases. c) Larger number of bone and lymph node metastases as compared to b or a. (Adapted from Kircher *et al.*, 2012).

Tumour stage can be determined by the measurement of the tumour size and spread. The Tumour Node Metastasis (TNM) determines the tumour stage based on three components:

- The T component shows the spread of the disease at the primary site
- The N component indicates whether the nodal metastases exist or not
- The M component determines the presence or absence of distant tumour metastases (McCall *et al.*, 2008).

Table 1.1: TNM classification used for Prostate cancer staging (Adapted from Clinical Practice Guidelines in Oncology: Prostate Cancer, 2013).

Stage	Description
TX	Primary tumour cannot be assessed
T0	No evidence of primary tumour
T1	Clinically unapparent tumour not palpable or visible by imaging
T1a	Tumour incidental histological finding in 5% or less of tissue resected
T1b	Tumour incidental histological finding in more than 5% of tissue resected
T1c	Tumour identified by needle biopsy (because of elevated prostate specific

Stage	Description
	antigen (PSA) level)
T2	Tumour confined within the prostate
T2a	Tumour involves one half of one lobe or less
T2b	Tumour involves more than half of one lobe, but not both lobes
T2c	Tumour involves both lobes
T3	Tumour extends through the prostatic capsule
T3a	Extracapsular extension (unilateral or bilateral)
T3b	Tumour invades seminal vesicle(s)
T4	Tumour is fixed or invades adjacent structures other than seminal vesicles: bladder neck, external sphincter, rectum, <i>levator ani</i> and/or pelvic wall
N	Regional lymph nodes
NX	Regional lymph nodes cannot be assessed

Stage	Description
N0	No regional lymph node metastasis
N1	Regional lymph node metastasis
M	Distant metastasis
MX	Distant metastasis cannot be assessed
M0	No distant metastasis
M1	Distant metastasis
M1a	Non-regional lymph node(s)
M1b	Bone(s)
M1c	Other site(s)

1.2.6. Grading of prostate cancer

Tumour grading classifies the tumour growth according to the degree of cellular differentiation. The Gleason grading system is one of the most used

systems for grading prostate cancer. In this system, the grade of tumours has a range from 1 to 5, with 5 having the worst prognosis. The prostate cancers can also be graded based on their microscopic appearance in which the Gleason scores range from 2 to 10 as follows: grade 2-4 (well differentiated), 5-7 (moderately differentiated) and 8-10 (poorly differentiated) with 10 having the worst prognosis (Gleason, 1992).

1.2.7. Prostate Cancer Treatment

The increased incidence of prostate cancer has led to some developments in diagnosis and treatment over the past century. However, the type of treatment is determined by the stage of prostate cancer. For example, localized prostate cancer has different treatment choices to those for metastasized cases.

Patients with localized carcinoma may be placed in a monitoring program. This pre-treatment program involves the regular application of various tests to monitor any changes in the cancer stage. Because prostate cancer generally affects older men and, in most cases, the cancer development is very slow (Klotz, 2006), this monitoring program aims to avoid or at least delay unnecessary side-effects of the treatment of prostate cancer which may affect the patient's quality of life.

There are two approaches for monitoring prostate cancer: active surveillance and watchful waiting. In the active surveillance, the cancer is observed for any growth before the patient can have appropriate treatment. On the other hand, watchful waiting keeps the treatment on hold if either the

cancer is a slow-grow disease or there is a medical condition that does not fit with different types of treatment due to age or other co-morbidity (Harlan *et al.*, 2003).

1.2.7.1. Surgery

Treatment of prostate cancer depends on the patient's age and the degree of spread of the cancer. There are several ways to treat this disease such as surgical intervention, which is considered to be one of the most important methods of treatment (Picard *et al.*, 2012), especially for those who are under the age of 70 (National Cancer Institute, 2006). A study on 1746 patients with prostate cancer showed that surgical excision of the tumour gave effective results in 83% of the total number of patients (Bianco *et al.* 2005).

1.2.7.2. Radiotherapy

The second major therapeutic modality for high-risk prostate cancer is radiotherapy (Picard *et al.*, 2012). However, using radiotherapy as a single modality therapy has a low rate of success for high-risk cancer. Recent studies based on the biochemical control rates of radiotherapy alone show that 38% of patients are at high-risk. Thus, the combination of radiotherapy and another therapeutic modality is indicated in the treatment of high-risk prostate cancer.

1.2.7.3. Hormonal therapy

Prostate cancer could also be treated by hormonal therapy with either medical or surgical castration, especially in patients with poor prognostic factors or

with other treatments. Immediate hormonal therapy has various benefits that improve the patient's quality of life, for instance, the reduction in pathologic fractures, urinary obstruction and spinal cord compression. However, the side effects of hormonal therapy include hot flashes, osteoporosis, increased sexual dysfunction, metabolic syndrome, anaemia, gynecomastia, dry eyes, body hair loss and vertigo (Picard *et al.*, 2012).

1.2.7.4. Chemotherapy

The early use of chemotherapy as a treatment for castrate-resistant prostate cancer (CRPC) was limited because of toxicity in old patients and the chemo-resistant nature of CRPC (Singh *et al.*, 2010). However, an early clinical trial involving patients with an advanced stage of CRPC treated using a combination of Mitoxantrone and Prednisone had approved that chemotherapy could help in the palliation of pain in patients with CRPC in its advanced stages (Tannock *et al.*, 1996), but did not show any survival advantage (Singh *et al.*, 2010). Since then, further treatments of CRPC using docetaxel-based chemotherapy have shown a survival benefit. However, the problem of toxicity and poor tissue specificity are still obstacles in the way of the success of this method. Today, the development of targeted gene therapies treating prostate cancer appears to be one of the best options to address these problems (Singh *et al.*, 2010).

1.2.7.5. Immunotherapy

Immunotherapy is one of the new techniques used as a central component for many cancer regimens. It is a central component for many cancer regimens. It is

sometimes used by itself for cancer therapy; however, it can be used together with standard treatment such as radiation, surgery and chemotherapy in order to enhance its effect (Dougan and Dranoff, 2009).

1.2.7.6. Cryotherapy

Cryotherapy is one of the new technologies used to destroy cancer cells by using extremely low temperatures to treat a variety of benign and malignant tissue damage. It can be used in localized prostate cancer which is not spread in prostate gland. In clinical trials, the technique of the treatment includes inserting thin needles into the prostate gland through the skin. Freezing gases are passed through the needles to kill cancer cells. However, freezing the prostate gland may cause small damages to healthy cells. In addition, cryotherapy may cause some side effects such as impotence, rectal problems and urinary symptoms.

1.2.7.7. Cancer Treatment based on Nanomedicine

Currently, the most common cancer treatments are surgical intervention, radiation therapy and chemotherapy. The outcome of these conventional treatments is still below expectations (Baird and Kaye, 2003; Wong *et al.*, 2007). In addition, these treatments have a number of side effects depending on the type of treatment. Chemotherapeutics, for example, have no tumour selectivity and are distributed randomly in the body. High doses are often required due to lack of specificity and the drugs are not targeted to tumour sites. In some cases, administrating high therapeutic doses of

chemotherapeutics also leads to serious systemic toxicity, as the drugs are distributed to non-cancerous cells at the same time (Wong *et al.*, 2007).

Effective treatment for cancer requires specific tumour targeting and efficient delivery of therapeutic agents. A better knowledge of cancer pathophysiology combined with developing novel technologies that deliver anticancer materials to their site of action is the ultimate goal which will lead to more effective therapies for cancer (Aldawsari *et al.*, 2011). Recent developments in nanotechnology have provided researchers in cancer treatment with new and promising tools for the treatment of cancer that aim to overcome the problems related to conventional treatments, such as toxicity and poor targeting for therapeutic agents. This technology involves the development of tumour-targeted delivery systems able to carry therapeutic agents, including antibodies, anticancer and genes.

1.3. Gene Therapy

1.3.1. Overview

Genes are units of heredity that consist of sequences of DNA contained in the chromosomes (Figure 1.5) (William and Kampmann, 1999; Mahale *et al.*, 2009). They determine the information about organisms which make each individual unique. For example, some genes are responsible in determining the eye, hair colour or blood type. Mutations in genes may cause serious diseases.

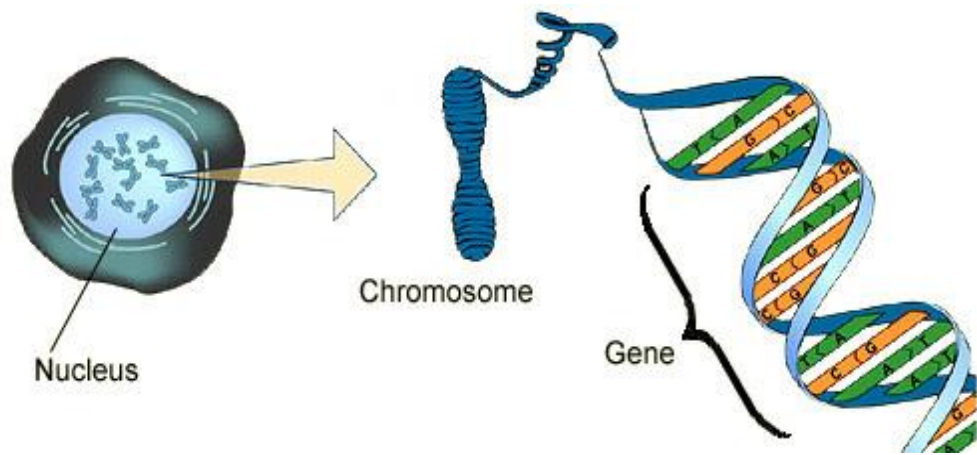


Figure 1.5: Gene in relation to a chromosome (Adapted from Cancer Research UK).

Gene therapy refers to the therapeutic delivery of exogenous genetic material containing DNA, RNA or oligonucleotides inside the cells of an organism for the treatment of a disease.

The development in human gene therapy occurred in the early 1970s, when Rogers proposed an initial procedure for the use of viruses as vectors to modify genes in human cells for therapy (Rogers *et al.*, 1973). In that study, two sisters suffering from hyperargininaemia were injected with papilloma virus to introduce the gene for arginase. Although it was successful in rabbits, the treatment failed to reduce the arginine blood levels in treated patients. The failure of this treatment was assigned to the virus instability (Escors and Breckpot, 2010).

In 1980, a first experimental attempting to use gene therapy on humans using recombinant DNA was conducted by Martin Cline. Following a successful gene transfer into mouse bone marrow stem cells, Cline performed a gene

transfer study on two patients suffering from β -thalassemia. The two patients were given infusions of autologous bone marrow cells that had been extracted from the patients and transformed with recombinant DNA. The treatment failed for both patients with no resulting harm for any of them (Marcum, 2005).

The focus on gene therapy as an approach for the treatment of human diseases increased during the 1990s. An approved gene therapy trial was initiated by Anderson *et al.* in September 1990 on a 4-year old girl born with severe combined immunodeficiency (SCID) as a result of a malfunctioning of a single gene called adenosine deaminase (ADA). In January 1991, a nine-year old girl suffering from the same disease was treated. Although the effect of these trials was temporary, they significantly reduced the amount of the (PEG)-ADA drug needed for their treatment (Anderson, 1995).

The 90s decade finished with a highly publicized case, when an 18-year old man, Jesse Gelsinger, took part in a gene transfer trial. He suffered from a rare liver disease due to a genetic disorder called ornithine transcarbamylase (OTC). Four days after having received a gene transfer with a very high dose of adenovirus, Gelsinger died after suffering a massive immune response triggered by the use of the viral vector used to transport the gene into his cells, leading to multiple organ failure and brain death. This failure was the first case that could be directly linked to the use of viral vectors for the treatment (Scollay, 2001). As a result of this severe event, the U.S. Food and drug

administration (FDA) suspended all clinical trials and conducted a re-evaluation of the ethical practices in the field (Morgan *et al.*, 2006).

In 2000, another successful gene transfer trial was reported by Alain Fischer and his team (Cavazzana-Calvo *et al.*, 2005). They treated nine male children who had an X-linked type of severe combined immunodeficiency (SCID), with most being cured. However, in 2002, two of the nine patients were diagnosed with a rare type of leukaemia. Examinations of their genomes showed that the retrovirus that had delivered the therapeutic gene into their cells had, as a side effect, activated silent oncogenes.

In 2003, China's State Food and Drug Administration (SFDA) approved the first gene therapy product for clinical use in human. Gendicine[®], manufactured by SiBiono Gene Tech Co., is a recombinant adenoviral vector to express human p53 cDNA for the treatment of neck and head squamous cell carcinoma. However, Gendicine[®], gained its approval based on a small scale phase II/III clinical trials with about 135 patients. As a consequence of this, there were concerns about the efficacy of Gendicine[®] (Xin, 2006). In this trial, all the 135 patients suffered from head and neck squamous cell carcinoma and Gendicine[®] was administered for a period of 12 weeks. The patients were randomly divided into two groups; one group received doses of Gendicine[®], in combination with radiotherapy, while the other group received radiotherapy alone. There were no significant differences in the other parameters, such as age, sex, or tumour size, between the two groups. Results of this trial showed a

complete regression in 64% of the patients from the first group in comparison with a complete regression in 19% of the patients from the other group. Moreover, in all the reported clinical trials, there was no serious side-effect. However, the most common side-effects of Gendicine® were fever, fatigue and some pain at the injection site. Observations from clinical trials also showed improvements in the appetite and general health of some patients approximately two days after the treatment.

Two years after the approval of Gendicine®, another gene therapy product, Oncorine®, gained approval by the Chinese SFDA on November 2005 for the treatment of head and neck cancer. Oncorine® is a selectively replicative oncolytic adenovirus with E1B 55kD deletion, which restricts the virus to bind and inactivate wild-type p53 protein. The design of these viruses allows them to replicate only in cancer cells and specifically kill these cells during the normal progression of the virus life cycle. Oncorine® was developed by Sunway Biotech Co. Ltd, which acquired approval to start clinical trials in September 2000. In phase I trial, 15 patients, with different cancers including head and neck cancer, melanoma, ovarian cancer, neuroblastoma and soft tissue sarcoma, were enrolled in the trial. Patients were treated with Oncorine® by intratumoural injection for 5 consecutive days. Among 15 patients, partial regression was observed in 3 patients. All patients tolerated Oncorine® well, and no dose limited toxicity and serious adverse event have been found. However, the most frequent side effects were pain at the injection site, fever and flu-like symptoms. This phase I trial concluded that Oncorine® is safe for

local treatment of cancers. Phase II clinical trials conducted between October 2001 and June 2002. A total of 50 patients with different cancers were recruited. All patients received viral injection for 5 consecutive days during the three weeks viral treatment cycle. Patients had at least 2 and up to 5 treatment cycles for their treatment. Four patients dropped from the treatment. Among the remaining 46 patients, a complete regression was observed in 3 patients and a partial regression in 11 patients. The focus in phase III clinical trial was on head and neck cancer. In this trial, a group of 66 patients was treated with a combination of Oncorine® and chemotherapy, while another group of 57 patients was treated with chemotherapy alone. The chemotherapy drugs used in this trial were 5-fluorouracil (f-FU), cisplatin (DDP) and Adriamycin (ADM) which were used in two different combinations as PF and AF regimens. The PF regimen conducted intravenous infusion of DDP at 20 mg/m² and f-FU at 500 mg/m² qd for 5 days. The AF regimen used intravenous injections of ADM at 50 mg/m² at day 1 and intravenous infusion of 5-FU at 500 mg/m² qd for 5 days. All patients were given the PF chemotherapy regimen first, unless no response was elicited, they were subsequently subjected to AF regimen therapy. Among the first group, there were 6 complete regressions and 42 partial regressions, whereas the other group had 2 complete regressions and 21 partial regressions. The response rate for both groups in the treatment was 72.7% and 40.0%, respectively, which concluded that the combination of Oncorine® with chemotherapy had a significant effect on the treatment of cancer (Campbell, 2008)

In 2004, another gene-based product, Cerepro[®], had the first Good manufacturing practice (GMP) certificate in the EU. Cerepro[®] is an adenoviral vector containing herpes simplex virus thymidine kinase gene (HSV-tk), developed by Ark Therapeutics Group plc for the treatment of malignant glioma. Cerepro[®] had completed three clinical trials and demonstrated significant efficacy in Phase III trial. In this trial, Cerepro[®] was injected through the wall of the cavity left behind by the surgical removal of the solid tumour, into the surrounding healthy brain tissue using 30-70 injections at a depth of 1cm (Wirth and Ylä-Herttuala, 2013).

Gene therapy clinical trials have been performed in 30 different countries but most of these trials (63.9%, as shown in Figure 1.6) were in the United States. These trials had been conducted to address various human diseases. However, the vast majority of gene therapy trials were for the treatment of cancer (64.6% of all gene therapy trials, as shown in Figure 1.7). These trials have made gene therapy for cancer a promising treatment approach for patients compared to traditional cancer therapies.

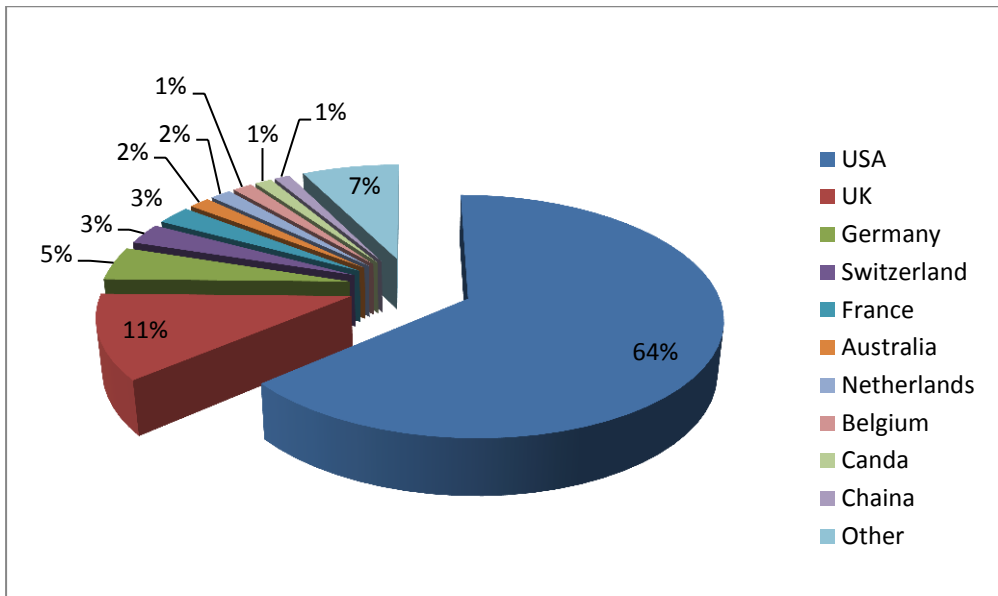


Figure 1.6: Geographical distribution of clinical trials for gene therapy (Adapted from Wiley, 2012).

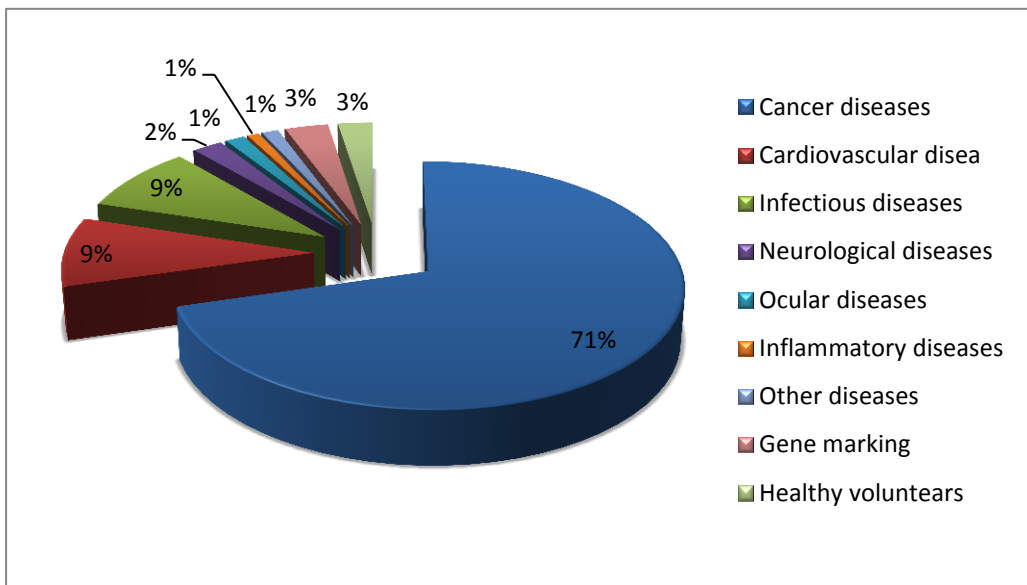


Figure 1.7: Clinical trials for gene therapy (Adapted from Wiley, 2012).

For gene therapy to be successful, the therapeutic gene has to be specifically and efficiently delivered to the targeted cell. However, the gene

cannot enter the targeted cell by itself because it is a large piece of DNA carrying negative charges (Balazs & Godbey, 2011). Therefore, carriers (known as vectors) are required to deliver a specific gene into the cell. There are two different types of vectors, viral vectors and non-viral vectors. Important parameters (Goverdhana *et al.*, 2005) to be considered in the definition of the best type of vector include:

- Size limitations for insertion of transgenes
- Purity and titre of the vector
- Transduction efficiency
- Ability to infect dividing and/or quiescent cells
- Long-term expression of transgenes
- Integration into the host genome
- Need for cell-type specifically or targeted delivery and vector-associated toxicity and immunogenicity

1.3.2. Viral Methods

The most common type of vectors used to carry therapeutic genes into target cells are viruses. The way that viruses encapsulate and deliver their gene to cause diseases in humans has been taken into account to use these viruses as

carriers to encapsulate and deliver therapeutic genes to targeted cells (Figure 1.8) (Mahale *et al.*, 2009).

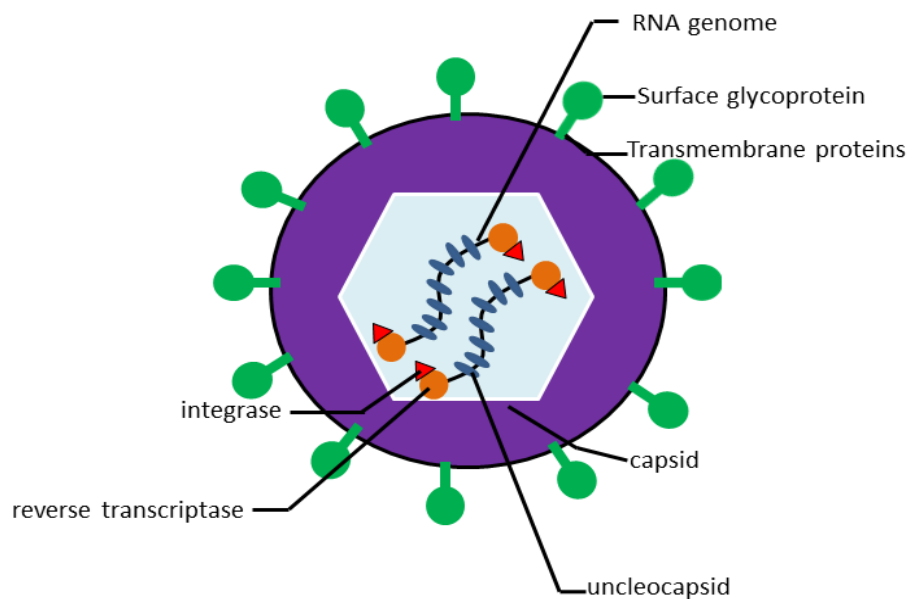


Figure 1.8: Viral vector Adapted from nano-life science (Mahale *et al.*, 2009).

There are three main requirements for viral vectors:

- The vector must be safe and immunologically latent.
- The delivery system must be able to protect the genetic material from degradation.
- The vector must encapsulate and effectively deliver a therapeutic gene to its target (Scheller and Krebsbach, 2009).

Different types of viruses can be used as gene vectors:

- **Retroviruses:** A family of viruses that duplicated to produce stranded DNA copies of their RNA genomes. These copies of genome can be integrated into the chromosomes of host cells (Mahale *et al.*, 2009) Retroviruses as vectors for delivering therapeutic DNA have been used in clinical trials for gene therapy for the treatment of cancer such as melanoma and ovarian cancer (Saraswat *et al.*, 2009).
- **Adenoviruses:** A family of DNA viruses known as “viruses of the common cold” (Goverdhana *et al.*, 2005). These viruses contain double-stranded DNA. They have been used as a delivery tools in gene therapy as their infection is non-fatal. These viruses have been used to deliver therapeutic DNA to metastatic breast ovarian and melanoma cancers (Saraswat *et al.*, 2009).
- **Adeno-associated viruses:** Adeno-associated viruses are linear, single-stranded DNA parvoviruses (Goverdhana *et al.*, 2005). They are not associated with any human diseases, which helps in reducing the risk of infection in host cells (Saraswat *et al.*, 2009).
- **Herpes simplex viruses:** These viruses are a class of double-stranded DNA viruses. They can remain latent in host cells and therefore provide a long-term expression of the therapeutic gene (Saraswat *et al.*, 2009). These viruses are common human pathogens that cause cold sore.
- **Lentiviruses and hybrid viruses:** The viral genome of this class of viruses is RNA (Goverdhana *et al.*, 2005). Hybrid viruses combine the positive features of more than one virus (Mahale *et al.*, 2009).

Table 1.2: Different viral vectors used in gene therapy (Adapted from Goverdhana *et al.*, 2005).

Vector	Viral genome	Cloning capacity	Tropism	Inflammation	Vector genome forms	Main limitations	Main advantages
Enveloped Retrovirus	RNA	8kb	Dividing cells only	Low	Integrated	Integration might induce on cogenesis in some applications	Stable gene expression Transduces dividing cells; integration might induce insertional mutagenesis and on cogenesis
Lentiviruses	RNA	8kb	Broad	Low	Integrated	Toxic and inflammatory; transient transgene expression in target tissues except neurons	Stable gene expression replicating cells
HSV-1	dsDNA	40kb ^a 150kb ^b	Neurons Broad	High	Episomal	Toxic and/or pathogenic properties	Stable gene expression in most tissues
AAV	ssDNA	<5kb	Broad	Low	Episomal (>90%) Integrated (<10%)	Small cloning Capacity	Broad cell tropism; non-inflammatory and non-pathogenic
Adenoviruses	dsDNA	7.9kb ^a 30kb ^c	Broad	High	Episomal	Capsid mediates an inflammatory response; pre-existing anti-Ad antibodies in most humans	Highly efficient transduction of most tissues; large cloning capacity; high titter and long-term expression

Viral vectors have emerged as the most commonly used carriers for many gene therapy trials today. However, viral vectors also have problems and limitations that restrict their applications in gene therapy (Seow and Wood, 2009). Among these problems are the immune response resulting from the administration of

viral vectors, and the risk for multiple cells of being infected with the virus (Porteus *et al.*, 2006).

1.3.3. Non-viral methods

Although viral vectors are efficient way to deliver genes, non-viral vectors are used to overcome the viral vectors drawbacks. They are preferred because of their safety, low cost, lack of immune response and toxicity, ease of chemical formulation and modification, and the lack of DNA size limitation (Park *et al.*, 2006; Scheller and Krebsbach., 2009).

The principle of non-viral delivery system is that a piece of DNA which carries a therapeutic gene is delivered to the targeted cell with the aid of a non-viral vector. These non-viral vector molecules are complexed with DNA that carries the therapeutic gene. The complexed DNA is formed by the interaction between the positively charged vectors and the negatively charged DNA. This complex is then capable of entering the plasma membrane of the target cells (Goverdhana *et al.*, 2005; Lungwitz *et al.*, 2005).

The complexes bind to endosomes upon their entry to the targeted cell. Successful non-viral vectors must be able to release themselves from endosomes before being destroyed by the lysosomal enzymes in the cell. The DNA must then be released from its carrier molecules to the nucleus of the cell (Goverdhana *et al.*, 2005) (Figure 1.9).

Several non-viral vectors are being explored to find the optimal carrier system. The majority of them are cationic lipids, polymers, or both lipids and polymers (Figure 1.10). In addition to these vectors, naked DNA was used in gene therapy and can be administered via two different methods, either *ex vivo* or *in vivo*. The *ex vivo* method has been successfully used to deliver the DNA to endothelial and smooth muscle cells. However, its dependency on the culture of the harvested cells makes it an unsuitable method for many cell types. On the other hand, the *in vivo* delivery of naked DNA, which was first demonstrated in skeletal muscles in 1990, has a low efficiency of expression (Wolff *et al.*, 1990). However, efficiency of the delivery had improved when administered in a pressure-mediated method using controlled, non-distending pressure. Enhanced delivery may be explained by an influence of absolute pressure on the microstructure of the tissue interstitium or may simply result from an altered interaction of the cell membrane with the DNA that is present at the cell surface. In fact, pressure has been found to alter both the fluid phase of biological membranes and the organization of membrane proteins and cytoskeletal elements, and these effects may be particularly important in protein-rich areas of cell membranes involved in channel formation or transmembrane transport (Mann *et al.*, 1999 ; Saraswat *et al.*, 2009).

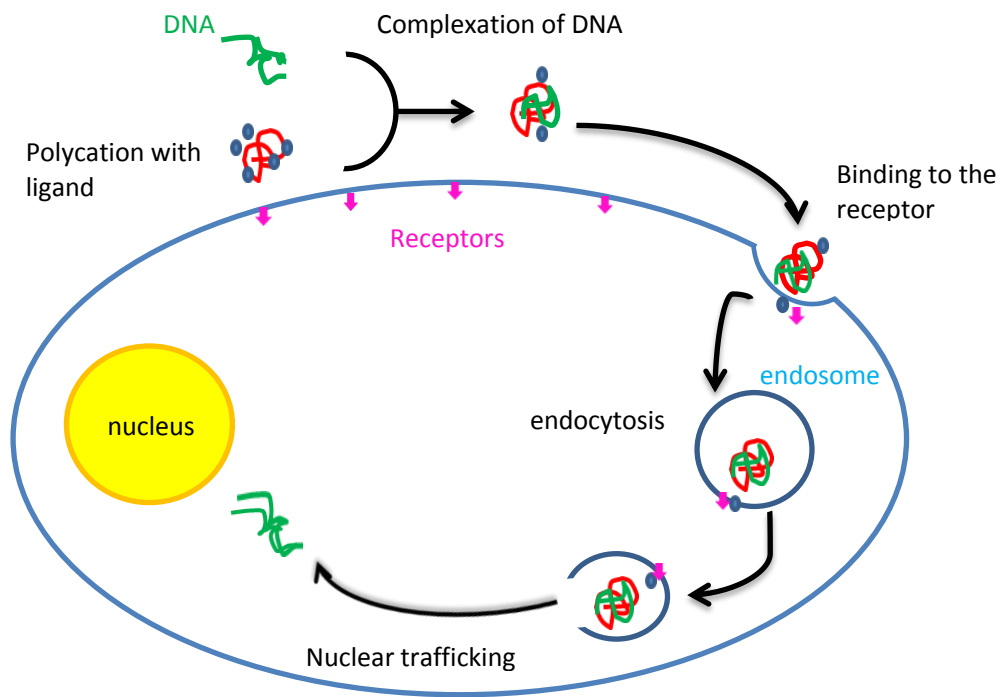


Figure 1.9: General scheme of gene delivery using non-viral vectors (Adapted from Lungwitz *et al.*, 2005).

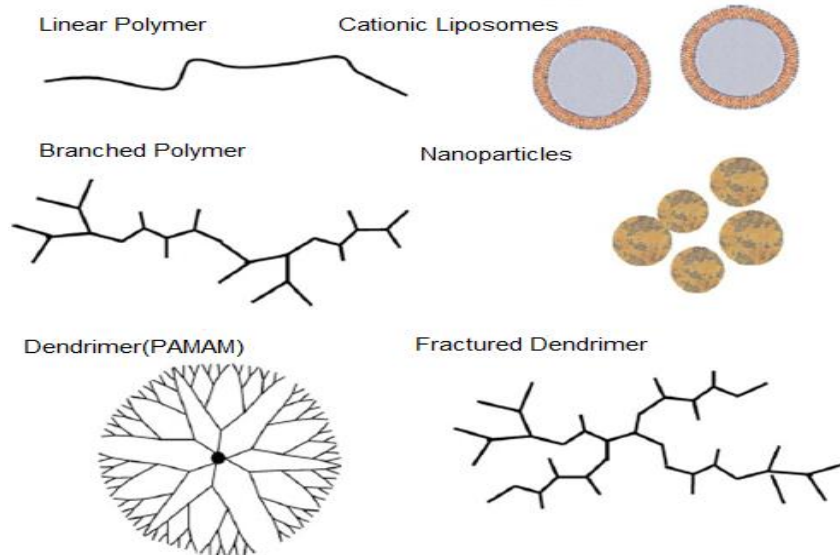


Figure 1.10: Non-viral vectors (Adapted from Dufès *et al.*, 2005).

Polymers have different architectures such as linear, branched or dendrimeric polymers. The architecture of polymer is closely related to its transfection efficiency (Gebhart & Kabanov, 2001; Kimura *et al.*, 2001). Nowadays, the non-viral gene delivery vectors used can be categorized into liposomes, polymersomes, dendrisomes and dendrimers.

1.3.3.1. Liposomes

Liposomes are considered to be one of the most versatile vectors for the use in gene delivery (Saraswat *et al.*, 2009). They are vesicular structures formed by the interaction between the self-assembly dissolved lipid molecules. Each molecule has a hydrophilic head group and a hydrophobic tail. These lipids are associated together by the tails facing each other and the head groups facing outward forming bilayer membrane (Figure 1.11). Both ends of the bilayer membrane are then attached to each other to form a closed vesicle known as liposome (Figure 1.11). This liposomal structure therefore overcomes the problem of hydrophobic parts being exposed to water (Balazs and Godbey, 2011).

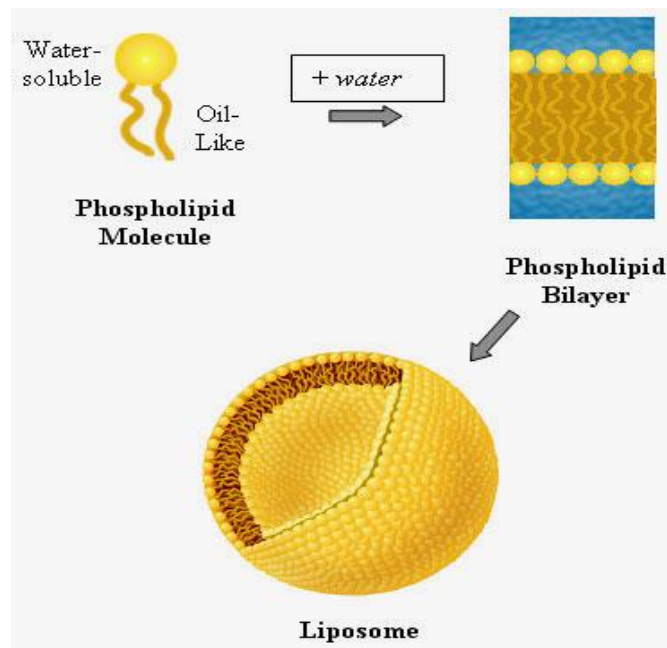


Figure 1.11: Lipids formulation of liposomes (Adapted from Balazs and Godbey, 2011).

There are three types of liposomes (Yanasarn *et al.*, 2011): neutral, negatively and positively charged liposomes.

Positively charged liposomes are known as cationic liposomes (Morille *et al.*, 2008). Their positive charge is due to the presence of one or more amines located in their hydrophilic heads (Balazs and Godbey, 2011). Cationic liposomes are one of the most commonly used non-viral vectors for gene delivery since their first introduction in 1987 by Felgner. (Felgner *et al.*, 1987; Morille *et al.*, 2008).

Cationic lipids that form cationic liposomes are classified into four groups (Figure 1.12) according to their structural characteristics (Morille *et al.*, 2008):

- Monovalent aliphatic lipids that contain single amino groups in their head group. N [1-(2, 3-dioleoyloxy) propyl]-N, N, N-trimethylammonium chloride (DOTMA) and 1, 2-dioleyl-3-trimethylammonium-propane (DOTAP) are examples of this group.
- Multivalent aliphatic lipids which contain several amine functions in their polar head group such as dioctadecylamidoglycylspermine (DOGS).
- Cationic cholesterol derivatives, such as 3β [N-(N',N'-dimethylaminoethane)-carbamoyl] cholesterol DC-Chol, bis-guanidinium-tren-cholesterol (BGTC).
- Neutral helper lipid such as dioleoylphosphatidylethanolamine (DOPE). Most liposomes used in gene therapy consist of both charged lipids and neutral helper lipids. Helper lipids are used to facilitate membrane fusion (Dass, 2002) and to improve transfection efficiency (Balazs & Godbey, 2011).

In cationic lipid-mediated gene delivery, DNA is surrounded by the cationic lipids in order to protect it from degradation and to facilitate its entry into the targeted cell. This interaction between DNA and the surface of liposomes forms cationic lipid-DNA-complexes known as lipoplex (Dass, 2002). As a result of the positive charge of the cationic lipids in lipoplexes, they interact with the cell membrane by the endocytosis of the lipoplex and the DNA is released into the cell (Gebhart and Kabanov, 2001).

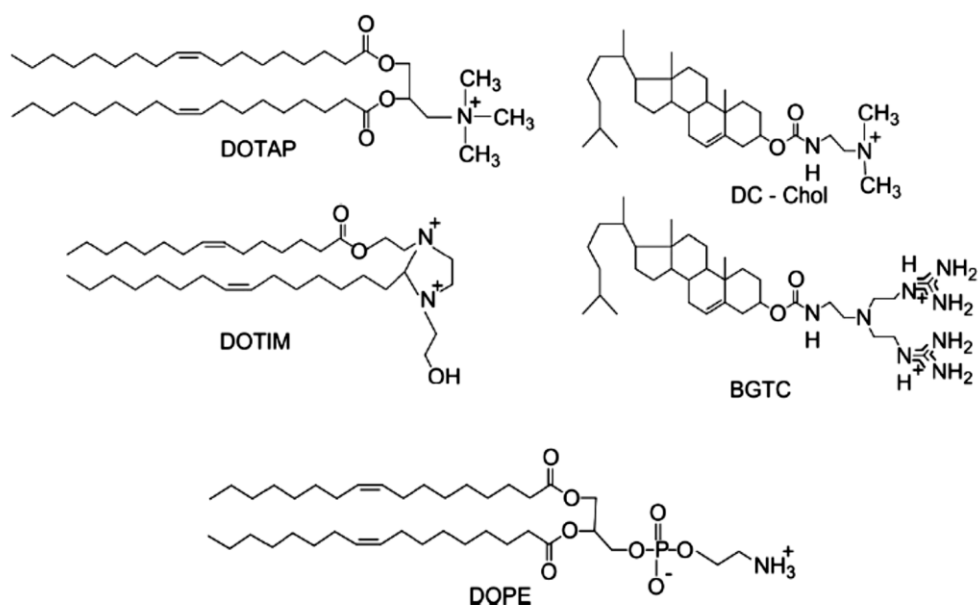


Figure 1.12: Structure of cationic lipids and the helper lipid DOPE used in gene therapy (Adapted from Morille *et al.*, 2008).

Several disadvantages of using cationic liposomes in gene delivery have been reported over the past 25 years. These include the changes in cell nature such as cell shrinking, reduced number of mitoses and vacuolisation (Dass, 2002). Cytotoxicity of cationic lipids has been reported in numerous *in vitro* and *in vivo* studies. Low transfection efficiencies has also been reported due to the heterogeneity and instability of cationic lipoplexes (Saraswat *et al.*, 2009).

As alternatives to cationic lipids, anionic lipids for DNA delivery have been used. In general, anionic lipids are not as efficient as cationic lipids due to the poor interactions between DNA molecules and anionic lipids as both are negatively charged.

However, liposomes present some advantages compared to other gene delivery vectors in that they are simple and quick to formulate, not as toxic as

viral vectors, commercially available and are easily adapted for specific applications (Dass, 2002).

1.3.3.2. Polymersomes

Another type of non-viral gene delivery vector is polymersomes. They are nano-sized vesicles that encapsulate therapeutic agents. Polymersomes are formed from amphiphilic blocks of copolymer bilayers, hydrophobic and hydrophilic (Christian *et al.*, 2009). The hydrophobic layer encapsulates the aqueous core and the hydrophilic layer forms a surrounding corona. A group of targeting moieties, such as antibodies, transferrin, folate or sugar (Saraswat *et al.*, 2009), is conjugated to the exterior surface of polymersomes for a specific cell targeting (Discher and Ahmed, 2006).

The amphiphilic bilayer of polymersomes makes them able to encapsulate both hydrophilic and hydrophobic molecules (Levine *et al.*, 2008).

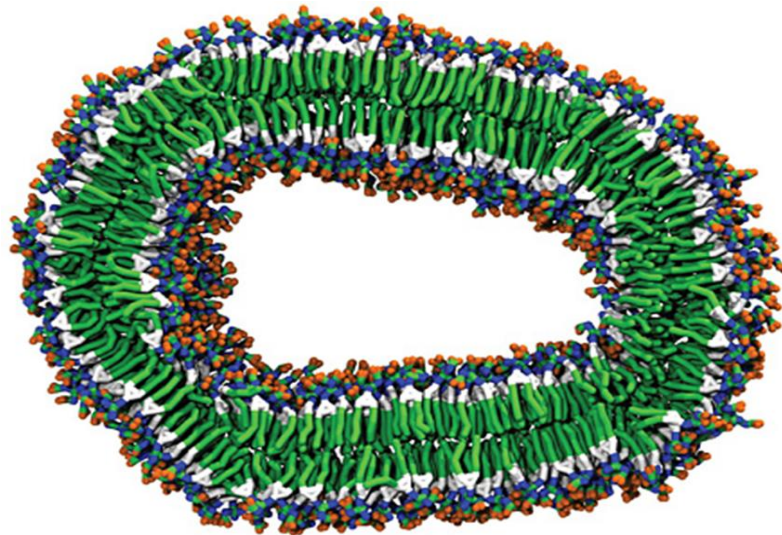


Figure 1.13: Structure of polymersomes (Adapted from Borman, 2010).

Polymers are classified into two groups:

- Synthetic polymeric delivery systems where most of these systems aim to generate cationic polymers that interact easily and efficiently with anionic DNA forming polymer-DNA complexes known as polyplexes. The commonly used synthetic polymers include polyethylenimine (PEI), poly-L-lysine (PLL) and polyethylene glycol (PEG).
- Natural polymers such as cyclodextrin, chitosan, collagen, gelatin and alginate. This group has a non-toxic effect at both low and high concentration.

PEI structures consist of two carbons atoms and one nitrogen atom. There are different forms of PEI based on the degree of branching and their molecular mass such as linear and branched PEI (Figure 1.14). The structure of PEI consists of two carbons atoms and one nitrogen (Boussif *et al.*, 1995).

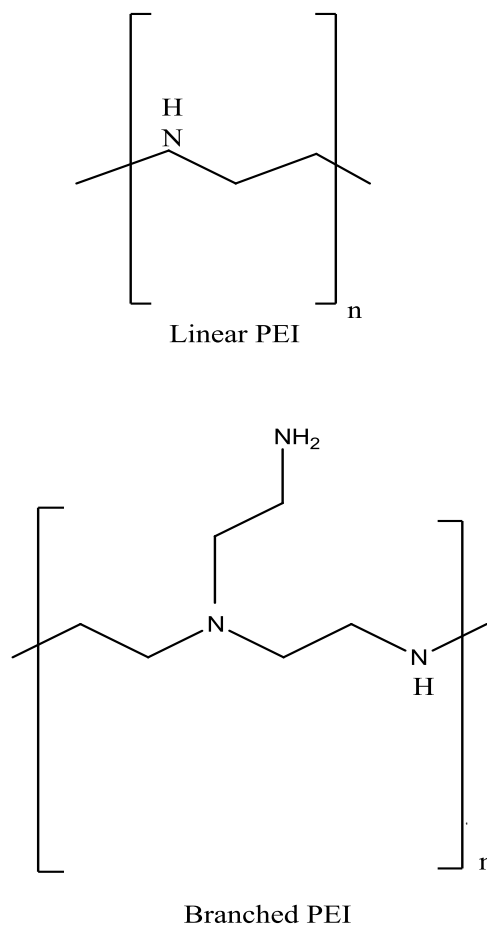


Figure 1.14: Linear and branched PEI.

The highly branched PEI has an excellent buffering capacity that provides an efficient release of DNA from the endosomes. In PEI-DNA the degree of toxicity and stability depends on the PEI-DNA ratio. Different ligands such as transferrin and antibodies are used in PEI-DNA complexes to increase specific cell-targeting (Goverdhana *et al.*, 2005).

In contrast to liposomes, gene delivery using polymer vesicles has several advantages, including their relative safety, low toxicity and immunogenicity, ease of formulation and administration, lack of DNA size

restriction (Park *et al.*, 2006; Scheller and Krebsbach., 2009). In addition, their bilayer characteristics such as thickness and chemical composition provide an enhanced mechanical stability and flexibility (Pata & Dan, 2003).

1.3.3.3. Dendrisomes

Dendrisomes are small vesicles of self-assembled cationic branched poly-lysine dendrons with a lipophilic core. The Transmission Electron Micrograph (TEM) images (Figure 1.15) showed that the polylysine head groups of dendrisomes form a membrane of 6 to 10 nm thick compared to liposomal membrane where the thickness is around 5 nm (Sakthivel & Florence, 2003). Dendrisomes are formed with or without cholesterol. Cholesterol has an effect on the morphology and size of dendrisomes but has no effect on their charge (Al-Jamal, 2005). The size of dendrisomes with cholesterol increases according to the cholesterol content while cholesterol-free dendrisomes are smaller in contrast.

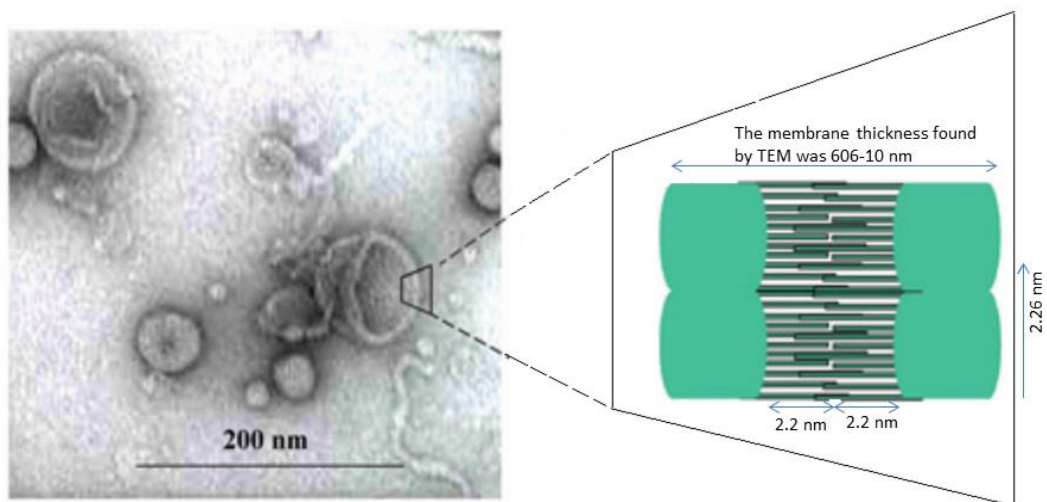


Figure 1.15: Transmission Electron Micrograph of dendrisomes with membranes from 6 to 10 nm thick (Adapted from Al-Jamal *et al.*, 2003).

1.3.3.4. Dendrimers

Dendrimers are highly branched, three dimensional polymerized macromolecules introduced by Donald A. Tomalia in the mid-1980s. Since their introduction, they have been increasingly used in several applications ranging from drug and gene delivery to processing, diagnostics and nanoengineering. Structurally, dendrimers are synthesised from a central core molecule and a number of highly branched arms forming a tree-like structure. The central molecule can be any molecule and the branches are constructed from any bi-functional molecules. Molecules forming the end group of the branches are modified chemically in order to be charged, hydrophilic or hydrophobic surfaces (Figure 1.16) (Sakthivel & Florence, 2003; Dufès *et al.*, 2005; Goindi & Maheshwari, 2009).

Dendrimers can be built in a repetitive sequence of reaction steps either in divergent synthesis starting from the core molecule to the periphery, or in a convergent synthesis from the outermost peripheral molecules to the core. Each completed sequence of reaction steps leads to a higher dendrimer generation. The size of dendrimers is described by the number of its generation (Figure 1.16).

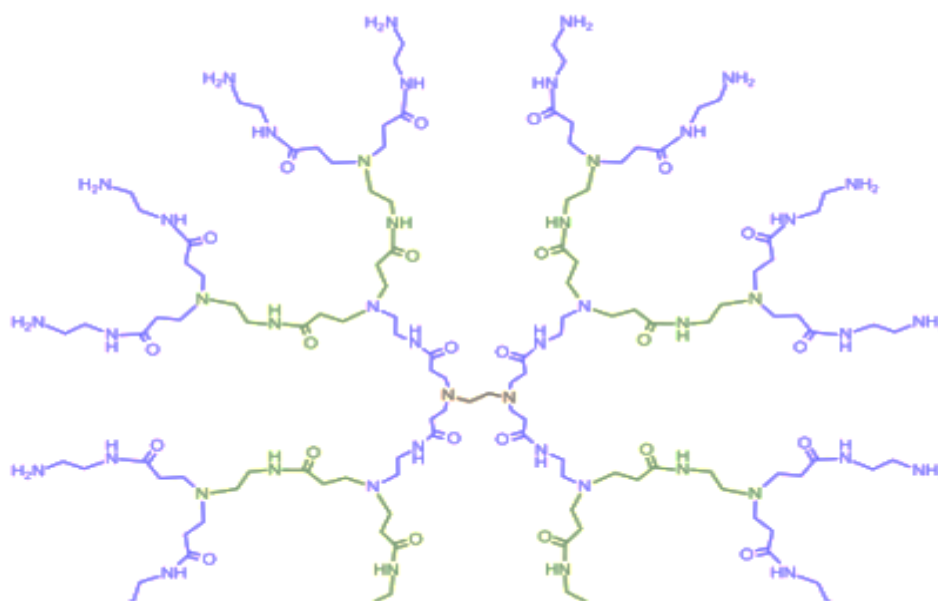


Figure 1.16: Dendrimer structure (Adapted from Brix, 2013).

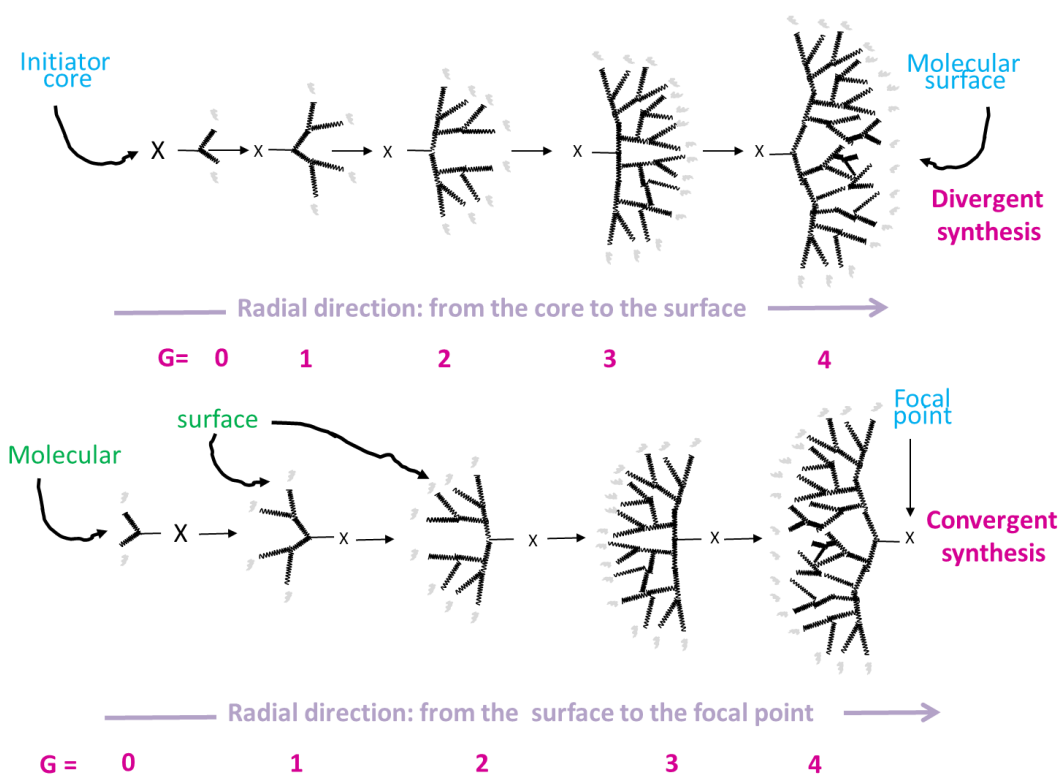


Figure 1.17: Divergent and convergent growth (Adapted from Mukeshgohel, 2009).

Two dendrimers are commercially available, polyamidoamine (PAMAM dendrimers) and polypropylenimine (PPI dendrimers). PAMAM dendrimers are based on ethylenediamine or ammonia for the core molecule with four and three branching points, respectively (Figure 1.17). PPI dendrimers can have diaminobutyric acid (DAB) as the core molecule. The repetitive sequence consists of the addition of acrylonitrile to a primary amino group followed by hydrogenation of nitrile groups to primary amino groups (Dufès *et al.*, 2005 ; Goindi & Maheshwari., 2009).

Different forms of dendrimers can be made by the process of engineering dendrimers and partial dendrimers (dendrimers without central

core) (Al-Jamal *et al.*, 2003; Al-Jamal *et al.*, 2005) which is made by controlling and altering the branching units, generation number and surface functionalities (Al-Jamal *et al.*, 2003) to be used in various applications. These forms include dendrisomes, dendriplexes and dendrimer aggregates (Goindi & Maheshwari, 2009).

- ***Dendriplexes***

Cationic dendrons and dendrimers are used as non-viral vectors for gene delivery as they are able to form complexes with DNA. Dendriplex is a dendrimer-DNA complex. *In vivo* applications show the ability of dendrimer complexes to protect the DNA from degradation by enzymes found in the serum. The performance of using these complexes as vectors for gene delivery depends on the physiochemical and colloidal properties of the complexes (Sakthivel and Florence, 2003).

1.3.4. Targeting Methods

Numerous delivery systems have been designed for entry into the cell by passive or active tumour targeting strategies.

1.3.4.1. Passive Tumour targeting

The normal blood vessels have well organized and functional structures, while the tumour blood vessels show heterogeneous and tortuous structures (Folkman 2007; Kang *et al.*, 2010). Researchers have demonstrated that the abnormal morphology includes large openings and fenestrations in the

vasculature network, lack of constant flow and pericytes, and dilated capillaries (Cassidy & Schätzlein, 2004; Alexis *et al.*, 2008; Maeda *et al.*, 2009). These defective vascular structures are likely to be the result of the rapid vascularisation to provide oxygen and nutrients for cancer cell growth and decrease lymphatic drainage, leading to cancer growth. Consequently, anti-tumour drugs can pass through tumour blood vessels and leading to accumulation in tumour cells, but not in normal tissue (Figure 1.18).

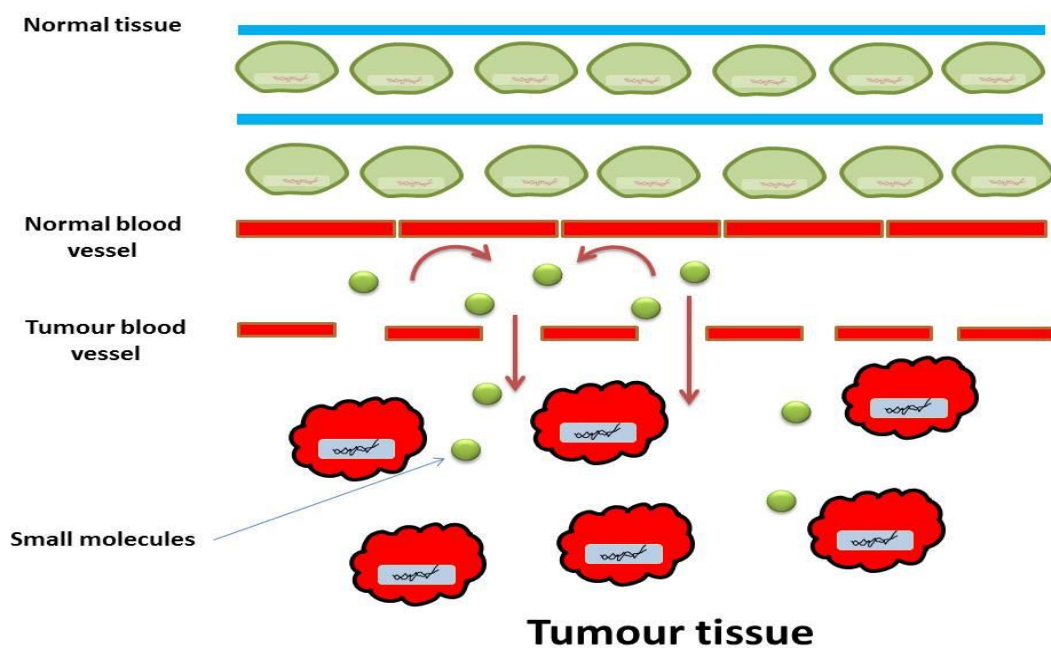


Figure 1.18: Passive tumour targeting method.

Matsumura and Maeda (1986) identified passive targeting phenomenon which called the “enhanced permeation and retention (EPR) effect”. Since this, several studies have shown that the EPR effect result in passive accumulation of macromolecules and nanosized particulates (liposomes, polymeric micelles, polymeric conjugates and dendrimers) in solid tumour tissues with the

resulting increase of the therapeutic index while decreasing side effects (Park *et al.*, 2008). According to Mislick and Baldeschwieler (1996), most of polyplexes have gained transport into cells by charge-mediated interactions with proteoglycans that are present on the cell surface.

Recently, cell penetrating peptides (CPPs) have been widely investigated for ability to allow membrane translocation. These peptides originally from viral proteins, are 5-40 amino acids in length, amphipathic in nature and positively charged. A number of CPPs used as DNA-binding and cell-penetrating components via the virtue of their overall positive charge (Rittner *et al.*, 2002; Ignatovich *et al.*, 2003; Rudolph *et al.*, 2003). The exact mechanism of CPPs is unclear but it is hypothesized that their uptake into cells is by one of the following mechanisms: formation of pores in cytoplasm, direct penetration or transient uptake by formation of micellar complexes as shown in Figure 1.19 (El-Andaloussi *et al.*, 2005).

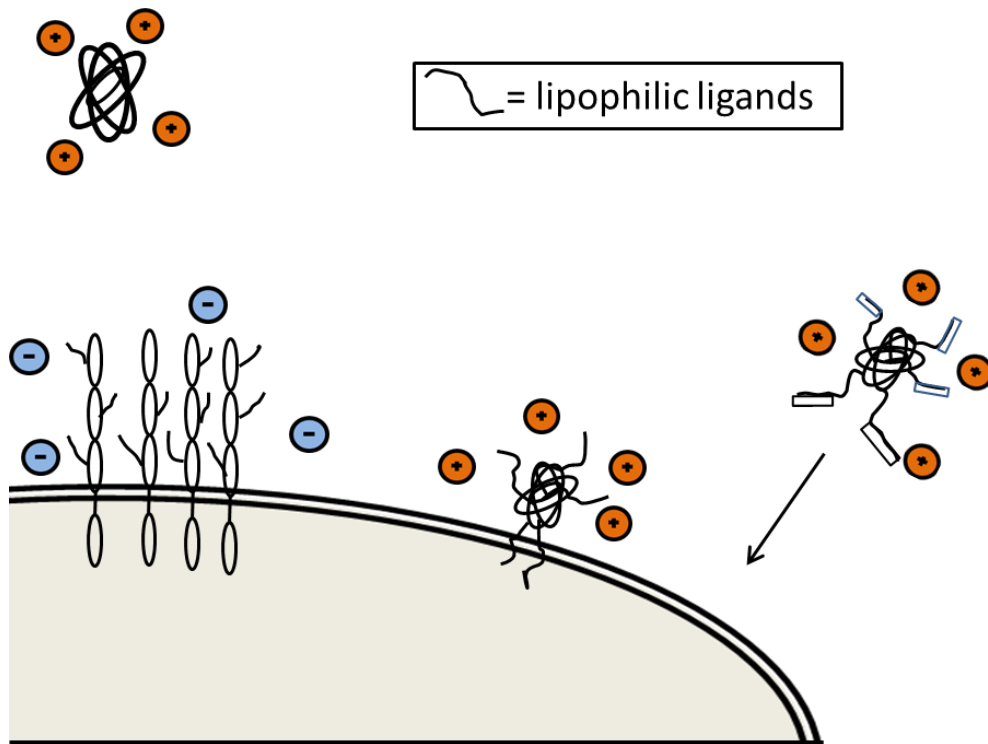


Figure 1.19: Cellular non-specific uptake strategies (Adapted from El-Andalousi *et al.*, 2005).

1.3.4.2. Active Tumour targeting

Cancer cells are characterized by an overexpression of cell surface proteins that are present in normal cells at low levels. Rapidly expanding necrotic mass of tumour requires an increase in supply of nutrients and therefore needs overexpression of receptors facilitating the uptake of these nutrients.

All intracellular signals and hyperactive receptors can become targets for tumour specific gene delivery. Active targeting is achieved by chemically pairing a targeting moiety which specifically interacts with receptors overexpressed on the target tissue. This process led to the accumulation of

therapeutics in targeted cells, organs and tissues as shown in Figure 1.20 (Park *et al.*, 2008).

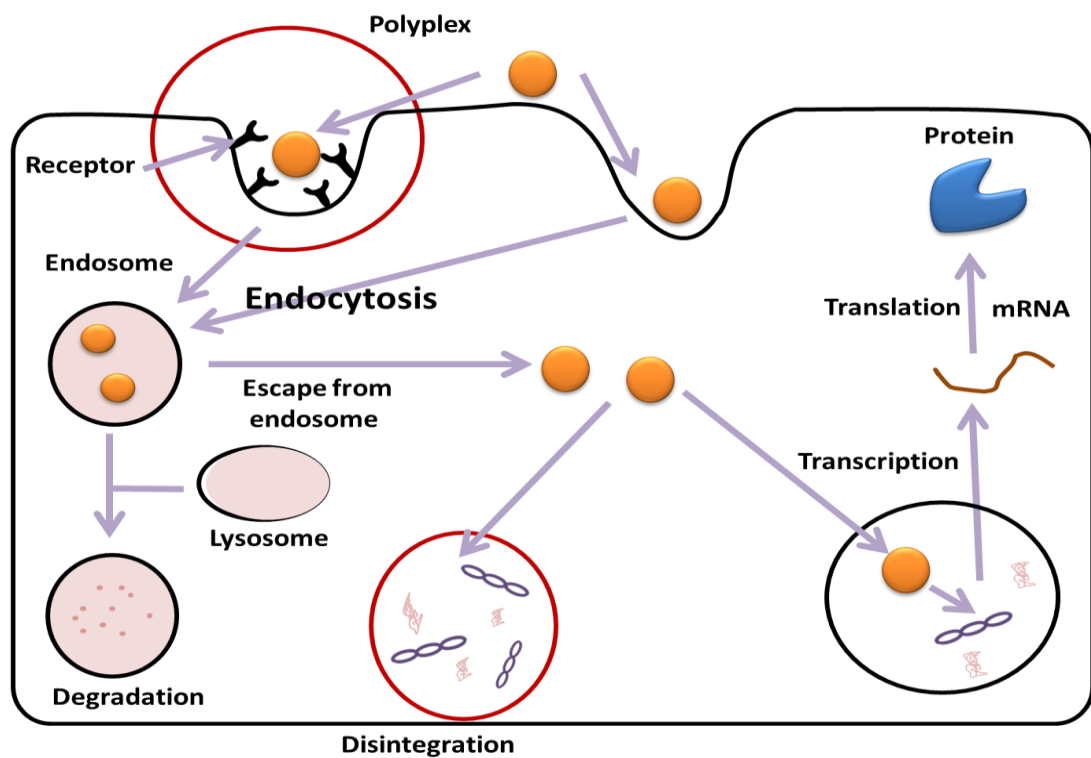


Figure 1.20: Active tumour targeting method (Adapted from Park *et al.*, 2008).

Targeted delivery systems carrying DNA are taken up by the cells via receptor-mediated endocytosis, mostly in the form of endocytic vesicles. The receptor and the carrier-ligand complex are then separated due to the influence of low pH environment of the endosome.

Delivery systems recognizing overexpressed receptors show reduced cytotoxicity to normal cells with high tumour affinity and increase in therapeutic effect. On the other hand, the efficiency of the delivery system can rely on several factors, for example the activated receptors concentration in the

tumour cells, the attraction of the attached ligands to each receptor and the pH (Khalil *et al.*, 2006; Bareford and Swan, 2007; Kang *et al.*, 2010).

Several ligands have been studied in cancer therapy for active targeting to tumour, for example transferrin (Kircheis *et al.*, 2001; Dufès *et al.*, 2004b; Yang *et al.*, 2009, Koppu *et al.*, 2010), glucose transporter (GLUT-1) (Dufès *et al.*, 2004a), epidermal growth factor (Park *et al.*, 2008), integrin receptors (Aina *et al.*, 2007; Merkel *et al.*, 2009) and folate receptors (Kim *et al.*, 2007; Low *et al.*, 2008). The role of these ligands is to effectively deliver DNA into the nucleus of cells. This method is mostly limited by barriers that exist between the administration site and the nucleus of the tumour target cells.

- ***Transferrin***

Transferrin (Tf) has been extensively studied by many researchers for more than 20 years. It is a targeting molecule for the transport of the drug and gene delivery systems as it is non-toxic and non-immunogenic to the cancer cells (Qian *et al.*, 2002).

Tf is a member of a family of ubiquitous iron-binding glycoproteins which includes melanotransferrin, ovotransferrin and lactoferrin. Iron is required for most of various biological processes, for example DNA synthesis, electron transfer and oxygen transport. As the presence of free iron in the circulation can be toxic to cells, the main function of Tf is to control the levels of free iron in biological fluids by the binding and transport of iron into cells via interactions with its receptors. Tf contains around 700 amino acids and has a

large molecular mass of approximately 80 kDa. The polypeptide chain is divided into two structurally similar lobes: N- and C- lobes connected by a small linear peptide like each lobe is capable to bind one iron atom. Therefore, each iron-free Tf molecule (apo-Tf) can transfer one iron atom and in this case it is called monoferric Tf. If both lobes of Tf molecule are bound to an iron atom, it is called diferric Tf. The association constant with Tf receptor (TfR) for diferric Tf is 30-fold higher than monoferric Tf and 500-fold higher than apo-Tf, which makes it the choice as a TfR ligand in targeting studies. Diferric Tf forms approximately 10—30% of circulating Tf, making other Tf to bind with other metal ions such as copper, gallium, zinc, manganese and aluminium ions (Daniels *et al.*, 2006).

The delivery and uptake of iron from Tf to the cells is done through TfR, which is a carrier protein involved in iron uptake and the regulation of cell growth. The uptake of iron into the cells is done by internalizing the transferrin-iron complex through receptor-mediated endocytosis of the cells. In the delivery process, Tf binds at least to two types of TfRs: Transferrin receptor I (TfRI) and Transferrin receptor II (TfRII). Both types are of type II transmembrane homodyne and have a similar amino acid sequence. They also contain two identical monomers which are bound by two disulfide bonds. However, in TfRII the affinity for Tf is lower than TfR1 by around 25 -fold (Qian *et al.*, 2002) . In addition, TfRII is expressed as two transcripts: the full-length (α -TfR2) and the shorter form (β -TfR2). Its α -transcript is largely expressed on liver cells, while its β -transcript is expressed at low levels on a variety of cell

types. In contrast, TfR1 is expressed on various cells, including red blood cells, erythroid cells, hepatocytes, monocytes and the blood–brain barrier. Therefore, it is an efficient target for Tf-mediated drug and gene delivery to the brain or cancer cells. TfRs are normally expressed at low levels on normal cells. These expression levels depend on the proliferation rate of the cells. In non- or low-dividing cells, TfR expressed at an extremely low level, while rapidly proliferating cells such as carcinoma cells have a high levels of TfR expression, which can be up to 100 000 TfRs per cell (Gomme *et al.*, α 2005) .

- ***Transferrin-targeted gene delivery system in cancer***

The possibility of using genes as medicines to treat patients suffering from cancer is hampered by the lack of safe carrier systems able to specifically deliver the therapeutic nucleic acids to the tumours after intravenous administration. There is therefore an urgent need to develop efficacious gene-delivery systems that should be target-specific, nontoxic, non-inflammatory, biodegradable and non-immunogenic. Among all the delivery systems currently being developed, non-viral delivery systems appear most suited to fulfill these requirements. Moreover, they have the advantages of being easy to prepare, flexible regarding the size of nucleic acid to be carried and suitable for repeated administrations as they are much safer than viral vectors (Elsabahy *et al.*, 2011). TfR-mediated gene delivery using these vectors is a promising strategy since it provides an opportunity to achieve specific gene delivery to tumours while increasing the transfection efficiency in cancer cells.

TfR-targeted liposomes

Cationic liposomes complexed with DNA have been used extensively for the delivery of nucleic acids to cancer cells *in vitro* and *in vivo*. The negatively charged DNA can be complexed to the positively charged liposomes by electrostatic interactions to form lipoplexes. The intravenous injection of a Tf-bearing lipoplex encoding for the tumour-suppressor protein p53 resulted in high level of *p53* gene expression in tumours, contrarily to that observed with non-targeted lipoplexes, in mice bearing subcutaneous DU145 human prostate tumours (Xu *et al.*, 2002) . In combination with radiotherapy, the TfR-targeting lipoplex encoding p53 exhibited complete tumour regression without recurrence 6 months after treatment.

TfR-targeted cyclodextrins

Cyclodextrins are a family of cyclic macromolecules consisting of 6–8 glucopyranoside units bound together by glycosidic bonds to form a ring. They are characterized by their toroidal molecular structure with hydrophilic outer surface. As a result, cyclodextrins are soluble in their aqueous environment while being able to host small hydrophobic drugs in their internal cavity to form inclusion complexes (Wenz *et al.*, 2006).

Cyclodextrins containing polycations have demonstrated efficacy in transporting nucleic acids such as plasmid DNA and siRNA. A TfR-targeting PEGylated imidazole-modified cyclodextrin was mixed with the siRNA targeting the EWS-FLI1 fusion protein known to be a transcription factor involved in

tumorigenesis. Intravenous administration of this system in mice decreased gene expression of EWS-FLI1 in tumours and decreased the growth of tumours with short-term effect (Hu-Lieskovan *et al.*, 2005).

TfR-targeted micelles

TfR-targeting micelles have demonstrated efficacy to deliver nucleic acids to tumours intravenously. Micelles made of a copolymer of PEG–poly(ethylenimine) biotin were associated to biotinylated Tf by avidin/biotin noncovalent binding (Vinogradov *et al.*, 1999). This micellar formulation was demonstrated to enhance the tumour delivery of antisense oligonucleotides against the human multidrug resistance protein-1 (which plays a role in multidrug resistance) in MCF-7ADR human breast carcinoma as well as in KBV human oral epidermoid carcinoma (Vinogradov *et al.*, 1999).

TfR-targeted polymers & dendrimers

Many Tf-bearing polycationic polymers have been used to condense negatively charged DNA and to deliver it to cancer cells. Among them, polylysine and polyethylenimine (PEI) have been widely used for this purpose and both were found to be very efficient vectors for gene transfer to cancer cells. In the K-562 human erythroleukemic cell line, most of the cell population was found to express the transfected reporter genes following intravenous treatment with the Tf-bearing polylysine polyplex (Cotton *et al.*, 1993). Similarly, Tf-bearing PEI was used to deliver a plasmid DNA encoding for TNF α , a cytokine with promising anticancer properties but also non-specific toxicity limiting its

potential use. Systemic treatment of mice bearing either subcutaneous Neuro2a neuroblastoma, MethA fibrosarcoma or M-3-melanoma cells with this targeted formulation resulted in anti-tumour effects on the three tumour models, with complete regression of MethA tumours (Kircheis *et al.*, 2002; Kursa *et al.*, 2003). The treatment was well tolerated by the animal.

In addition to their role as drug carriers, dendrimers have also been investigated as potential vehicles for nucleic acids. PAMAM dendrimer coated with PEG was targeted to TfR by conjugation with the peptide T7. It was able to co-deliver the drug doxorubicin together with a therapeutic plasmid encoding TNF-related apoptosis-inducing ligand (Han *et al.*, 2011). A synergistic efficacy was observed between the two therapeutic agents following intravenous administration on mice bearing subcutaneous Bel-7402 human hepatoma tumours. The TfR-targeting system inhibited 77% of tumour growth, which was much higher than that obtained with non-targeted dendriplex or the free drug. The inhibition was also achieved using a smaller dose (Han *et al.*, 2011).

Recent research has also demonstrated that an intravenously administered generation 3-diaminobutyric polypolypropylenimine dendrimer conjugated to Tf by crosslinking and complexed to plasmid DNA encoding TNF α led to complete disappearance of 90% of A431 human epidermoid carcinoma tumours, compared with the 40% complete tumour regression observed with the non-targeted dendriplex (Koppu *et al.*, 2010).

In another study, this targeted dendrimer was used to assess the therapeutic potential of p73, a member of the p53 family of transcription factors. The study demonstrated that the intravenous administration of Tf-bearing, p73-encoding 3-diaminobutyric polypropylenimine dendrimer dendriplex led to a sustained inhibition of tumour growth and complete tumour suppression for 10% of A431 and B16-F10 tumours in mice (Lemarié *et al.*, 2012) . The treatments with both dendriplexes were well tolerated by the animals.

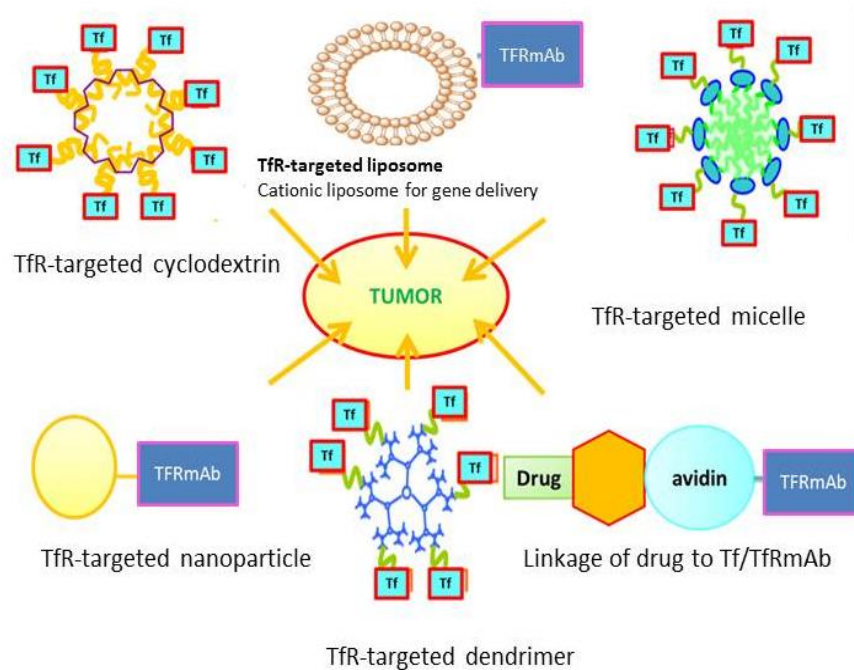


Figure 1.21: Formulation strategies used for the delivery of drugs and nucleic acids to the tumour. (Adapted from Dufès *et al.*, 2013).

- ***Lactoferrin***

Lactoferrin (Lf) and lactoferricin (Lfc) are other promising targeting ligands of transferrin family. They are iron-binding proteins able to bind the transferrin receptors. In addition to their tumour delivery properties, these iron-carriers have recently been shown to have intrinsic anti-tumour activity, which recently make them highly attractive moieties as gene medicine.

Lactoferrin (Lf) is a glycoprotein with a molecular weight of about 80 kDa, which shows high affinity for iron. In 1939, lactoferrin was isolated from bovine milk (Adlerova *et al.*, 2008). It was identified to be the main iron-binding protein in human milk in 1960 (Tomita *et al.*, 2008; Adlerova *et al.*, 2008).

Lf is produced by mucosal epithelial cell in various mammalian species, including humans. Studies have shown that Lf is also produced by fish. The Lf function is to transport iron in blood serum and it is involved in various physiological function, such as regulation of iron absorption in the bowel, immune response, anti-carcinogenic, anti-inflammatory, antioxidant and antimicrobial.

There are three different isoforms of lactoferrin: Lactoferrin- α is the iron binding form, but have no ribonuclease activity; lactoferrin- β and lactoferrin- γ demonstrate ribonuclease activity but they are not able to bind iron (Furmanski *et al.*, 1989).

Lf consists of a single polypeptide chain containing 703 amino acids folded into two globular lobes called C – (carboxy) and N – (amino) terminal regions. Each lobe consists of two domains known as C1, C2, N1 and N2 respectively. These domains are capable of binding one iron atom in each lobe. Thus, lactoferrin molecule is capable of binding two ferric ions Fe^{3+} and one carbonate ion. This iron binding capability of lactoferrin is two times higher than that of transferrin (Adlerova *et al.*, 2008). However, it has been shown that at pH value of 4, lactoferrin was found to be saturated in 2-2.5% (Majka *et al.*, 2013). There are three forms of lactoferrin based on its iron saturation: apo-lactoferrin (iron free), monoferric lactoferrin (one ferric ion) and holo-lactoferrin (two ferric ions).

In addition to binding and transport of iron, lactoferrin is also capable of binding other macromolecules. These include other milk proteins such as albumin, lysozyme and f1-lactoglobulin. It also can bind other metal ions such as Al^{3+} , Ga^{3+} , Mn^{3+} , Co^{3+} , Cu^{2+} , and Zn^{2+} . Besides this, one of the most important properties of lactoferrin is its ability to bind with nucleic acid (Sanchez *et al.*, 1992; Adlerova *et al.*, 2008).

Lactoferrin has the ability to inhibit the production of many cancer cell lines, including nasopharyngeal carcinoma, head and neck cancer cell lines and breast carcinoma through induction of cell cycle arrest and modulation of the mitogen-activated protein kinase (MAPK) signalling pathway *in vitro*.

Like Lf, Lfc has anti-tumour effects against a number of cancer cell lines including colon and ovarian carcinoma, neuroblastoma and melanoma. Lfc has also been reported to exert potent *in vivo* anti-tumour activity in mouse models of cancer (Zhou *et al.*, 2008).

Lactoferricin (Lfc) has received much attention recently due to its broad host defence properties. It can be released from the multifunctional protein Lf through proteolysis by pepsin under acidic conditions (Gifford *et al.*, 2005). The two most-studied Lfc are those derived from bovine (LfcB) and human Lf (LfcH). The primary structure of LfcB is well established as a 25-residue peptide that forms into a looped structure through an intramolecular disulfide bond. However, LfcH consists of the N-terminal 49 residues in a single continuous chain (Gifford *et al.*, 2005). (Figure 1.22)

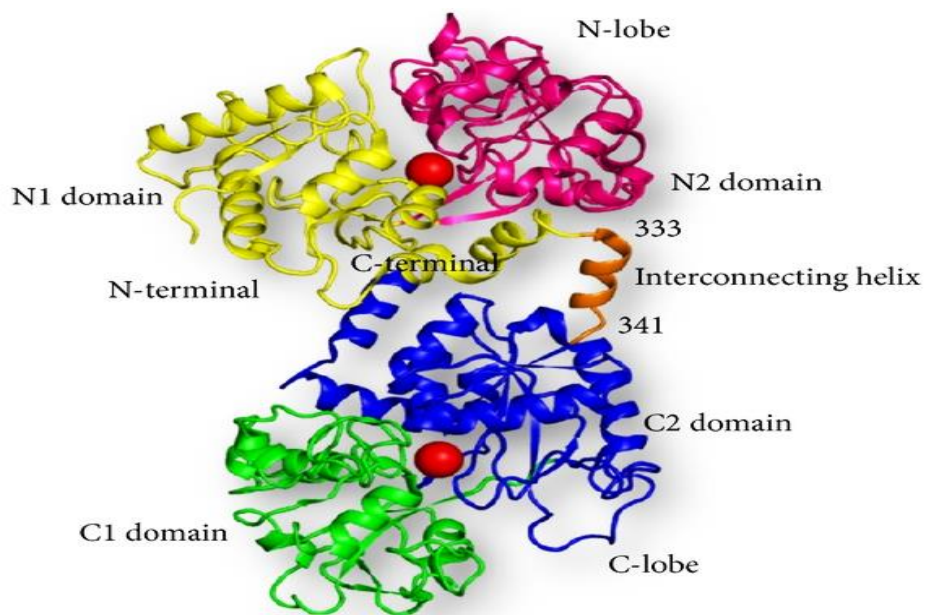


Figure 1.22: Schematic diagram of the bovine lactoferrin molecule. The N1 and N2 domains are colored in yellow and pink, respectively, while the C1 and C2 domains are colored in green and

blue, respectively. The interconnecting helix between the lobes is colored in orange. The two iron atoms are shown as red spheres. (Adapted from Sharma *et al.*, 2013).

1.4. Aims and Objectives

Improvements in the treatment for prostate cancer are critically needed in order to overcome metastasis and lethal recurrence. Intravenously administered gene therapy would be an attractive anticancer treatment strategy. However, the lack of suitable carrier system able to selectively deliver therapeutic gene to tumours has so far limited this investigation. Given that transferrin receptors are overexpressed on prostate cancer cells, the aim of this research project is to investigate if novel transferrin-targeted DAB dendrimers complexed with various therapeutic DNA improve the therapeutic efficacy on prostate cancer cells *in vitro* and on xenograft models after intravenous administration. Specifically, the key objectives are to evaluate the efficacy of DAB-Tf, DAB-Lf and DAB-Lfc dendriplexes in tumour targeting and gene transfection on different prostate cancer cell lines *in vitro* and experimental tumour-bearing models.

CHAPTER 2.

GENERAL MATERIALS AND METHODS

2.1. Material

Suppliers Materials	Suppliers
A431 human epidermoid carcinoma	European Collection of Cell Cultures (Salisbury, UK).
AgarGel H/M agarose	Continental Laboratory Products (Northampton, UK)
Bioware® B16-F10-luc-G5 mouse melanoma	Calliper Life Sciences (Hopkinton, MA)
DDAO-Galactoside	Invitrogen (UK)
Dimethylsuberimidate	Sigma Aldrich, (Poole, UK).
DU145 prostate cancer cell lines	European and American Collection of Cell Cultures , Salisbury, UK
Endotoxin-free Giga Prep Plasmid purification Kit	Qiagen, Hilden, Germany
Expression plasmid encoding β -galactosidase (pCMVsport β -galactosidase)	Invitrogen (Paisley, UK)

Suppliers Materials	Suppliers
Expression plasmid encoding Tumour necrosis factor (TNF) α (pORF9-mTNF α)	InvivoGen (San Diego, CA)
Generation 3- Diaminobutyric polypropylenimine dendrimer (DAB)	Sigma Aldrich (Poole, UK).
HyperLadder	Bioline (London, UK).
Label IT [®] Cy3 Nucleic Acid Labelling kit	Cambridge Biosciences, Cambridge, UK
Lactoferrin and lactoferricin	Sigma Aldrich (Poole, UK).
LNCaP prostate cancer cell lines	European and American Collection of Cell Cultures , Salisbury, UK
Passive lysis buffer	Promega (Southampton, UK).
PC3 prostate cancer cell lines	European and American Collection of Cell Cultures , Salisbury, UK
pORF9-mTNF α plasmid DNA	InvivoGen (San Diego, CA)
Quanti-iT [™] PicoGreen [®] dsDNA reagent	Invitrogen (Paisley, UK).
T98G human glioblastoma	European Collection of Cell Cultures (Salisbury, UK).
Tissue culture media	Invitrogen (Paisley, UK).
Transferrin	Sigma Aldrich (Poole, UK)

Suppliers Materials	Suppliers
Vectashield® mounting medium with DAPI	Vector Laboratories (Peterborough, UK)

2.1.1. Cell lines

2.1.1.1. PC3

This human prostate carcinoma cell line was established from the bone marrow metastasis isolated post-mortem from a 62-year-old Caucasian man with grade IV prostate cancer (poorly differentiated adenocarcinoma) (Kaighn *et al.*, 1979). These cells are epithelial-like and grow adherently in monolayers or in multilayer foci. PC-3 cells have the highest metastatic potential compared to DU145 cells which has a moderate metastatic potential and to LNCaP cells which has a low metastatic potential (Pulukuri *et al.*, 2005).

In addition, PC-3 cell lines do not express prostate-specific antigen (PSA) (Jarrard *et al.*, 1998) and are PSMA-negative (prostate-specific membrane antigen) (Ghosh *et al.*, 2005). These cell lines are also reported to be human androgen receptor (AR)-negative by examining the levels of specific 5 α -dihydrotestosterone binding sites present in the PC-3 cell lines. Scatchard analysis of these ligand binding data indicates that PC-3 cell lines express no detectable specific 5 α -dihydrotestosterone binding (Tilley *et al.*, 1990) However, other study have provided evidence that PC-3 cell lines express AR in

lower levels compared to other AR-positive cell lines such as LNCaP (Alimirah *et al.*, 2006)

In contrast, it was shown previously that PC-3 cell lines express significant levels of high affinity transferrin receptor TfR when assessed *in vivo* by performing Scatchard analysis following the administration of [¹²⁵I]-transferrin (Keer *et al.*, 1990). Moreover, a more recent study to examine the binding sites of Tf receptor on PC3, DU145, and LNCaP cells showed that PC-3 cells have a higher level of Tf receptor expression (Liu, 2000).

2.1.1.2. DU145

This cell line was established from tumour cells removed from a metastatic central nervous system lesion from a 69 year old male Caucasian man with prostate cancer in 1975 (Mickey *et al.*, 1977). The cells are epithelial-like, adherent and grow as monolayers. Like PC3, DU-145 cell lines do not express PSMA (Yao *et al.*, 2006) and express lower levels of the AR and PSA than the AR-positive LNCaP cells (Alimirah *et al.*, 2006) as their growth is inhibited by androgen withdrawal (Tai *et al.*, 2011). This cell line also expresses high levels of Tf receptors on their surface (Liu, 2000).

2.1.1.3. LNCaP

Cells are androgen-sensitive human prostate adenocarcinoma cells derived from the left supraclavicular lymph node metastasis from a 50-year-old Caucasian male in 1977. They are adherent epithelial cells growing in

aggregates and as single cells (Horoszwicz *et al.*, 1983). LNCaP cell lines are positive for PSA (Papsidero, *et al.*, 1981) and PSMA (Troyer *et al.*, 1997).

2.1.1.4. B16-F10-luc-G5

B16-F10-luc-G5 is a luciferase-expressing cell line that was derived from B16-F10 mouse melanoma cells by stable transfection of the North American Firefly Luciferase gene expressed from the SV40 promoter into B16-F10 Cells. This cell lines overexpress Tf receptors (Fu *et al.*, 2011).

2.1.1.5. A431

A431 is a human epidermoid carcinoma cell line obtained from an 85-year-old female patient. This cell line expresses high levels of transferrin receptors (Hopkins, 1983).

2.1.1.6. T98G

This cell line was derived from a human glioblastoma multiform tumour (Mercer *et al.*, 1990). Like B16-F10-luc-G5 and A431, T98G cell line overexpresses transferrin receptors (Dufès, 2011).

2.2. Methods

2.2.1. Nuclear Magnetic Resonance (NMR) spectroscopy

Nuclear Magnetic Resonance (NMR) is a technique used to elucidate chemical structures. It is efficient for providing detailed information about the dynamics, topology and a three-dimensional structure of molecules. The most commonly studied nucleus is proton (^1H) due to its highest sensitivity to NMR as protons are magnetically active and therefore detectable by NMR. The atomic nucleus employed for NMR spectroscopy in this work is ^1H (proton, 99.98% natural abundance) (Williams & Fleming, 1980; Akitt & Mann, 2000).

The methodology of ^1H -NMR involves the placement of a proton between the poles of an induced magnetic field (Figure 2.1). Many nuclei have spin and all nuclei are electrically charged. The spin (I) of a nucleus may either be integral (e.g. $I = 1, 2, 3 \dots$) or fractional (e.g. $I = 1/2, 3/2, 5/2 \dots$) or null ($I=0$), i.e. no spin at all. The case of no spin is considered to be the characteristic of a particular nucleus. As a consequence of the spin of the nucleus a magnetic field is generated around the nucleus. If an external magnetic field is applied, an energy transfer is possible between the base energy to a higher energy level (generally a single energy gap). The energy transfer takes place at a wavelength that corresponds to radio frequencies are irradiated on the sample nucleus which will undergo a change in its spin state due to energy (radio waves) being absorbed. While retaining the original spin, these nuclei emit energy of a particular wavelength at the same frequency which is received and processed

by a receiver coil in order to yield an NMR spectrum or map, which is called a ^1H -NMR spectrum, for the nucleus concerned (Figure 2.2) (Fessenden & Fessenden, 1990). The map is expressed as a plot of energy being absorbed against the delta values (δ). Delta values refer to the resonating position of an atom in a given spectrum expressed in units of frequency of the waves generated by the instrument ($1 \delta = 1$ part/million of the instrument's wave frequency). The zero value on the map represents the absorption of the standard compound tetramethylsilane (TMS) $[(\text{CH}_3)_4\text{Si}]$ and is used as reference point. After the absorption of a particular frequency, most of the protons present show a decrease in the δ value which is known as downfield shift. The difference between downfield shift and the original δ value creates the signals (Fessenden & Fessenden, 1990).

The case of the spin-1/2 nucleus

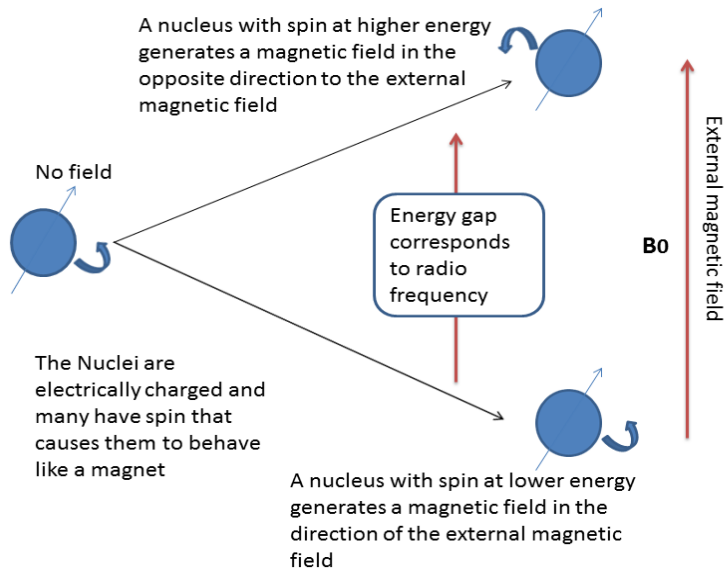


Figure 2.1: The basis of NMR (Adapted from Hoffman & Ozery, 2013)

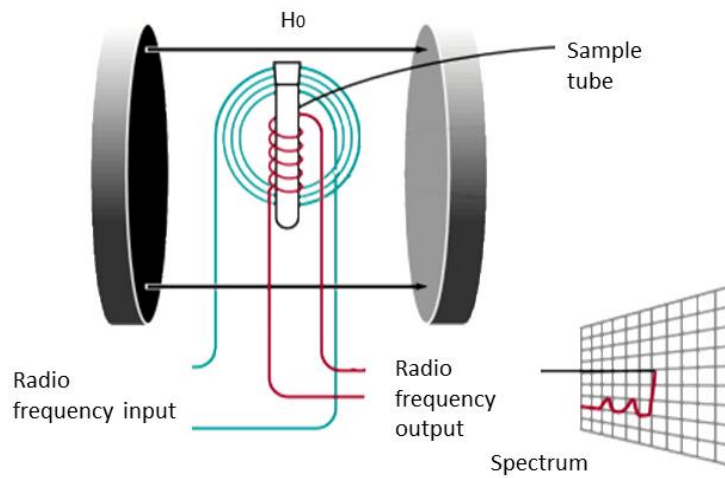


Figure 2.2: NMR Spectroscopy (Adapted from McGraw-Hill Education, 2013)

2.2.2. Plasmid Deoxyribonucleic acid (DNA) preparation

Plasmids are self-replicating circular pieces of DNA. They can carry and transfer a rich variety of genes including antibiotic resistance genes, which may be located on a section of DNA capable of transfer from one plasmid to another or to the genome (Hawkey, 1988). Plasmids have three common elements (Figure 2.3):

- An origin of replication (replicating autonomously within a living organism).
- A selectable marker gene (usually a gene encoding resistance to a particular antibiotic).
- A cloning site (a place for inserting foreign DNAs) (Feinbaum, 1998).

Plasmid preparation is a method used to isolate plasmid DNA from transformed bacteria. Since the 1970s, plasmids have been constructed using *Escherichia coli* (*E. coli*). Transformation of *E. coli* with a high copy number plasmid can produce hundreds of clones per bacterial cell. These can be readily separated out from chromosomal DNA, owing to their relatively small size (Feinbaum, 1998).

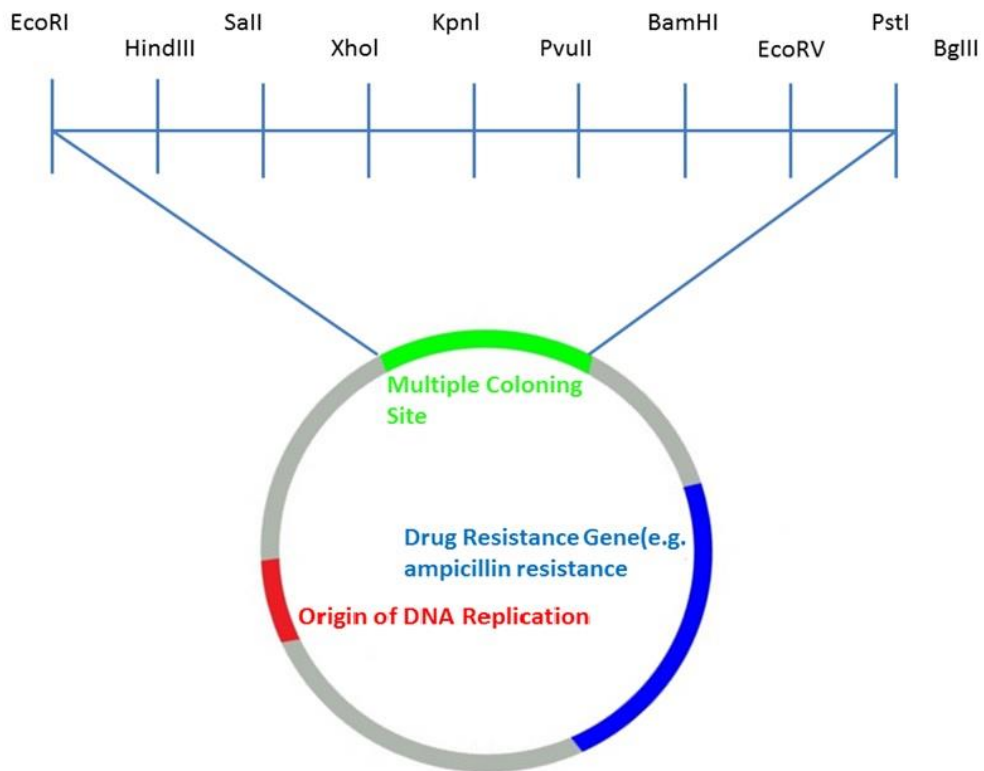


Figure 2.3: Plasmid DNA (Adapted from oregonstate.edu).

The process of plasmid preparation involves three steps:

- Growth of bacterial culture
- Harvesting and lysis of bacteria
- Purification of plasmid DNA.

The process of plasmid preparation and purification are performed according to the following procedure. Plasmid DNA encoding β -galactosidase (pCMV β -Gal) was grown in *Escherichia coli* (using 100 mg/mL ampicillin as selective antibiotic resistance gene) at 37° C in standard L-Broth (LB) medium.

The culture was then harvested by centrifugation for 20 minutes after incubation, achieving a density of $\sim 2 \times 10^9$ cells / mL (Wilfinger *et al.*, 1997).

The next step involves the extraction of plasmid DNA which is carried out by lysis. Cell lysis can be performed by exposing the cells to a chemical agent, usually ethylenediaminetetraacetate (EDTA) that affects the integrity of bacterial cell membranes. EDTA works by removing magnesium ions which are essential for the cellular envelope's structural integrity. It also inhibits the DNA degrading enzymes (DNAses) and also serves to stabilise the DNA phosphate backbone. Separately, alkaline lysis which consists of anionic detergent sodium dodecyl sulphate (SDS) and Sodium hydroxide (NaOH) is prepared and used. The high pH of the lysis mixture (pH 12) allows for denaturing both plasmid DNA and chromosomal DNA by breaking down hydrogen bonds of DNA molecule. Sodium dodecyl sulphate is used due to its ability to remove lipid molecules from the membrane and hence produce cell lysis. Upon bacterial cell lysis, a cell extract is produced which must be purified to remove the cellular components and collect the purified plasmid DNA.

The final step is the purification process of the plasmid DNA which was achieved by using a Qiagen endotoxin-free Giga Plasmid Kit according to the manufacturer's instructions. Plasmid DNA purification is carried out to remove RNA, proteins and other low molecular weight impurities as these components may cause fever and endotoxin shock syndrome. They may also sharply reduce cell transfection efficiency (Feinbaum, 1998). The purification of plasmid DNA

is based on the principle of anion-exchange column chromatography. In this method, the column employed contains a resin that has molecules with high density positive charges that bind with the DNA which carries a strong negative charge. To elute plasmid DNA, a high-salt buffer is used to destabilize the ionic interactions between the DNA and resin particles. Finally, the DNA is concentrated, desalted by ethanol precipitation and collected by centrifugation.

The amount of the purified plasmid DNA was measured by UV absorbance spectrophotometry using a GeneQuant RNA/DNA calculator at a wavelength of 320 nm. The A₂₆₀/ A₂₈₀ ratio is a reliable estimate of DNA purity with few limitations, and a value of 1.8-2.2 represents a high-quality DNA sample (Wilfinger *et al.*, 1997).

2.2.3. DNA complexation studies

DNA is a long negatively charged molecule. DNA diameter is about 2 nm (Marko, 1997) while the actual size of a DNA is about 3 meters in length (Campbell *et al.*, 1997). In gene delivery, DNA is condensed by vectors to form complexes that allow for a cellular uptake of the therapeutic gene. To condense DNA, such vectors usually rely upon electrostatic interactions between their positively charged cationic moieties, such as amino groups, and the highly negatively charged phosphate groups of DNA. This electrostatic interactions result in decreasing internal charge repulsions between phosphates charge within the DNA backbone and consequently DNA condensation (Labat-Moleur *et al.*, 1996).

The vector used in gene delivery has to be able to condense DNA in order to produce stable complexes with variable molecular properties (size and charge) to yield a more desirable biodistribution and cellular uptake that ultimately lead to a better gene expression (Singer *et al.*, 1997).

In addition to enhancing cellular uptake of the genetic material, condensation represents a process by which the genetic information is packaged and protected from degradation by the hostile environment of circulation (Gao and Huang, 1995).

In this study, both gel retardation and PicoGreen® assay studies were carried out to ensure that DAB-Tf, DAB-Lf and DAB-Lfc are capable of condensing DNA

2.2.3.1. Gel retardation assay

Gel retardation assay, also referred to as the Electrophoretic Mobility Shift Assay (EMSA), is a sensitive technique for studying protein-DNA/RNA interactions.

This procedure can evaluate the ability of a gene delivery system to condense DNA. In this study, gel retardation assay was used to evaluate DNA complexation with different vectors: DAB-Tf, DAB-Lf and DAB-Lfc. It is based on the principle that molecules of different sizes, molecular weights, and charges will have different electrophoretic mobility in agarose gel (a non-denaturing gel). In the case of vector-DNA complexes, the mobility of DNA-

binding vector is typically less than that of free DNA (Laniel *et al.*, 2001). In this assay, ethidium bromide, a planar aromatic fluorescent dye, is used as a DNA intercalator. When fluorescence molecules are exposed to light they may absorb the light and reflect a light of different colour; this process is known as fluorescence. Ethidium bromide binds with DNA and when exposed to ultraviolet light, a significant increase of the fluorescence intensity of the ethidium bromide is observed. When DNA condensation occurs in vector-DNA complexes, the ethidium bromide is excluded from binding to the DNA and a decrease of the fluorescence intensity of the ethidium bromide is observed (LePecq *et al.*, 1967).

In this assay, vector-DNA complexes are subjected to electrophoresis through agarose gel. After electrophoresis, the negatively charged particles will move along the gradient while the positively charged as well as the neutral ones stay at the origin. Therefore, vector-DNA complexes migrate more slowly than the corresponding free DNA (Hellman *et al.*, 2007). The electrophoretic mobility of the nucleic acid is detected by the fluorescence imaging using ethidium bromide which produces fluorescence and enables DNA visualisation on the agarose gel under UV illumination (Gershon *et al.*, 1993).

2.2.3.2. PicoGreen assay

PicoGreen[®] is an ultra-sensitive fluorescent probe that binds to the double-stranded DNA (dsDNA), resulting in an increase in the fluorescence as compared to the free dye in solution. PicoGreen[®] assay was introduced a

decade ago and is now reputed as one of the most prominent fluorescent dyes used in biomedical research and bio-analytical techniques (Ahn *et al.*, 1996; Singer *et al.*, 1997). This assay can assess the ability of DNA to form complexes with gene delivery vectors. In this study, PicoGreen assay was used to evaluate DNA complexation with DAB-Tf, DAB-Lf and DAB-Lfc systems.

This assay is based on the concept that the dye shows a significant fluorescence enhancement upon intercalation with the double strands of the DNA. In DNA complexes, when the anionic DNA interacts with cationic groups of the polymer, the DNA condenses, which results in less binding sites for the dye to bind to the DNA. Thus, lower fluorescence intensity of the dye.

The PicoGreen® assay provides a highly sensitive means of dsDNA quantitation in solution compared to other dyes such as ethidium bromide. The main disadvantage of using ethidium bromide dye for dsDNA quantitation is the contribution of signal from single-stranded DNA (ssDNA) and other contaminants, such as protein and extraction buffers. In contrast, PicoGreen® reagent selectively binds to dsDNA and circumvents such contributions from interfering substances by exhibiting an emission peak at 530nm when bound specifically to dsDNA (Dragan *et al.*, 2010).

2.2.4. Fluorescence Spectrophotometry

Fluorescence spectrophotometry is a technique that assays the state of a biological system by studying its interactions with fluorescent probe molecules (Damez *et al.*, 2008). It is one of the most common, simple, sensitive, specific

and fast analytical technique in pharmaceuticals. In our study, the efficiency of DAB-Lf and DAB-Lfc systems to condense DNA was determined by using fluorescence spectrophotometry. The measurement is based on the principle that a molecule can be excited from its ground electronic state to an excited electronic state by absorbing energy in the form of visible or ultraviolet light. Since this transit state is not stable, the sample emits a lower energy light and returns to the most stable state (Ground state).

This emitted lower energy light is known as fluorescence (Connors, 2002). This energy is detected by a fluorescence detector and DNA concentration is shown in LCD display. A schematic illustration of a spectrophotometer is shown in (Figure 2.4)

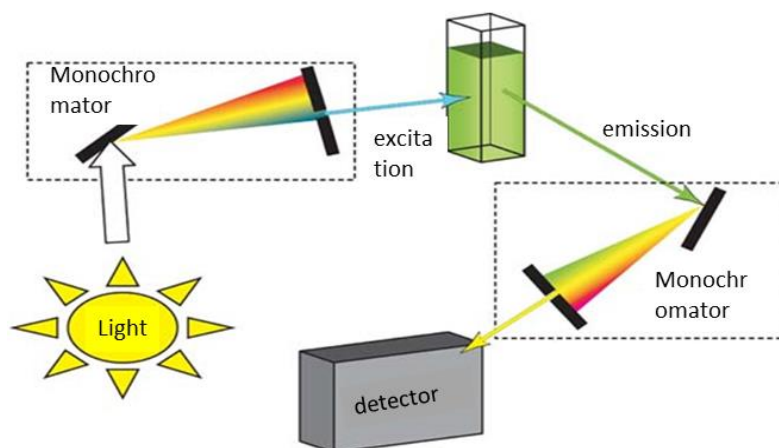


Figure 2.4: Physical Methods in Chemistry and Nano Science. (Adapted from Barron, 2013).

2.2.5. Transmission Electron Microscopy (TEM)

The transmission electron microscopy is a technique that is well established for structure characterization, in both physical and biological sciences. It was developed in the 1950s to improve the images resolution by giving atomic-resolution for nanoparticles from less than 1 nm to 100 nm (Williams & Carter, 1996). TEM constructs images when a beam of electrons passes through a sample ($< 1\mu\text{m}$) and the electrons interact with the sample used. The process of producing these images is illustrated in Figure 2.5. Briefly, a beam of electrons is generated from the heated tungsten filament within the electron gun, with a voltage from 20 to 200 kV. The condenser lens is in place to focus the electron source. The electron beam travels through the specimen stage, in which samples are placed on a thin circular metallic mesh of about 3 mm in diameter. TEM images are then constructed by the objective lens. Finally, the projector lens then can be optimized to reduce or magnify the images before collecting the images from a photographic recording camera.

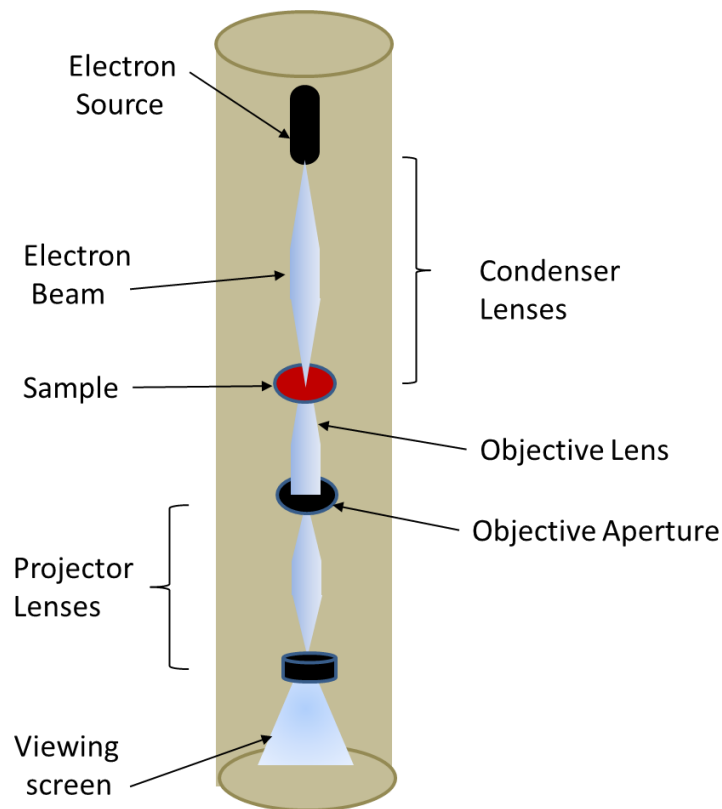


Figure 2.5: Diagram outlining the internal components of a basic TEM system (Adapted from Barrett Research Group).

2.2.6. Photon Correlation Spectroscopy (PCS)

Particle size and zeta potential are essential factors in the characterization of any vector/DNA complex that determines the behaviour of these systems *in vitro* and *in vivo*. They are generally measured using Photon Correlation Spectroscopy (PCS).

Particle size, typically in the sub-micron region, is determined by measuring the diffusion of the particles due to Brownian motion. Brownian motion is a constant random movement of particles which results from the interaction with solvent molecules that surround them. In photon correlation

spectroscopy (PCS) or dynamic light scattering, the Brownian motion of sub-micron particles is measured as a function of time. The technique is based on the principle that the larger the particle, the slower the Brownian motion will be. It is considered to be the most popular technology in sizing nanoparticles. It utilizes a laser beam to probe a small volume of a particle suspension (Figure 2.6) (Malvern Instruments Ltd., 2004). The Brownian motion of particles in suspension causes laser light to be scattered at different intensities. The interference between scattered light produces fluctuations in the intensity at different times. These fluctuations are detected by a photon detector (normally a photomultiplier). This temporal fluctuation, containing information on the motion of particles, is registered and processed by a digital correlate (Filella *et al.*, 1997).

PCS calculates the diameter of particles (usually ranging from 1 to 5000 nm) under controlled temperature and viscosity. As the diameter obtained by PCS refers to how a particle diffuses within a fluid, measurements were referred to as hydrodynamic diameter ($d(H)$):

$$d(H) = (\kappa T) / (3 \pi \eta D)$$

$d(H)$ = hydrodynamic diameter, κ = Boltzmann's constant, T = absolute temperature, η = viscosity, D = translational diffusion coefficient.

Surface interaction forces of particles are the key to understanding dispersion stability and aggregation. Zeta potential is a useful indicator of particle surface charge. The surface charge of a particle dispersed in a

suspension is determined by the ionization state of the ionisable groups on the particle surface and the pH of the medium (Shaw & Costello, 1993). When such a charged solid surface is in contact with a liquid, an electrical potential develops at the interface. Each particle is surrounded by an electrical double layer (EDL) consisting of an inner region (Stern layer) where the ions are strongly bound and an outer (diffuse) region where they are less firmly associated (Figure 2.6) (Goddard & Hotchkiss, 2007). Although ions in the Stern layer are fixed in place, ions in the diffuse or mobile layer are free to migrate. The common practice is to determine the electric potential of a particle at a location away from the particle surface, somewhere in the diffuse layer. The plane between the Stern layer and diffuse layer is called the shear plane. The potential at this plane is called the zeta potential which is the electrostatic potential difference between the stern layer and the diffuse layer.

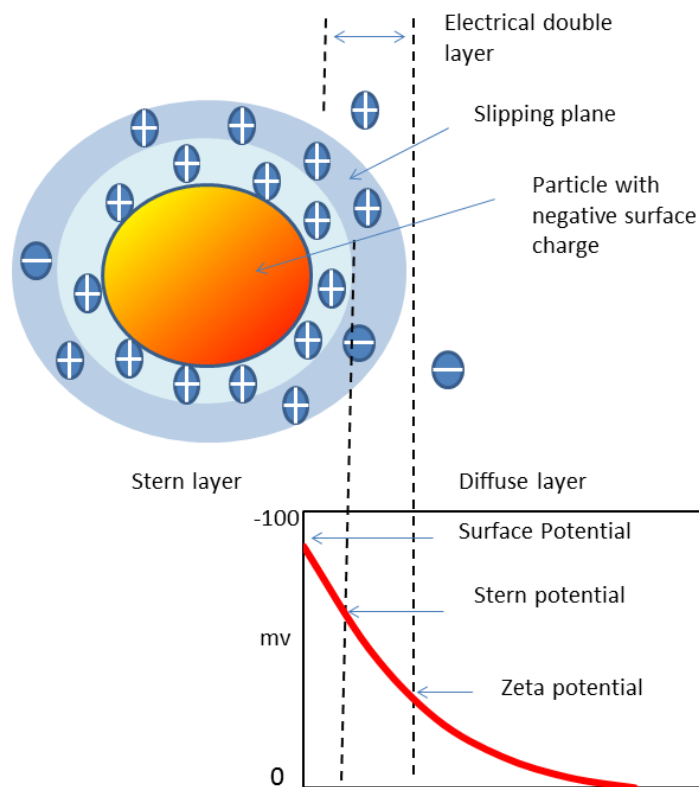


Figure 2.6: Electrical double layer (adapted from Morfesis, 2010).

Zeta potential is a physical property important for many applications from the development of biomedical polymers to the design of microfluidic devices (Sze *et al.*, 2003). Measurement of zeta potential facilitates the understanding of vesicles-cell interactions *in vitro*. For example, reports suggested that particles bearing positive charges have enhanced interaction with negatively charged cell membrane which facilitates their cellular uptake (Torchilin, 2006). In this study, PCS is used to measure size and zeta potential of DNA complexation with DAB-Lf and DAB-Lfc systems at various vector: DNA weight ratios ranging from 0.5 to 20 (Delgado *et al.*, 2007). Measuring zeta potential of DNA complexes facilitates the understanding of the surface charge

that could efficiently condense DNA and result in smaller size DNA complexes and therefore enhance their cellular uptake.

2.3. Introduction to *In vitro* and *In vivo* studies

2.3.1. *In vitro* studies

In the last decade, there has been a significant development in the knowledge of the fundamental molecular processes that are involved in the growth of cancer and its response to treatment (Stratton *et al*, 2009). This includes rapid improvements in prevention, diagnosis and treatment of cancers particularly malignant disease that need more effective therapies. Moreover, the identification of the genes and pathways that give rise to cancer dependencies has promoted the development of individualised, molecularly targeted therapies. This has led to the development of new *in vitro* and *ex vivo* methodologies and research techniques that should improve our understanding of cancer (Workman and de Bono, 2008). This should help to ensure that improved methods for diagnosis, therapy and prevention will be developed more effectively for patient benefit.

In vitro studies in cancer research are those that are conducted using cancer cells in isolation from the host under reasonable conditions in the laboratory. The main advantage of this method is its good control over the cultural environment such as nutrients, temperature or salt concentrations, which simplifies the system under study and makes the investigator focus on a

small number of components. In addition, *in vitro* methods are the methods of choice for large-scale studies because of the ease of culture, compared with the use of animals, and because of economic considerations (Association, Educational, & Testing, 1999). Commonly, experiments based on *in vitro* methods include process that uses cells derived from multicellular organisms (cell culture), subcellular components, and cellular or subcellular extracts or purified molecules such as proteins, DNA or RNA.

However, some of the properties of a tested delivery system that produce successful *in vitro* results may differ from those required for effective *in vivo* delivery (Ledley, 1995) , as *in vitro* transfection experiment is carried out in a less complex environment than that encountered *in vivo*. In addition, media components and volume and the cell type being investigated can be controlled in an *in vitro* environment (Freshney, 2000). Such a controlled environment is not encountered if systems are delivered *in vivo* and hence this adds to the lack of predictability that *in vitro* transfection results have on *in vivo* efficiency. In addition, cellular properties are often modified upon removal from their normal *in vivo* environment (Freshney, 2000). Moreover, the *in vitro* systems often involve using dividing cells and mitosis that may present beneficial effectiveness results for many non-viral systems by enhancing nuclear uptake (Mortimer *et al.*, 1999).

However, *in vitro* transfection experiments can be a useful tool for studying specific aspects of gene delivery systems and to establish if

transfection can occur, thus reducing the number of animal experiments conducted (Aldawsari *et al.*, 2011)

2.3.1.1. Cell culture

Cell culture is the process of isolating cells from the whole organism of an animal or plants into an artificial environment and growing them under controlled conditions for days or weeks to obtain a sufficient number of cells (Green, 1966). The cells may be obtained by the direct removal from the tissue before cultivation: this process is called primary culture. They can also be derived from a subculture process where cells are obtained from cell line that has been already established by primary culture (Ryan, 2008).

For *in vitro* studies, the three prostate cell lines PC3, DU145 and LNCaP (described earlier in section 2.1.1.) were used. These three cell lines were used to investigate the effect of conjugation of Tf, Lf, and Lfc to DAB dendrimer (DAB-Tf, DAB-Lf and DAB-Lfc, respectively) on enhancing the gene expression. The prostate cell lines overexpressing Tf receptors were grown in either Minimum Essential Medium (MEM) (for PC-3 and DU145 cells) or Roswell Park Memorial Institute Medium (RPMI) medium (for LNCaP cells), at 37°C in a humidified atmosphere under 5% CO₂. Both media were supplemented with 10% (v/v) foetal bovine serum, 1% (v/v) L-glutamine and 0.5% (v/v) penicillin-streptomycin. Ten mM N-2-hydroxyethylpiperazine-N'-2-ethanesulfonic acid (HEPES) (5 mL) and 1 mM sodium pyruvate (5 mL) were also added to RPMI medium.

2.3.1.2. Cell transfection

Transfection refers to the process whereby the genetic material is introduced to host cells, taken up, transported to the nucleus and expressed as the desired protein (Lemoine, 1999). Each of these stages is exposed to delivery failure when naked DNA is used. This is because naked DNA tends to be rapidly degraded in tissues or in the systemic circulation (Nishikawa & Huang, 2001). This extracellular degradation is due to the characteristics of DNA such as its hydrophilic nature, large size and polyanionic character. Therefore, to achieve an effective gene therapy, the low transfection efficiency of naked DNA must be overcome with the aid of delivery systems such as polymers and dendrimers (Uchegbu *et al.*, 2008). However, these systems will face many barriers that have to be overcome for successful transfection to occur, such as inefficient cellular uptake, poor endosomal escape and low nuclear uptake (Nishikawa and Huang, 2001).

The efficiency of gene expression to target cells is commonly measured by using gene reporter assays. The reporter assay is based on the reporter gene, the protein it encodes, and the assays available for detecting presence of the reporter. Reporter assays are used to study promoter and enhancer sequences, trans-acting mediators such as transcription factors, mRNA processing and translation. Reporters are also used to monitor transfection efficiencies, protein-protein interactions and protein subcellular localization. In gene delivery systems, reporter assays allow gene delivery efficiency to be measured via the uptake and expression level of a known reporter protein being investigated

using different delivery vectors. These systems are usually sensitive, easy to use and yield rapid results.

Reporter proteins can be assayed by detecting endogenous characteristics such as enzymatic activity or spectrophotometric characteristics, or indirectly with antibody-based assays. Reporter gene is used as indicator of transcriptional activity within cells where the reporter gene or cDNA is joined to a promoter sequence in an expression vector that is transferred into cells. This is followed by an assay of the cells for the presence of the reporter by directly measuring the amount of reporter mRNA, the reporter protein itself, or the enzymatic activity of the reporter protein (Schenborn and Groskreutz, 1999).

The ideal reporter gene should be biologically inert, i.e. not influence the cell metabolism or interfere with cellular signalling and should not itself modulate expression (Torbett, 2002). Moreover, the readouts from reporter gene assays should be a true reflection of cellular transcription or translation process (Zinselmeyer *et al.*, 2003). A common genetic reporter used to study gene expression is the *E. coli lacZ* gene, which encodes the protein β - galactosidase which is the reporter gene used in our *in vitro* and *in vivo* studies (Ogris *et al.*, 1999; Brown *et al.*, 2003; Shcharbin *et al.*, 2010).

- ***β -galactosidase transfection assay***

In 1972, Jeffrey Miller published a protocol for determining the amount of β -gal with o-nitrophenyl- β -D-galactosidase (ONPG). This protocol is known as β -

galactosidase transfection assay or Miller assay (Miller, 1972). The standardized amount of β -gal activity is a “Miller Unit”. β -galactosidase is commonly used as biomarker both *in vivo* and *in vitro* as it provides a convenient method for β -galactosidase (a prokaryotic enzyme) expression to be detected (Shcharbin *et al.*, 2010). β -galactosidase enzyme can be assayed by measuring hydrolysis of the chromogenic substrate, o-nitrophenyl- β -D-galactoside (ONPG), a colourless solution, which is cleaved to yield galactose and o-nitrophenol which is yellow in alkaline solution (Figure 2.7). The amount of o-nitrophenol formed indicates the enzyme concentrations and can be measured by reading the photometrical absorbance with a microplate reader.

Briefly, the procedure of the assay in our study involves a 72 h incubation after transfection with β -galactosidase reporter vector, such as pCMV SPORT β -gal plasmid, the cells were lysed with 1X passive lysis buffer (PLB) (50 μ l/well) for 20 min. Then, the cell lysates were subsequently analysed for β -galactosidase activity in the supernatant and measured in a buffer containing ONPG (1.33 mg/ml). The β -galactosidase enzyme cleaves the β -bond of colourless ONPG to form o-nitrophenol (a yellow solution). Finally, the samples were analysed by measuring the absorbance photometrically at 405 nm with a microplate reader.

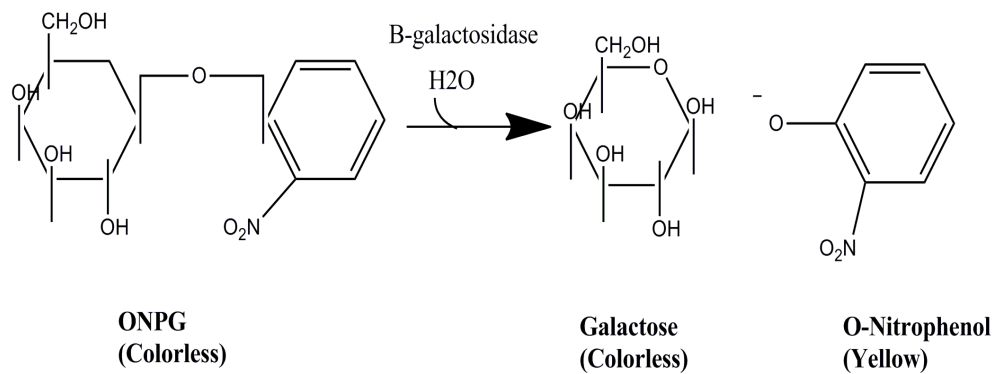


Figure 2.7: Miller Assay (Adapted from: <http://www.sci.sdsu.edu/>).

2.3.1.3. Confocal Laser Scanning Microscopy (CLSM)

Confocal microscopy is used to obtain biological images with very high degree of specificity and sensitivity. The key elements in the design of the confocal microscopy are the use of pinhole apertures and point-by-point illumination of the specimen of spatial filtering to suppress unwanted out-of-focus light or flare in specimens that are thicker than the plane of focus (Figure 2.8). Because of these elements, confocal microscopy offers several advantages over conventional microscopy. For example, confocal microscope creates sharp images of a specimen compared to the blurred images when viewed with a conventional microscope. This is accomplished by suppressing the out-of-focus light from the specimen and therefore the image has less haze, better contrast and improved details of the confocal image than that of a conventional microscope (Semwogerere and Weeks, 2005 ; Claxton *et al.*, 2006). Confocal microscopy provides improvements in speed, image quality, and storage of the generated images. Thus, apart from its improvements on the quality of the

images, CLSM offers a feature for building three-dimensional (3D) reconstructions of the specimen (Conchello *et al.*, 2005).

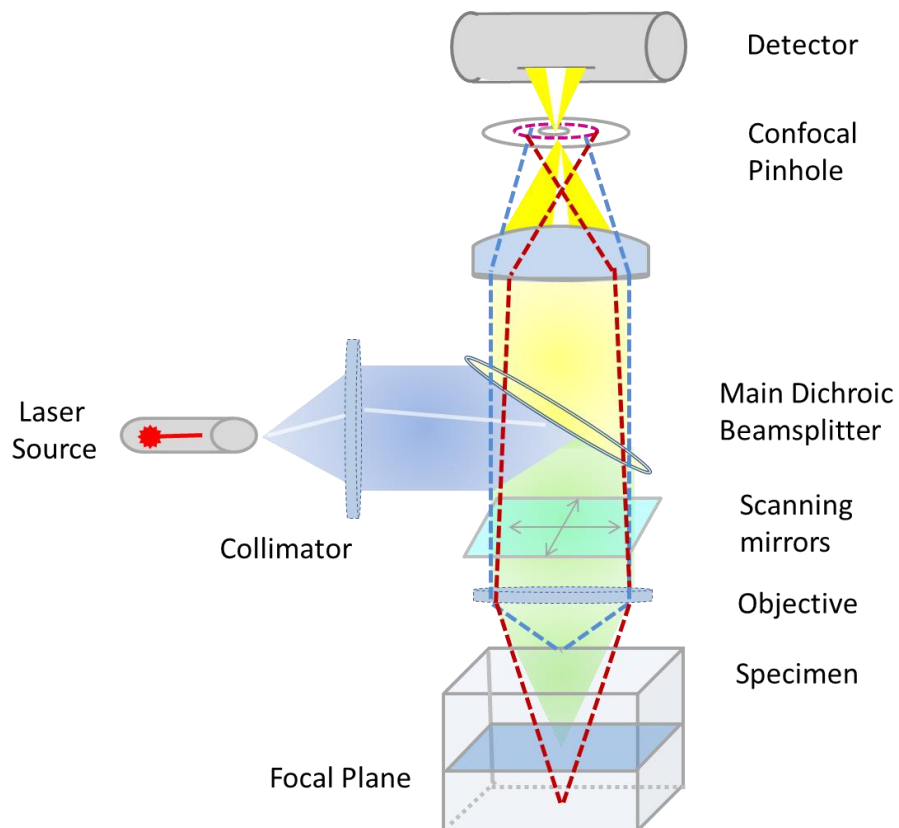


Figure 2.8: Confocal Laser Scanning Microscope (Adapted from Carl Zeiss, Inc.).

The majority of confocal images are produced either by reflecting light off the specimen or stimulating fluorescence from fluorophores. However, the most commonly used confocal microscopy in biological applications is fluorescence confocal microscopy. When fluorescence molecules are exposed to light (for example a laser beam), they may absorb the light and reflect a light of different colour; this process is known as fluorescence. Fluorescein is a common fluorophore that emits emission wavelength of green light when exposed to excitation wavelength of blue light. The emission wavelength is

always higher than the excitation wavelength. Fluorescence confocal microscopy has several advantages over confocal microscopy that works in the reflected mode. These advantages include the possibility of attaching fluorescence molecules to specific parts of specimen. In addition, it is possible to add more than one type of fluorophore to different parts of specimen in order to distinguish these parts, this feature is called multi-label or multi-colour confocal imaging (Sheppard & Pearlman, 1997).

2.3.1.4. Anti-proliferative assay: MTT assay

Anti-proliferative assays are required in many biological applications for the measurement of surviving and/or proliferating mammalian cells. MTT (3-(4,5-dimethylthiazol-2-yl)-2,5-diphenyltetrazolium bromide) assay is one of the most commonly used proliferation and cytotoxicity assays to measure the anti-cancer therapeutic efficacy (Wang *et al.*, 1994). It was first developed in 1983 by Mosmann for measuring cytotoxicity in cells (Mosmann, 1983).

MTT assay is based on the conversion of MTT into formazan crystals by the mitochondrial activity of the living cells. Since for most cell populations the total mitochondrial activity is related to the number of viable cells, this assay is broadly used to measure the *in vitro* cytotoxic effects of drugs on cell lines (Plumb, 2004).

MTT is a yellow tetrazolium salt that can easily enter mammalian cells. The unique chemical and biological properties of MTT have led to its use in cytotoxicity assays that measures only living cells. Tetrazolium salts are

organic compounds consisting of five membered unsaturated ring contains four nitrogen atoms and one carbon atom. This structure is surrounded by three aromatic groups which usually involve phenyl moieties. This structure forms a yellow or colourless compound which is transformed into a deeply purple product known as formazan (Figure 2.9) (Berridge *et al.*, 2005).

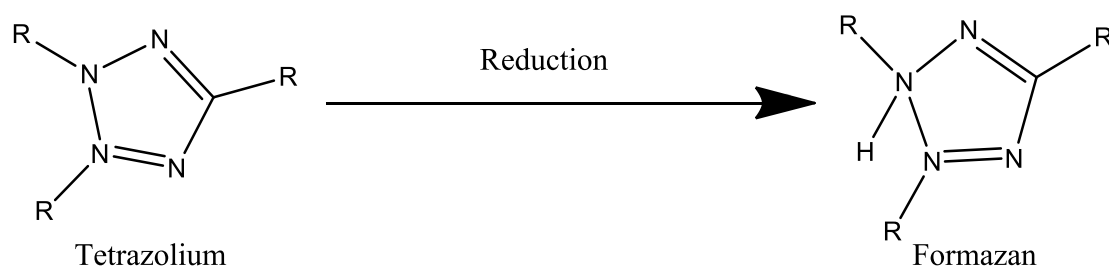


Figure 2.9: Transformation of Tetrazolium salt into formazan.

The reduction of MTT and production of formazan are results of the cellular metabolic activity due to the intracellular NAD (P) H-dependent NADH which is responsible for most MTT reductions. However, other factors may contribute to the reduction of MTT. The amount of the produced formazan can be dissolved in a suitable organic solvent, in this work dimethylsulfoxide (DMSO), to give peak intensity at 570 nm that can be colorimetrically determined. Thus, the result of the MTT assay is based on the assumption that the amount of the produced formazan is linear with the number of living cells (Berridge *et al.*, 2005).

2.3.2. *In vivo* studies

The *in vivo* study is considered to be one of the most essential studies prior to clinical trials in a drug evaluation process (Kelland, 2004).

Cell culture techniques and *in vitro* characterization studies have significantly contributed in recent advances in gene therapy. However, *in vivo* study remains an essential tool in developing a successful gene delivery system due to the complexity of the biological system (Kelland, 2004).

In non-viral gene delivery systems, the efficiency can be improved by learning from the characteristics of their *in vitro* transfection data which enable predict their performance across biological membranes (*in vivo* study). However, one of the difficulties faced by the science is the lack of correlation between *in vitro* and *in vivo* results as the *in vitro* transfection is more efficient than the corresponding *in vivo* gene delivery (Wells *et al.*, 2000), since the whole organism imposes the extracellular matrix, inhibitory biological fluids and many other barriers (Brown *et al.*, 2001). Hence carrier characteristics favouring efficient transfection *in vitro* may be ineffective *in vivo* (Brown *et al.*, 2001).

In non-viral gene delivery systems, several biological barriers must be overcome to achieve efficient gene delivery (Brown *et al.*, 2001). The various barriers to gene delivery have been identified as being both at the extracellular and intracellular levels. These barriers include binding to the cell surface,

traversing the plasma membrane, escaping lysosomal degradation, and overcoming the nuclear envelope (Khalil *et al.*, 2006).

2.3.2.1. Animal models

To develop new treatments, animal models are essential for investigation of the pathogenesis of the disease. The appropriate animal model should be representative for the human disease. Several animal models are used in research and investigation of human disease such as mice, rats, guinea pigs, rabbits, etc. Mice are the most commonly used species: over 95% of human disease studies are conducted in mice. (Figure 2.10) (Workman *et al.*, 2010).

For cancer therapy, animal studies are important to understand how cancers develop and spread within living organisms and to discover the more effective ways to diagnose and treat cancer. Animal studies are also required by regulatory authorities before any trials of new drugs can be tested in humans. However, they are only performed after every possible test has been conducted on cancer cells in the laboratory and where no alternative exists (Workman *et al.*, 2010).

Selection of tumour models is based on molecular characteristics, for example, expression or mutation of a target of interest together with desired properties such as metastatic potential, the rate of growth and chemosensitivity (Brown *et al.*, 2001).

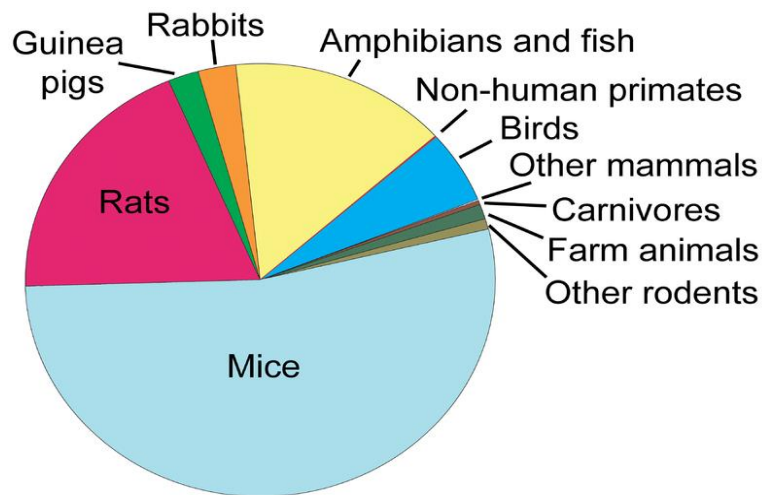


Figure 2.10: Types and percentage of vertebrates used in animal studies in Europe in 2005 (Adapted from Commission of the European Communities, 2007).

In 1959, Russell and Burch published *The Principles of Humane Experimental Technique* in which they stated that all animal experiments should incorporate, as far as possible, the 3Rs: replacement (of animals with alternative methods), reduction (in the numbers of animals used to achieve scientific objectives) and refinement (of methods to minimise animal suffering). These principles underpin the guidelines and working practices for the use of animals in scientific procedures. The 3Rs must be taken into account when planning cancer research using animals (Russell and Burch, 1959). Workman and co-workers provided updated guidelines on the use of animals in cancer research. They also presented recommendations on all aspects of cancer research, including study design, statistics and pilot studies, and choice of tumour models focusing on animal welfare (Workman *et al.*, 2010).

The Animals (Scientific Procedure Act) 1986 regulates the designated procedures where animal welfare and health must constantly be maintained and monitored by authorized personal, and project licences are appropriately justified, trained and supervised (Wolfensohn and Lloyd 1998). Animal housing should be maintained according to the highest standards, including environmental enrichment as the most reliable results are most likely obtained when healthy animals are used in the study (Tsai *et al.*, 2006). Mice should be kept in animal unit for at least one week before starting the experiment. Ideally, mice are housed in groups of 5-6 with temperatures ranging between 19- 23°C, 40-70% humidity, 12 to 15 air changes per 143 h, and 12 h daylight cycle for circadian rhythm regulation. The normal fed for adult mice is about 3-5 g of pelleted mouse diet/day and 6-7 mL water/day. Light wavelength should be between 350-400 nm, and noise level should be kept low as mice are sensitive to ultrasounds (Wolfensohn and Lloyd 1998). Local ethical review will come first before any experimental animal studies. In addition, these guidelines should be used in conjunction with appropriate national legislation: UK Animals (Scientific Procedures) Act 1986.

2.3.2.2. Biodistribution of gene expression

The identification of new reporter genes considers a key factor in development of novel gene delivery systems. As discussed earlier in section 2.3.1.2., the presence of reporter gene allowed accurate evaluation of delivery vectors both *in vitro* and *in vivo*. It is also important in the process of comparison of transgene expression by different promoters (Zinselmeyer *et al.*, 2003).

An example of a reporter gene in bacteria is the chloramphenicol acetyltransferase (CAT) gene, which confers resistance to the antibiotic chloramphenicol. CAT is a bacterial enzyme from *Escherichia coli* that has been used for describing genetic reporter vector and assay systems designed for the analysis of transcriptional regulation *in vivo* (Gorman *et al*, 1982). In this assay, the polar H-acetyl-Coenzyme A (CoA) substrate is cleaved and released chloramphenicol. However, this assay is limited due to environmental issues (Sleigh, 1986). Since then, several reporter genes and assays have been developed which include β -galactosidase, luciferase, alkaline phosphatase (AP), growth hormone (GH), β -glucuronidase (GUS), and the recently used green fluorescent protein (GFP) and β -lactamase (Schenborn and Groskreutz, 1999). These available genetic reporters have potential applications in gene expression and regulation studies.

Table 2.1: Advantages and Limitations of the Commonly Used Reporter Genes (from Schenborn and Groskreutz, 1999).

Reporter Gene	Advantages	Limitations
CAT	<ul style="list-style-type: none"> - Widely accepted standard in literature - Visual confirmation of enzyme activity 	<ul style="list-style-type: none"> - Relatively low sensitivity - High costs for isotope and Thin Layer Chromatography (TLC) systems - Requires luminometer for high sensitivity assay - Relatively labile protein
Luciferase	<ul style="list-style-type: none"> -Fast assay -High sensitivity -Large linear range 	<ul style="list-style-type: none"> - Protein instability
β-Galactosidase	<ul style="list-style-type: none"> -Easy to assay -Variety of assay formats for use with cell extracts -Widely used for in situ staining 	<ul style="list-style-type: none"> -Endogenous activity in some cell types -Lower sensitivity in non chemiluminescent assays
β-Glucuronidase (GUS)	<ul style="list-style-type: none"> -Wide variety of formats -Used for in situ staining -Fusion proteins 	<ul style="list-style-type: none"> -Endogenous activity in mammalian cell
hGrowth Hormone(hGH)	<ul style="list-style-type: none"> -Secreted -Low background in most cells 	<ul style="list-style-type: none"> - Radioimmunoassay (RIA) or Enzyme Immunoassays (EIA) formats -Low sensitivity
Alkaline Phosphatase(AP)	<ul style="list-style-type: none"> -Wide variety of assay methods -High sensitivity in some assays 	<ul style="list-style-type: none"> -Endogenous activity in most cells

Reporter Gene	Advantages	Limitations
Secreted Alkaline Phosphatase (SEAP)	<ul style="list-style-type: none"> -Secreted -Low background activity 	<ul style="list-style-type: none"> - Poor sensitivity
Green Fluorescent Protein(GFP)	<ul style="list-style-type: none"> -No substrates required -Stable reporter protein -GFP and blue mutants can be detected in the same cell -<i>In situ</i> and <i>in vivo</i> applications 	<ul style="list-style-type: none"> -Low sensitivity; high level expression may be toxic -Expensive microscope or fluorimeter required
β -Lactamase	<ul style="list-style-type: none"> -Easy to use colorimetric assay with secreted from of reporter protein -Fluorescent substrates allow analysis with flow cytometry 	<ul style="list-style-type: none"> -Colorimetric assay comparable in sensitivity to CAT. -Intracellular localization not currently available for <i>in situ</i> analyses -Expensive instrumentation required

Cell transfected with pCMV sport β -galactosidase plasmid DNA will express the β -galactosidase enzyme. β -galactosidase is an example of glycosidase enzymes which are known to catalyse the hydrolysis of glycosidic bonds (Zinselmeyer *et al.*, 2003).

In the *in vivo* transfection in our studies, the activity of β -galactosidase was quantified by measuring the enzymatic cleavage of 9H-(1,3-dichloro-9,9-dimethylacridin-2-one-7-yl)-D-galactopyranoside (DDAO-G,) to 7-hydroxy-9H-(1,3-dichloro-9,9-dimethylacridin-2-one) (DDAO) moiety as the substrate for β -galactosidase enzyme expressed in successfully transfected cells. The product, DDAO, absorbs and emits light at a much longer wavelength ($\lambda_{\text{excitation}} = 630$ nm/ $\lambda_{\text{emission}} = 650$ nm) than the substrate DDAO-G ($\lambda_{\text{excitation}} = 460$ nm/ $\lambda_{\text{emission}} = 610$ nm).

2.3.2.3. Bioluminescence imaging

Current imaging techniques have contributed to the improvement in translational cancer research due to high detection ability and the simple analytical format of bioluminescence. The main function of imaging is for monitoring tumours and metastases with or without treatment. Other utility include studies of basic biological processes and tissue pharmacokinetics and pharmacodynamics responses to treatment (Galbraith *et al.*, 2003; Tennant *et al.*, 2009).

According to the 3Rs in animal studies (“reduce, replace and refine”), bioluminescence imaging offers a powerful imaging methodology that is more

sensitive, non-invasive and less toxic. This imaging system is a versatile tool that is based on the detection of light emission from cells or tissues (Sato *et al.*, 2004).

In addition to its use in monitoring tumour growth, bioluminescence imaging is also used for imaging gene expression and protein – protein interactions.

Bioluminescence imaging has many advantages over other techniques in that it is a highly sensitive tool that can be used in gene reporters at low costs. However, in most cases, this method requires genetic modification of tumour cells for detection. (Workman *et al.*, 2010).

In vivo bioluminescent imaging concept is based on the expression of luciferase in the living animal following an intraperitoneal (i.p.) dose of D-luciferin, and imaging of the bioluminescence tissue by a cooled, charge-coupled device (CCD) camera (Sadikot *et al.*, 2005). This imaging modality has been broadly used in the examination of molecular processes, in particular, bioluminescent has been used to study tumour metastasis (van der Pluijm *et al.*, 2005) and monitor potential cancer therapeutics (Hoffman, 2005) due to its technical simplicity in quantifying photons emitted by the enzyme-catalysed, chemiluminescent reaction. The intensity of emitted light can be converted into a pseudo-colour graphic which provides a visual interpretation of tumour growth and regression for monitoring the efficacy of a therapeutic intervention (Sato *et al.*, 2004).

A major advantage of bioluminescence imaging is the ability to construct longitudinal studies in living organisms where multiple measurements can be made in the same animal over time, thus providing information on the various stages of tumour development (Sadikot *et al.*, 2005; Klerk *et al.*, 2007). This will potentially reduce the number of animals required for experimentation while minimizing the effects of biological variation (Sadikot *et al.*, 2005).

Compared to other methods for detecting *in vivo* transgene expression, bioluminescence imaging eliminates tissue harvesting. As a result, the same animals can be monitored over a time course, and the number of animals needed is significantly reduced (Workman *et al.*, 2010). The whole animal is imaged using sensitive optical detectors, which may or may not incorporate a tomographic facility (Wells *et al.*, 2006). It is known that exogenous illumination such as fluorescence labelling bleaches tissues, which causes phototoxic damage to the cells (Welsh and Kay, 2005). Bioluminescence imaging potentially avoids this problem, and therefore can be considered an ideal system for long-term studies in living organisms (Welsh and Kay, 2005).

In our study, the biodistribution of gene expression was visualized by bioluminescence imaging, using an IVIS Spectrum. Treated mice were intraperitoneally injected with the luciferase substrate D-luciferin before imaging. Production of luciferase enzyme is able to catalyse the oxidation of substrate D-luciferin to non-reactive oxyluciferin, emitting photons of light at 562 nm (Sato *et al.*, 2004). The depth of light emission is able to penetrate

tissues of several millimeters-centimeters, thus allowing organ-level resolution (Sato *et al.*, 2004). The light emitted from the bioluminescence tumours was detected for 2 min using Living Image® software and displayed as a pseudo-colour overlay onto a grey-scale image of the animal.

CHAPTER 3.

THERAPEUTIC EFFICACY OF INTRAVENOUSLY ADMINISTERED TRANSFERRIN CONJUGATED DENDRIPLEXES ON PROSTATE CARCINOMAS

3.1. Introduction

Radiation therapy, chemotherapy, radical prostatectomy and cryoablation can be effective therapies for localized tumours. However, there is still no efficacious treatment modality for patients with recurrent or metastatic disease (Lu, 2009). New treatment approaches are therefore critically needed for these patients (Al Robaian *et al.*, 2013)

Among these novel experimental approaches, gene therapy holds great promise for the intravenous treatment of prostate cancer. However, its use is currently limited by the lack of delivery systems able to deliver the therapeutic genes selectively to the tumours by intravenous administration, without secondary effects to normal tissues.

In order to overcome this limitation, safe and efficacious gene delivery systems able to selectively deliver therapeutic genes to tumours by intravenous administration.

On the basis that iron is essential for tumour cell growth and can be effectively carried to cancer cells by using transferrin, whose receptors are overexpressed on cancer cells (Lemarié *et al.* 2011), we recently demonstrated that the conjugation of transferrin to generation 3- diaminobutyric polypropylenimine (DAB) dendrimer led to gene expression mainly in the tumours after intravenous administration.

3.2. Aims and Objectives

In this chapter, we investigated the conjugation of DAB dendrimer with transferrin (Tf) whose receptors are overexpressed on prostate cancer cells. The objectives of this study were therefore 1) to prepare and characterize transferrin -bearing DAB dendrimer and 2) to evaluate their targeting and therapeutic efficacy on prostate cancer cells *in vitro* and *in vivo* after intravenous administration.

3.3. Methods

3.3.1. Preparation of the Tf-bearing polypropylenimine dendrimer

Generation 3- diaminobutyric polypropylenimine dendrimer (DAB, 24 mg) was conjugated to transferrin (Tf, 6 mg) by cross-linking with dimethylsuberimidate (DMSI, 12 mg) in triethanolamine HCl buffer (pH 7.4, 2 mL), as previously described (Koppu *et al.*, 2010; Lemarié *et al.*, 2012). The conjugation reaction took place at 25°C for 2 h whilst stirring. DAB-Tf dendrimer was then purified by size exclusion chromatography using a Sephadex G75 column, freeze-dried, before having its identity confirmed by ¹H NMR spectroscopy, using a Jeol Oxford NMR AS 400 spectrometer (Koppu *et al.*, 2010).

3.3.2. Cell culture

PC-3M-luc-C6, DU145 and LNCaP prostate cell lines overexpressing Tf receptors were grown in either MEM (for PC-3 and DU145 cells) or RPMI medium (for LNCaP cells), at 37°C in a humidified atmosphere under 5% CO₂. Foetal bovine serum (10% (v/v), L-glutamine (1% (v/v) and penicillin-streptomycin (0.5% (v/v) were added to both media. In addition, RPMI medium was also supplemented with 10 mM HEPES (5 mL) and 1 mM sodium pyruvate (5 mL).

3.3.3. Cellular uptake of DNA

Plasmid DNA encoding β -galactosidase was labelled with the fluorescent probe Cy3 using a Label IT[®] Cy3 Nucleic Acid Labelling kit, as described by the manufacturer. PC-3, DU145 and LNCaP cells were seeded on coverslips in 6-well plates (10⁴ cells/ well) and grown at 37°C for 24 h. They were then incubated with Cy3-labeled DNA (2.5 μ g DNA / well) complexed by mixing to DAB-Tf and DAB at their optimal dendrimer: DNA weight ratios (leading to complete DNA condensation and highest transfection) respectively of 10:1 for DAB-Tf and 5:1 for DAB. Control slides were treated with naked DNA. Following 24 h treatment, the cells were then washed three times with PBS and fixed with methanol for 10 min. DAPI was then used to stain the nuclei and the cells were examined using a Leica TCS SP5 confocal microscope. DAPI was excited with the 405 nm laser line (bandwidth: 415-491nm), whereas Cy3 was excited with the 543 nm laser line (bandwidth: 550-620 nm). Cy3-related fluorescence

intensity was then quantified in each of the confocal microscopy pictures by using Adobe Photoshop Elements software. Results were expressed as fluorescence intensity (in arbitrary units) per cell.

3.3.4. *In vitro* transfection

Transfection efficacy of the plasmid DNA encoding β -galactosidase and carried by DAB-Tf dendrimer was evaluated by a β -galactosidase transfection assay. Following seeding at a density of 2000 cells/ well in 96-well plates, PC-3, DU145 and LNCaP cells were left to grow at 37°C for 72 h. They were then incubated for a further 72 h with DNA (10 μ g/mL), alone or complexed to DAB-Tf and DAB (dendrimer: DNA weight ratios of 10:1 for DAB-Tf and 5:1 for DAB). The cells were then lysed with 50 μ L/well of 1X passive lysis buffer (PLB) for 20 min, before being incubated with 50 μ L/well of assay buffer (2 mM magnesium chloride, 100 mM mercaptoethanol, 1.33 mg/mL *o*-nitrophenol- β -galactopyranoside, 200 mM sodium phosphate buffer, pH 7.3) for 2 h at 37°C. The absorbance of the samples was then read at 405 nm with a plate reader (Thermo Lab Systems, Multiscan Ascent, UK) (Koppu *et al.*, 2010)

3.3.5. Anti-proliferative assay: MTT

Following seeding at a density of 2000 cells/ well in 96-well plates, PC-3, DU145 and LNCaP cells were left to grow at 37°C for 72 h. They were then incubated with DAB-Tf dendriplexes encoding TNF α , TRAIL and IL-12, at final DNA concentrations of 1.28×10^{-3} to 100 μ g/mL. After 72 hours incubation with the treatment, anti-proliferative activity was assessed by using a standard MTT

assay (three independent experiments with n=5 for each concentration level). The incubation of the treatments with the cells was maintained for 72 h, in order to allow comparison with our previous cytotoxicity results, obtained with DAB-Tf dendrimer but with different therapeutic DNA and different cancer cells.

3.3.6. *In vivo* tumoricidal activity

The *in vivo* experiments described below were approved by the local ethics committee and performed in accordance with the UK Home Office regulations.

PC-3M-luc-C6 and DU145 cancer cells in exponential growth were subcutaneously implanted to both flanks of male immunodeficient BALB/c mice (1×10^6 cells per flank). When tumours became palpable, vascularized and reached a diameter of 5 mm, the mice were split into groups of five before being intravenously injected with the treatments, namely Tf-bearing DAB dendrimer complexed with TNF α , TRAIL or IL-12 expression plasmids, the targeted dendrimer and naked DNA (50 μ g of DNA) once daily for 10 days. The weight of the mice was measured every day to evaluate the toxicity of the treatments and tumour volume was determined by calliper measurements (volume = $d^3 \times \pi/6$).

Bioluminescence imaging using an IVIS Spectrum (Calliper Life Sciences, Hopkinton, MA) was also used to monitor the therapeutic efficacy of the treatments. To this end, mice bearing subcutaneous PC-3M-luc-C6 tumours were intravenously injected with treatments as described above. Ten minutes

before imaging, they were intraperitoneally injected with the luciferase substrate D-luciferin (150 mg/kg body weight), before being anaesthetized by isoflurane inhalation on Days 1, 3, 5, 7, 9 of the experiment. The light emitted from the bioluminescent tumours was detected for 2 min using Living Image® software and displayed as a pseudo-colour overlay onto a grey scale image of the animal. Identical illumination settings were used for acquiring all images (Aldawsari *et al.*, 2011)

3.3.7. Statistical analysis

Statistical significance was assessed by one-way analysis of variance (ANOVA) and Bonferroni multiple comparison post-test (GraphPad Prism software). *P* values lower than 0.05 were considered statistically different. Results were expressed as means ± standard error of the mean (S.E.M).

3.4. Results

3.4.1. *In vitro* studies

In order to examine the *in vitro* gene delivery efficiency of the conjugation of DAB-Tf complexed to TNF- α , TRIAL and IL-12 compared to the unconjugated dendriplexes, confocal microscopy experiments was performed to investigate the cellular uptake efficiency of the delivery systems in PC-3M-luc-C6 and DU145 cancer cell lines. In addition, transfection experiments were performed to investigate the best carrier: DNA ratio that exhibit the optimum transfection efficacy compared to controls. These experiments are of a particular importance as they provide insight information regarding the intracellular

behaviour of both the conjugated and unconjugated dendriplexes when accumulated in cancer cells. Finally, anti-proliferative activity of the optimum formulations was investigated using MTT assay.

3.4.1.1. Cellular uptake of DNA

Confocal microscopy experiments confirmed that Cy3-labelled DNA was taken up by PC-3, DU145 and LNCaP cells (Figure 3.1). The fluorescently-labelled DNA was found to be disseminated in the cytoplasm following treatment with DAB-Tf and DAB dendriplexes in the three tested cell lines. However, the DNA uptake appeared to be much more pronounced after treatment with Tf-bearing dendriplex than with the non-targeted dendriplex, corresponding to an increase in fluorescence intensity of respectively 1.5-fold in PC-3 cells, 6-fold in DU145 cells and 15-fold in LNCaP cells (Figure 3.1). DNA appeared to be more efficiently taken up by PC-3 cells when delivered by means of the targeted dendriplex, compared to LNCaP and DU145 cells. However, these results need to be taken with caution, as they correspond to the quantification of one single representative confocal microscopy picture. No statistical analysis can therefore be applied to these results.

Co-localization of DNA in the nuclei was visible in the 3 cell lines following treatment with Tf-bearing dendriplex, as well as in PC-3 cells following treatment with DAB dendriplex, but to a lesser extent. By contrast, no Cy3-derived fluorescence was visible in cells treated with naked DNA. The conjugation of Tf to DAB therefore improved the uptake of DNA by PC-3, DU145 and LNCaP prostate cancer cells.

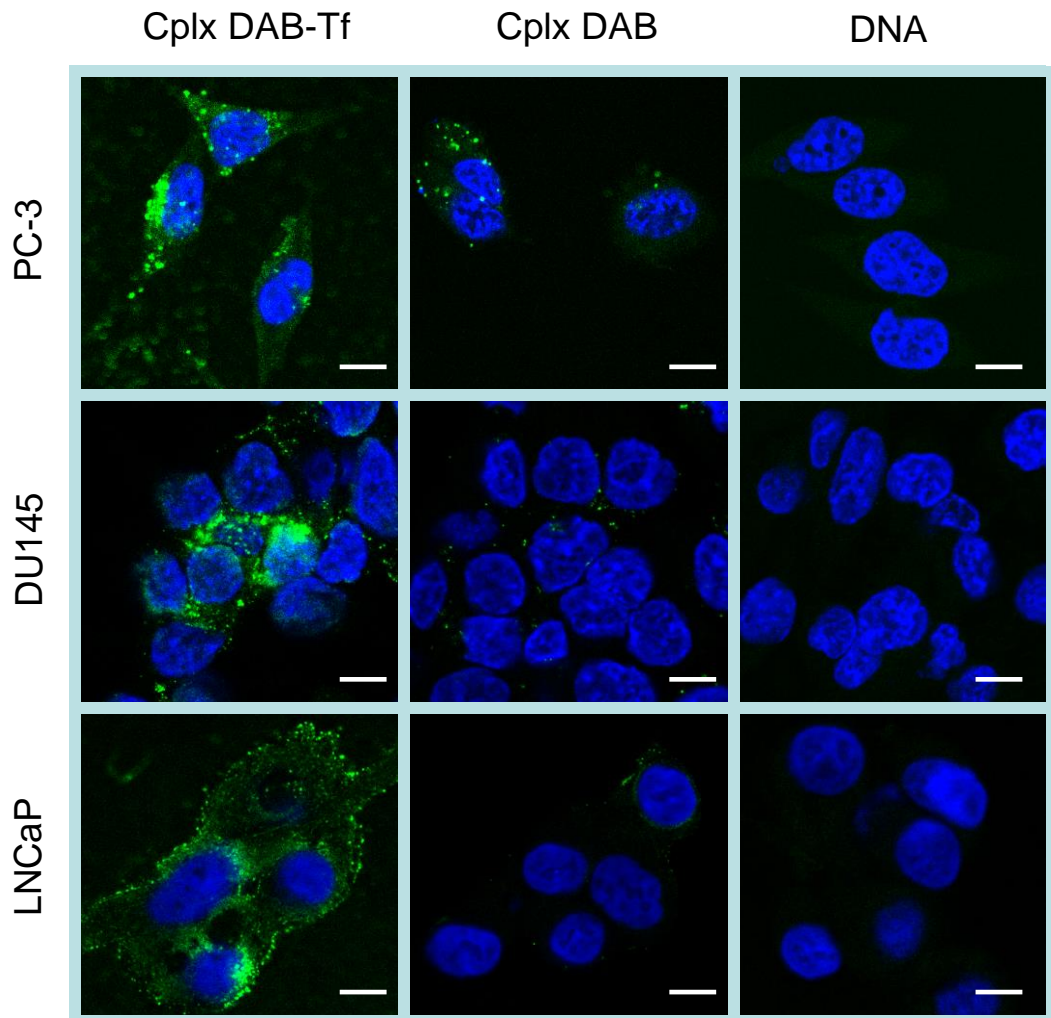


Figure 3.1: (A) Confocal microscopy imaging of the cellular uptake of Cy3- labelled DNA (2.5 μg / well) either complexed with DAB-Tf, DAB or in solution, after incubation for 72 hours with PC-3 (top), DU145 (medium) and LNCaP cells (bottom) (Blue: nuclei stained).

3.4.1.2. *In vitro* transfection

Treatment with DAB-Tf dendriplex led to an increase in gene expression on both PC-3 and LNCaP cells (Figure 3.2). On PC-3 cells, gene expression following treatment with DAB-Tf dendriplex ($2.69 \times 10^{-3} \pm 0.09 \times 10^{-3}$ U/mL) was 1.3-fold higher than with unconjugated DAB dendriplex ($2.08 \times 10^{-3} \pm 0.09 \times 10^{-3}$ U/mL). Similarly, it was slightly higher following treatment with DAB-Tf dendriplex ($1.77 \times 10^{-3} \pm 0.11 \times 10^{-3}$ U/mL) than that observed with DAB

dendriplex ($1.53 \times 10^{-3} \pm 0.05 \times 10^{-3}$ U/mL) on LNCaP cells. However, there was no significant difference between gene expression following treatment with DAB-Tf dendriplex and DAB dendriplex on DU145 cells ($1.47 \times 10^{-3} \pm 0.10 \times 10^{-3}$ U/mL and $1.29 \times 10^{-3} \pm 0.11 \times 10^{-3}$ U/mL respectively). Treatment with control dendrimer and naked DNA only resulted in weak levels of gene expression, as expected.

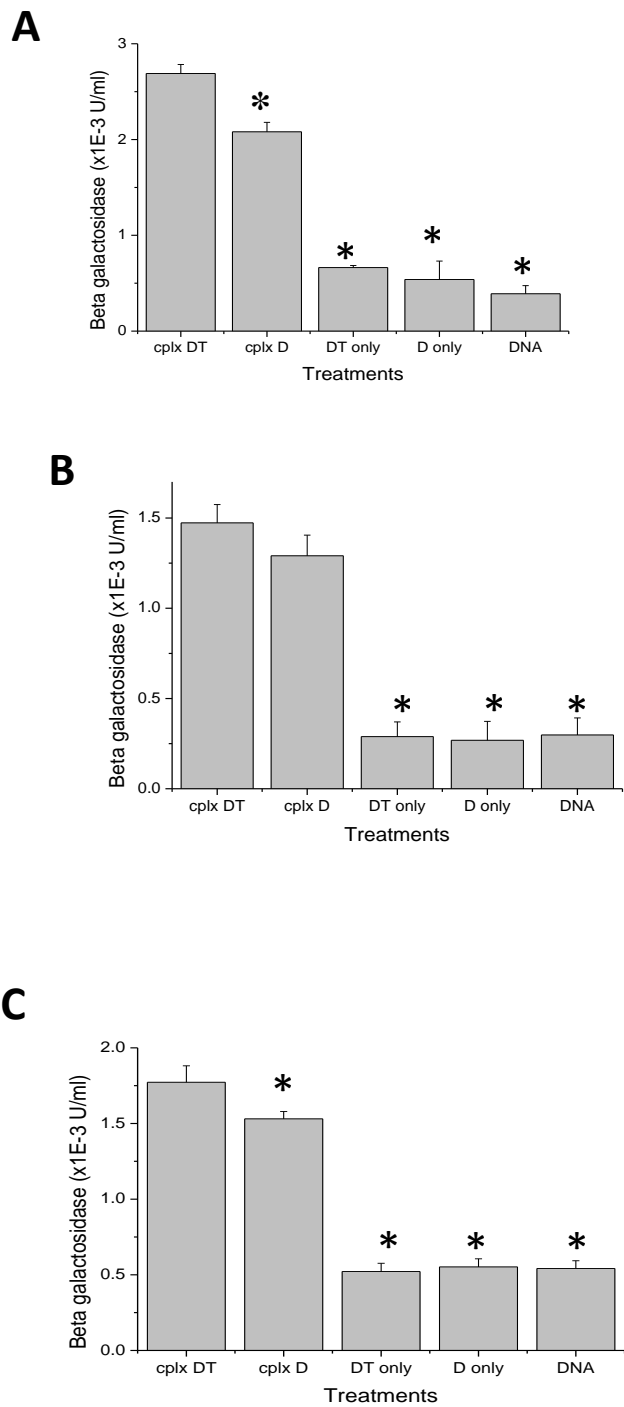


Figure 3.2: Transfection efficacy of DAB-Tf (“cplx DT”) and DAB dendriplexes (“cplxD”) in PC-3 (A), DU145 (B) and LNCaP cells (C). DAB-Tf and DAB dendriplexes were dosed at their optimal dendrimer: DNA ratio of 10:1 and 5:1 respectively. (Controls: DAB-Tf (“DT only”), DAB (“D only”) and naked DNA). Results are expressed as the mean \pm SEM of three replicates (n=15). *: P < 0.05 vs. the highest transfection ratio. Cplx D: Diaminobutyric dendriplex; cplx DT: Diaminobutyric polypropylenimine-transferrin dendriplex.

3.4.1.3. *In vitro* anti-proliferative activity

DAB-Tf complexed to TNF α , TRAIL and IL-12 expression plasmids significantly enhanced the *in vitro* anti-proliferative efficacy on the three prostate cancer cell lines when compared to the unconjugated dendriplex (Table 3.1). When complexed to TNF α expression plasmid, it significantly increased the *in vitro* therapeutic effect by 5.1-fold in PC-3 cells (IC₅₀: 0.27 \pm 0.04 μ g/mL), 1.7-fold in DU145 cells (IC₅₀: 1.26 \pm 0.11 μ g/mL) and by more than 100-fold in LNCaP cells (IC₅₀: 1.01 \pm 0.07 μ g/mL), compared to the unconjugated dendriplex. It was most efficacious on PC-3 cells, followed by LNCaP cells and then DU145 cells.

When complexed to TRAIL expression plasmid, DAB-Tf also increased the anti-proliferative activity, this time by 21-fold in PC-3 cells (IC₅₀: 0.85 \pm 0.03 μ g/mL), 3.5-fold in DU145 cells (IC₅₀: 0.81 \pm 0.04 μ g/mL) and 5.2-fold for LNCaP cells (IC₅₀: 1.16 \pm 0.24 μ g/mL), compared to the unconjugated dendriplex. DAB-Tf dendriplex expressing TRAIL was most efficacious on DU145 cells, closely followed by PC-3 cells and then LNCaP cells.

On the other hand, DAB-Tf complexed to IL-12 expression plasmid led to an increased anti-proliferative activity in comparison with the unmodified dendriplex, by 1.7-fold for PC-3 cells (IC₅₀: 1.11 \pm 0.16 μ g/mL), 1.5-fold for DU145 cells (IC₅₀: 0.80 \pm 0.09 μ g/mL) and more than 30-fold for LNCaP cells (IC₅₀: 3.31 \pm 0.25 μ g/mL). It was most efficacious on DU145 cells, followed by PC-3 cells and then LNCaP cells, as observed with TRAIL-expressing DAB-Tf dendriplex.

Table 3.1: Anti-proliferative efficacy of TNF- α , TRAIL-and IL-12 encoding DNA complexed with Diaminobutyric polypropylenimine-transferrin and Diaminobutyric polypropylenimine in PC-3, DU-145 and LNCaP prostate cancer cells.

IC ₅₀ ($\mu\text{g}/\text{mL}$) (mean \pm S.E.M.)						
Cell line	DNA	Formulation				
		DAB-Tf-DNA	DAB-DNA	DAB-Tf only	DAB only	DNA only
PC-3	TNF-alpha	0.27 \pm 0.04	1.40 \pm 0.47	>100	>100	>100
	TRAIL	0.85 \pm 0.03	17.90 \pm 0.19	>100	>100	>100
	IL-12	1.11 \pm 0.16	1.94 \pm 0.17	>100	>100	>100
DU-145	TNF-alpha	1.26 \pm 0.11	2.19 \pm 0.17	>100	>100	>100
	TRAIL	0.81 \pm 0.04	2.88 \pm 0.19	>100	>100	>100
	IL-12	0.80 \pm 0.09	1.25 \pm 0.03	>100	>100	>100
LNCaP	TNF-alpha	1.01 \pm 0.07	>100	>100	>100	>100
	TRAIL	1.16 \pm 0.24	6.06 \pm 4.96	>100	>100	>100
	IL-12	3.31 \pm 0.25	>100	>100	>100	>100

3.4.2. *In vivo* study

The intravenous administration of DAB-Tf dendriplex encoding TNF α resulted in PC-3 tumour regression within 24h (Figure 3.3). This effect was maintained

for 4 days, allowing the tumours to shrink to nearly half their initial size. From Day 5, some tumours kept regressing while others started growing, resulting in an overall slowdown of PC-3 tumour growth compared to the other treatments (Figure 3.3). From Day 15, the mice bearing growing tumours had to be euthanized due to their tumours reaching the maximum allowed size. The remaining mice, whose tumours were regressing or had completely disappeared, were kept until the end of the study.

The replacement of TNF α by TRAIL expression plasmid led to a different tumour growth pattern following administration of DAB-Tf dendriplex. A smaller number of PC-3 tumours were regressing compared to that observed with TNF α gene therapy, resulting in an overall slowdown of PC-3 tumour growth compared to controls.

Following administration of DAB-Tf dendriplex encoding IL-12, PC-3 tumours slowly started regressing until Day 5. From that day, some of them started growing, resulting in an overall slowdown of PC-3 tumour growth compared to controls. Unlike that observed with TNF α , none of the tumours completely disappeared.

Treatment of the DU145 tumours with DAB-Tf dendriplex encoding TNF α resulted in an overall slowdown of tumour growth compared to controls, although some tumours were regressing (Figure 3.4). From Day 20, only the mice bearing regressing tumours or no longer any tumours were still in the study.

DAB-Tf dendriplex encoding TRAIL initially led to an overall stable response for 9 days, followed by tumour growth.

The administration of DAB-Tf dendriplex encoding IL-12 resulted in an initial tumour regression for 5 days, followed by a very slow tumour growth. By contrast, all the PC-3 and DU145 tumours treated with DAB-Tf, naked DNA or left untreated, were growing throughout the experiment.

On the last day of the experiment, 60% of PC-3 and 50% of DU145 tumours treated with DAB-Tf dendriplex encoding TNF α had completely disappeared, while another 10% of DU145 tumours showed a partial response (Figures 3.3 and 3.4). As a result of treatment with DAB-Tf dendriplex encoding TRAIL, 10% of PC-3 tumours showed a complete disappearance, 20% of these tumours were regressing, while no DU145 tumours were responsive to this treatment. Finally, treatment with DAB-Tf dendriplex encoding IL-12 did not lead to any tumour disappearance on both tumour types. Only 20% PC-3 tumours showed a partial response, while another 20% remained stable. For DU145 cell line, 20% of the tumours also showed a partial response, while 10% were stable. All the tumours treated with DAB-Tf, naked DNA or left untreated were progressive for both tumour types.

The therapeutic effect resulting from treatment with DAB-Tf dendriplexes was also qualitatively confirmed by bioluminescence imaging on mice bearing subcutaneous PC-3M-luc-C6 tumours (Figure 3.5). Following treatment with DAB-Tf dendriplex encoding TNF α , luciferase expression in the

tumours gradually decreased from Day 1 to Day 11, to completely disappear at Day 11 as a result of the suppression of the entire tumour. Following treatment with DAB-Tf dendriplex encoding TRAIL, the tumours were regressing without completely disappearing at Day 11. As a result of the treatment with DAB-Tf dendriplex encoding IL-12, the tumours appeared to remain stable. All the other treatments led to an increase of luciferase expression in the growing tumours.

The improved therapeutic efficacy observed with DAB-Tf dendriplexes treatment resulted in an extended survival of 22 days compared to untreated tumours, for both cell lines (Figures 3.3 and 3.4). Treatment with naked DNA only extended the survival of the animals by 1 or 2 days compared to untreated mice.

No apparent sign of toxicity or significant weight loss were observed, suggesting that all treatments were well tolerated by the mice (Figures 3.3 and 3.4).

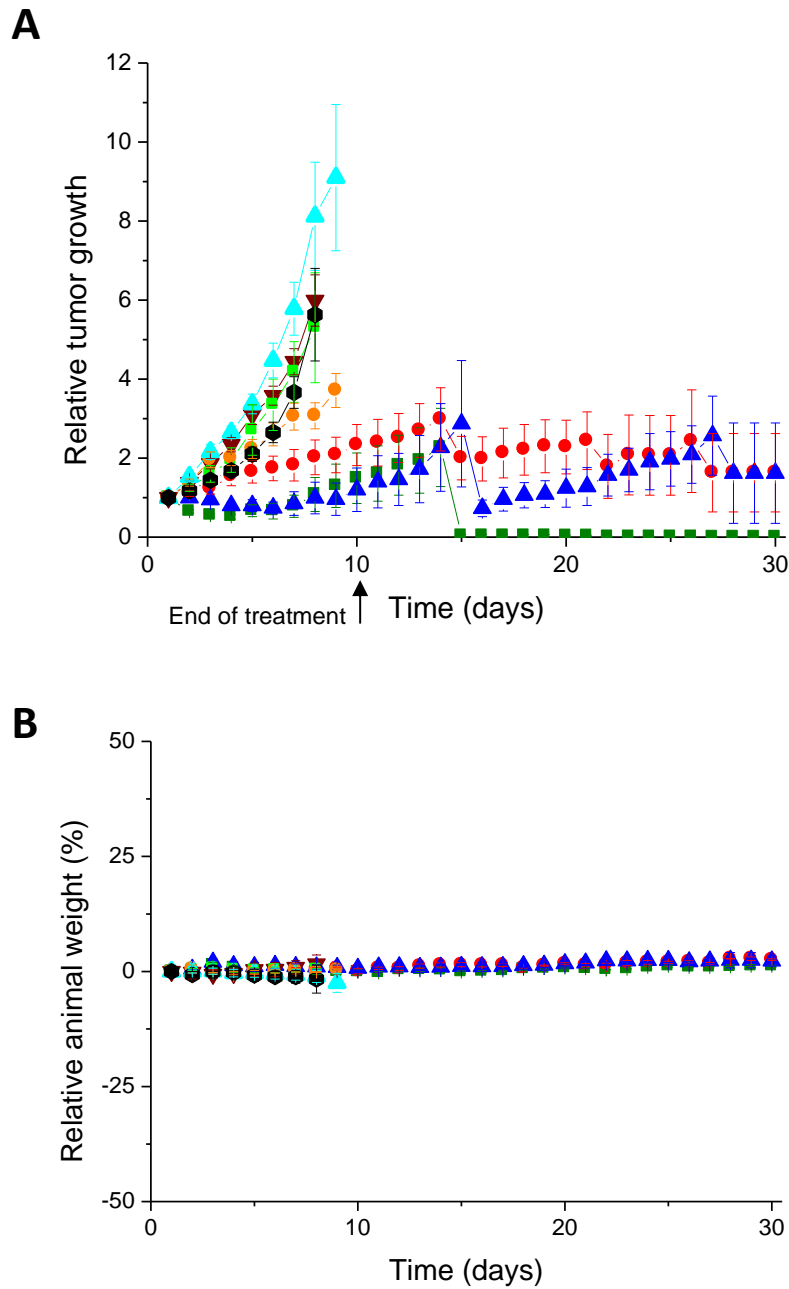


Figure 3.3: (A) Tumour growth studies in a PC-3 xenograft model after intravenous administration of transferrin- bearing DAB dendriplex carrying plasmid DNA encoding TNF α (green), TRAIL (red), IL-12 (blue) (50 μ g DNA / injection), uncomplexed DAB-Tf (brown), naked DNA encoding TNF α (pale green), naked DNA encoding TRAIL (orange), naked DNA encoding IL-12 (pale blue), untreated tumours (black) . (B) Variations of the animal body weight throughout the treatment (Colour coding as in A).

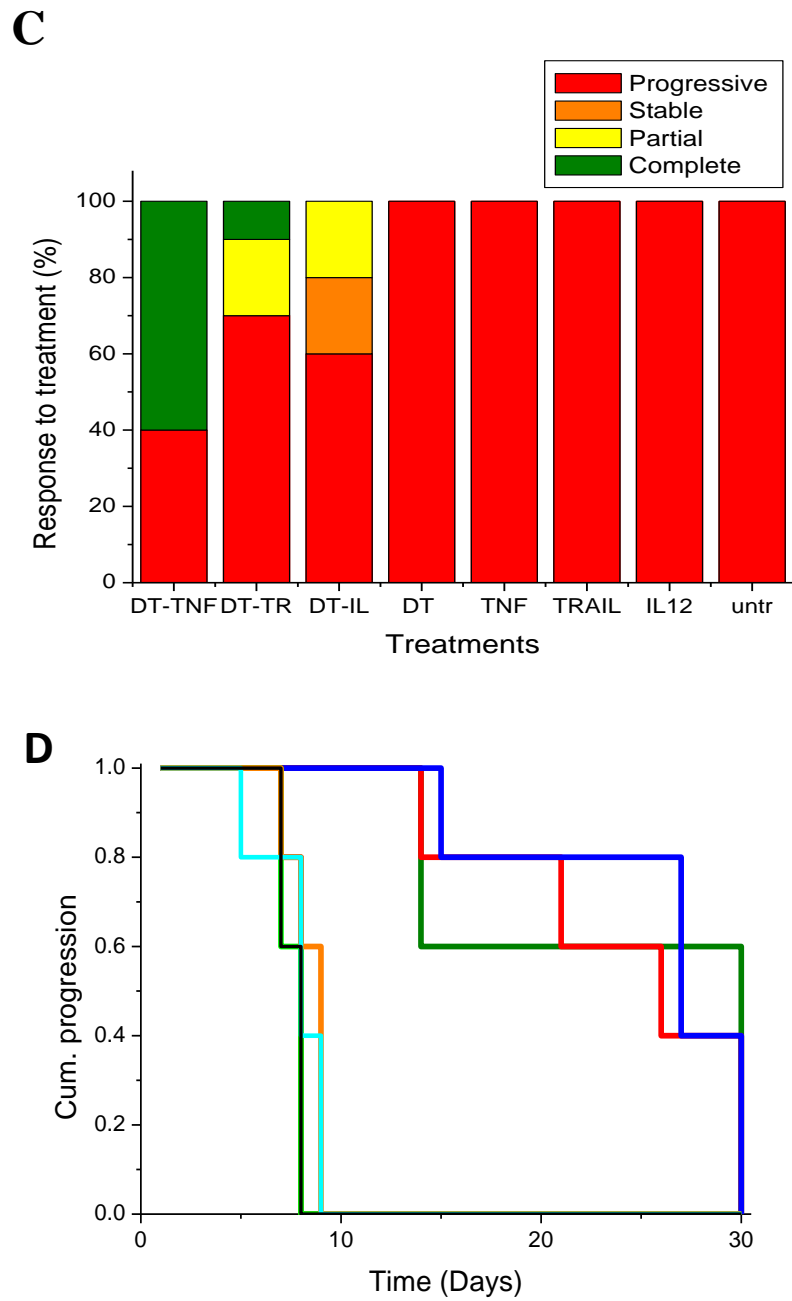


Figure 3.3 (continued): (C) Overall tumour response to treatments at the end of the study. (D) Time to disease progression. The Y axis gives the proportion of surviving animals over time. Animals were removed from the study once their tumour reached 12 mm diameter (Colour coding as in A).

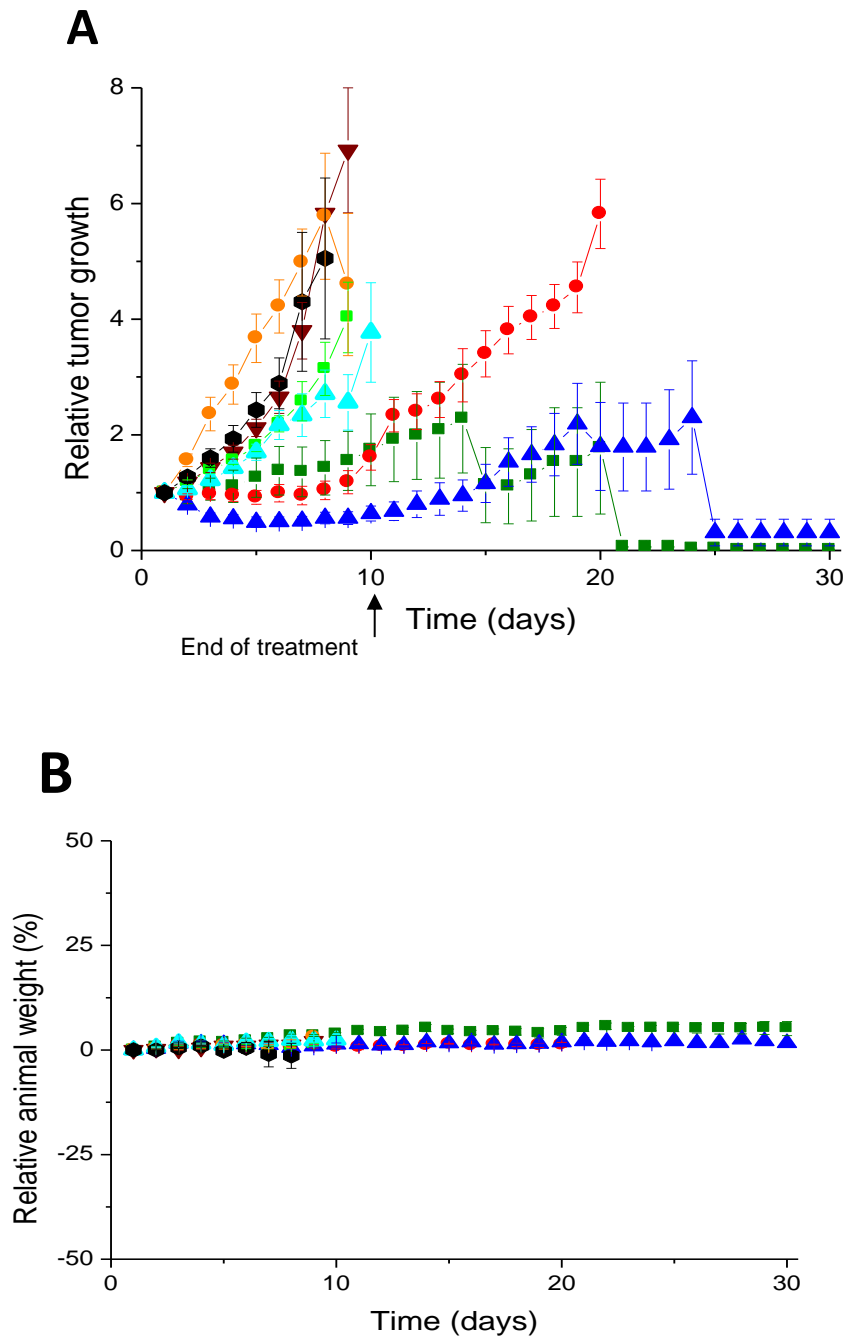


Figure 3.4: (A) Tumour growth studies in a DU145 xenograft model after intravenous administration of transferrin- bearing DAB dendriplex carrying plasmid DNA encoding TNF α (green), TRAIL (red), IL-12 (blue) (50 μ g DNA / injection), uncomplexed DAB-Tf (brown), naked DNA encoding TNF α (pale green), naked DNA encoding TRAIL (orange), naked DNA encoding IL-12 (pale blue), untreated tumours (black) . (B) Variations of the animal body weight throughout the treatment (Colour coding as in A).

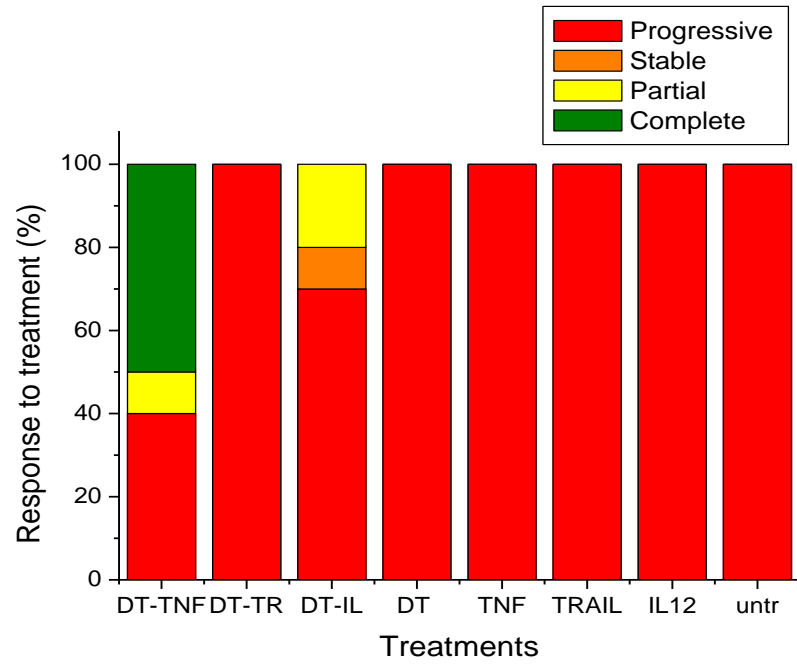
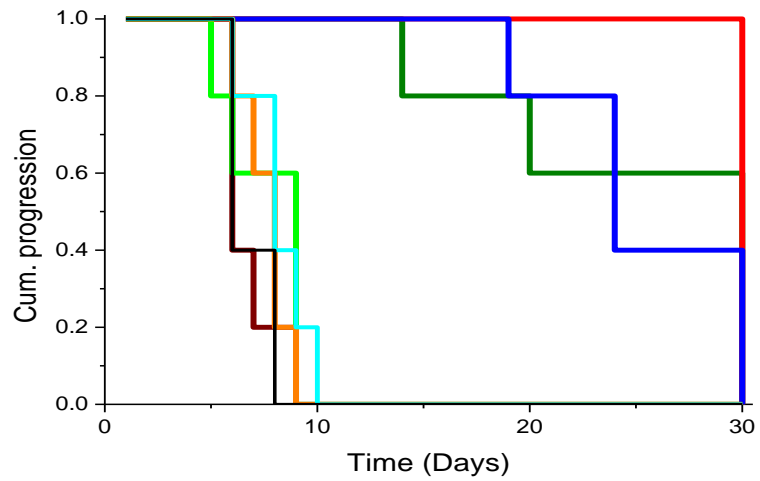
C**D**

Figure 3.4 (continued): (C) Overall tumour response to treatments at the end of the study. (D) Time to disease progression. The Y axis gives the proportion of surviving animals over time. Animals were removed from the study once their tumour reached 12 mm diameter (Colour coding as in A).

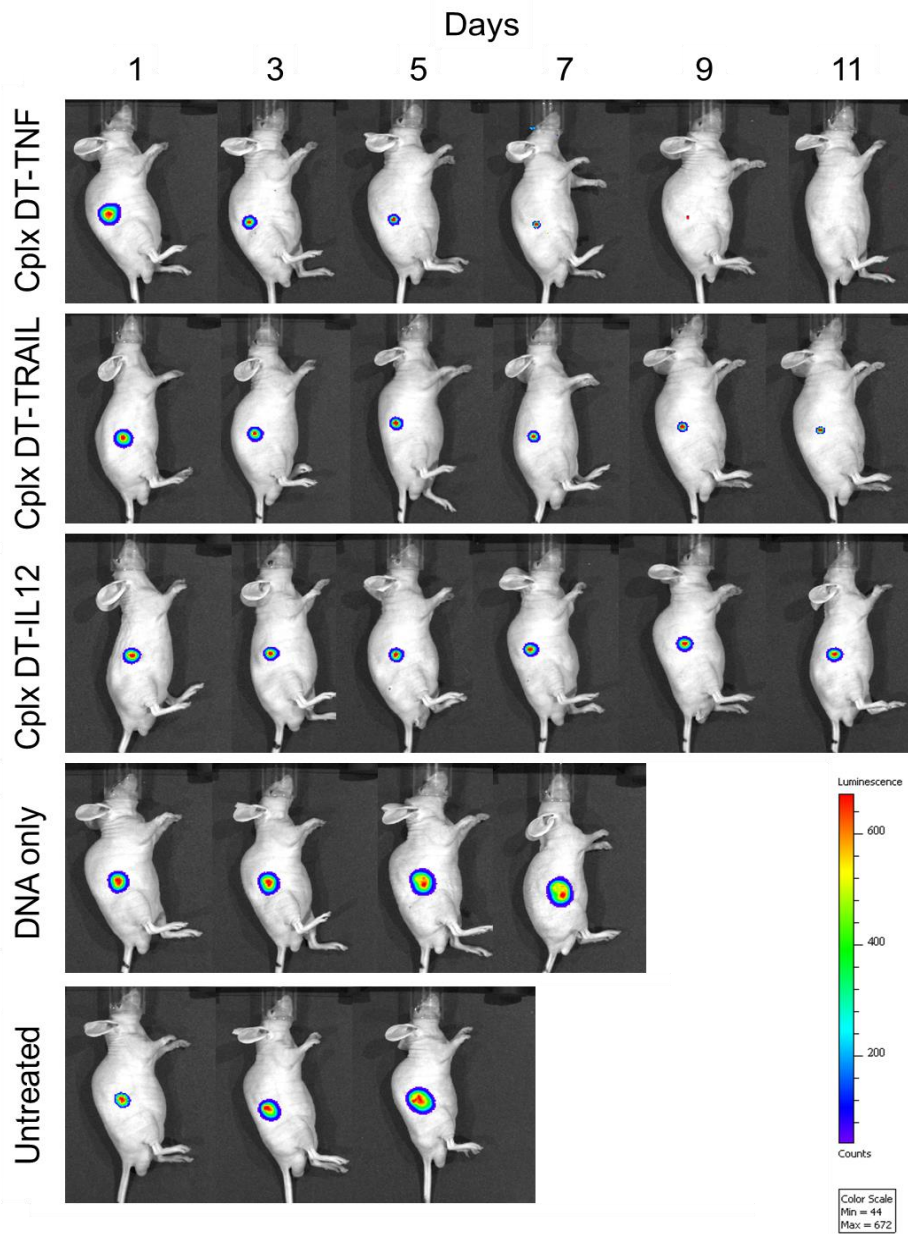


Figure 3.5: Bioluminescence imaging of the tumoricidal activity of transferrin - bearing DAB dendriplex carrying plasmid DNA encoding TNF α ("cplx DT-TNF"), TRAIL ("cplx DT-TRAIL"), IL-12 ("cplx DT-IL12") in a PC-3M-luc-C6 tumour model.

3.5. Discussion

The use of gene therapy for the treatment of recurrent prostate cancer and its metastasis is currently hampered by the lack of safe and efficacious gene delivery systems able to deliver therapeutic genes to their site of action following intravenous administration, without secondary effects to normal tissues. In order to remediate to this problem, we hypothesized that a generation 3- diaminobutyric polypropylenimine (DAB) dendriplex encoding TNF α , TRAIL and IL-12 and conjugated to transferrin, would improve the delivery of therapeutic DNA and suppress the growth of prostate cancer cell lines *in vitro* and *in vivo*. Transferrin receptors are abundantly expressed on prostate cancer cells (Liu., 2000) and have been successfully used for the delivery of liposomes to prostate tumours (Hwang *et al.*, 2008), thus making a transferrin -based tumour targeting strategy particularly interesting to explore on prostate cancer cells with the DAB dendrimer delivery system. In addition, the combination of transferrin-based active targeting and passive targeting due to the accumulation of dendriplexes resulting from the enhanced permeability and retention effect should provide a tumour-selective targeting to these dendriplexes.

Furthermore, generation 3-DAB dendrimer presents the advantage of having 100% proton able nitrogen's (van Duijvenbode., 1998), making it particularly suitable for binding the negatively charged DNA by electrostatic interactions (Kabanov., 1999).

In this study, we successfully demonstrated that the conjugation of Tf on the dendriplexes improved DNA uptake by the three prostate cancer cell lines studied, compared to control dendriplexes and naked DNA treatment. Tf receptor-mediated uptake of DNA and drugs has been extensively studied on numerous cancer cell lines (Dufès *et al.*, 2004; Fu *et al.*, 2009; Fu *et al.*, 2011; Calzolari *et al.*, 2007; Han *et al.*, 2010; Han *et al.*, 2011), but rarely on prostate cancers. Although the difference between treatments was less pronounced in our study, our results were in accordance with previous data obtained by Sahoo and colleagues (Sahoo *et al.*, 2004), who demonstrated that the uptake of Tf-conjugated, paclitaxel-loaded nanoparticles was about 3-fold higher than that of unconjugated nanoparticles in PC-3 cells. The enhanced DNA uptake resulting from treatment of the cells with a transferrin-bearing delivery system could be explained by the level of transferrin receptor protein expression on these prostate cancer cell lines. Liu previously demonstrated that transferrin receptors were overexpressed on PC-3, DU145 and LNCaP cells, with a higher level of expression on the surface of PC-3 cells (Liu, 2000).

As a consequence of this improved uptake, the treatment of the cells with DAB-Tf dendriplex resulted in an increase in gene expression on PC-3 and LNCaP cells, the improvement on DU145 being not significantly different from the gene expression level obtained with unconjugated DAB dendriplex. Overall, the most efficacious treatment observed in the *in vitro* study was DAB-Tf dendriplex expressing TNF α on PC-3 cells. By contrast, uncomplexed DAB-Tf, DAB and naked DNA did not exert any cytotoxicity to the cells at the tested

concentrations, thus demonstrating that 1) DAB-Tf and DAB dendrimers were safe for the cells in the range of concentrations used in our experiments and 2) that a tumour-targeted delivery system is needed for the effective delivery, transfection and subsequently efficacy of the therapeutic DNA on prostate cancer cells.

Our results were in agreement with the similarly improved gene expression observed by Yu *et al.* (2004) when using immunolipoplexes targeting Tf receptors on prostate cancer cells.

The use of DAB-Tf as a delivery system for TNF α , TRAIL and IL-12 expression plasmids significantly enhanced the *in vitro* therapeutic efficacy of the plasmids on the three prostate cancer cell lines studied, with improvements of up to 100-fold in LNCaP cells compared to the unconjugated dendriplex. The most efficacious treatment observed in this study was DAB-Tf dendriplex expressing TNF α on PC-3 cells, which resulted in an IC₅₀ of 0.27 ± 0.04 $\mu\text{g/mL}$. Our results were in accordance with previously published works. Kaliberov and colleagues (2004) have demonstrated that an adenoviral vector encoding the TRAIL gene under the control of the vascular endothelial growth factor receptor FLT1 promoter significantly increased DU145 cell death in comparison with the PC-3 cell line, following a similar trend to that observed in our results. In another study (Griffith *et al.*, 2000), adenoviral-mediated TRAIL treatment led to a significant increase in cytotoxicity on PC-3 cells, with 85.5% of cells dead. However, the lack of IC₅₀ values for these cell lines prevents

comparison of the anti-proliferative effects of the viral and non-viral strategies. Furthermore, we could not find any studies describing the anti-proliferative effect of TNF α - and IL-12-mediated gene therapy on PC-3, DU145 and LNCaP prostate cancers to allow a comparison with our results.

In our experiments, the IC₅₀ obtained following administration of DAB-Tf dendriplex expressing TNF α was higher than those of TRAIL and Il-12 in DU145 cells, despite being the lowest in PC-3 and LNCaP cells. This may be explained by the sensitivity of these cell lines to the Fas ligand. TNF α is well known for its ability to induce apoptosis in a wide variety of cells. However, Rokhlin and colleagues (1997) previously reported that Fas-sensitive PC-3 cell line was more sensitive to TNF α mediated apoptosis and growth inhibition than Fas-resistant DU145 and LNCaP cell lines. These results, in line with our observations, suggested that TNF α mediated apoptosis might be determined by factors that are common in both Fas and TNF α pathways.

In vivo, we demonstrated that the intravenous administration of DAB-Tf dendriplex encoding TNF α resulted in tumour eradication of 60% of PC-3 and 50% of DU145 tumours. In addition, treatment with DAB-Tf dendriplex encoding TRAIL also led to tumour eradication of 10% of PC-3 tumours. To our knowledge, it is the first time that the intravenous administration of tumour-targeted dendriplexes encoding TNF α , TRAIL and IL-12 on mice bearing prostate tumours, inhibited tumour growth and even led to complete tumour suppression in some cases. Other researchers have previously demonstrated

the ability of TNF α , TRAIL and IL-12-encoding DNA to induce a therapeutic effect on prostate tumours, but following intratumoural injection rather than intravenous administration, while using a viral delivery system rather than a non-viral one, and often in conjunction with other therapeutic modalities, such as radiotherapy (Fujita *et al.*, 2007), co-administration with oncolytic herpes simplex viruses (Varghese *et al.*, 2006), with adenoviral vector-mediated Herpes Simplex Virus / thymidine kinase and ganciclovir (Nasu *et al.*, 2001), or in addition with the drug mifepristone (Gabaglia *et al.*, 2010). For example, the intratumoural administration of an adenoviral vector encoding the TRAIL gene under the control of FLT1 promoter, in combination with radiation treatment, was shown to produce significant slowdown of the growth of DU145 tumour xenograft in athymic nude mice (Kaliberov *et al.*, 2004). In another work, the intratumoural administration of a recombinant adenovirus expressing IL-12 was shown to significantly slowdown the growth of RM-9 prostate tumours (Nasu *et al.*, 1999). Similar results were obtained by Saika and colleagues (2006) following the intratumour administration of an adenovirus-mediated IL-12 on a 178-2 BMA prostate cancer model. The effects observed in these studies were generally a slowdown of tumour growth, rather than the tumour regression or suppression observed in some instances in our experiments.

In the DU145 xenograft model, the therapeutic effect of DAB-Tf dendriplex encoding TNF α was more pronounced than that obtained with TRAIL and IL-12, contrarily to what was observed in our anti-proliferative assay *in vitro*. This could be explained by the fact that TNF α exerts its potent

cytotoxic effects on tumours *in vivo* via the death receptor-dependent apoptotic pathway, like TRAIL, but also via its anti-angiogenic effects, believed to be critical for its anti-cancer activity (Mocellin *et al.*, 2005; Mahalingam *et al.*, 2009). It actually highlights the limitation of *in vitro* experiments for predicting the anti-cancer outcome of novel therapeutic systems *in vivo*.

In this study, we have chosen to use, among other therapeutic agents, a plasmid DNA encoding IL-12. The biological effects of IL-12 encompass stimulation of unspecific immunity, such as via activation of NK cells, and stimulation of specific immunity as mediated by cytotoxic T lymphocytes. In our experiments, we had to use immunodeficient BALB/c mice unable to produce T cells in order for them to grow subcutaneous tumours of human origin. We therefore hypothesize that the therapeutic effect observed could be further improved by using a fully immunocompetent mouse bearing a murine prostate tumour model (Heinzerling *et al.*, 2002)

Our previous work, carried out with a therapeutic DNA encoding TNF α on A431 epidermoid carcinoma tumours, demonstrated the tumour targeting capability of Tf-bearing DAB dendrimer and led to a more pronounced therapeutic effect than that observed when using prostate tumour models (Koppu *et al.*, 2010). These results highlight the difficulties encountered for the treatment of prostate tumours, independently of the therapeutic strategy chosen, and explain why so many studies use combinatorial modalities to improve the overall therapeutic effect. In this study, we wanted to evaluate the

therapeutic efficacy of Tf-bearing DAB dendriplexes encoding TNF α , TRAIL and IL-12 on prostate tumour models following intravenous administration. Tumour-targeted TNF α gene therapy was more efficacious than TRAIL and IL-12, leading to tumour regression and even some tumour disappearance. Still, TRAIL and Il-12-mediated gene therapy actually improved the therapeutic efficacy on prostate tumour models, compared to the slowdown of tumour growth generally observed following intratumoural administration of adenovirus-based gene medicines, and this without any combinatorial treatment. In addition, these tumour-targeted systems are intravenously delivered, thereby allowing them to reach metastases as well as primary tumours, which is particularly important for the treatment of prostate tumours.

CHAPTER 4.

TUMOUR REGRESSION FOLLOWING INTRA- VENOUS ADMINISTRATION OF LACTOFERR- IN- AND LACTOFERRICIN-BEARING DENDR- IPLEXES

4.1. Introduction

The use of gene therapy is currently limited by the lack of delivery systems able to deliver therapeutic DNA into cancer cells efficiently and selectively without secondary effects to healthy cells (Luo *et al.*, 2000). In order to overcome this problem, numerous non-viral gene delivery systems are currently under development. Non-viral gene delivery systems vectors have attracted great interest due to their low toxicity, stability and high flexibility regarding the size of the transgene delivered (Dufès *et al.*, 2005; Li & Huang, 2007). Among these delivery systems, generation 3 diaminobutyric polypropylenimine dendrimer (DAB) appears to be particularly promising. In the previous chapter, we have demonstrated that the intravenous administration of this dendrimer conjugated to transferrin (Tf), whose receptors are overexpressed on cancer cells, resulted in gene expression mainly in the tumours. Building on our previous study, we proposed in this chapter a novel gene-based therapeutic system with improved tumour targeting and therapeutic efficacy. Basically, we propose to replace the transferrin moiety by other promising tumour-targeting ligands of the same family that additionally have intrinsic anti-tumoural activity, such as lactoferrin (Lf) and lactoferricin (Lfc).

Lf has a greater iron-binding affinity than that of transferrin and is the only protein in the transferrin family with the ability to bind to this metal over a wide pH range, including extremely acidic pH. It also exhibits a greater resistance to proteolysis. In addition, Lf's positive charges allow to bind to the negatively charged DNA (González-Chávez *et al.*, 2009) Thus, we hypothesize

that the conjugation of DAB with Lf will improve the condensation of DNA and it may also increase the electrostatic interaction of the dendriplex with the negatively charged cellular membrane, and this therefore, may improve the cellular uptake of the DNA. In addition, the concentration of its receptors on prostate cancer cells is higher than on normal cells (van Sande & Van Camp 1981), which improves the selectivity of DAB-Lf delivery system. Like Lf, Lfc not only retains the activities of Lf but is more active in terms of its strong antimicrobial and weak antiviral activities, and its potent antitumor and immunological properties (Gifford *et al.*, 2005).

Lf has been shown to inhibit the proliferation of many cancer cell lines, including nasopharyngeal carcinoma, breast carcinoma as well as head and neck cancer cell lines, through induction of cell cycle arrest and modulation of the mitogen-activated protein kinase (MAPK) signalling pathway *in vitro* (Zhou *et al.*, 2008). The inhibition of tumour cell growth by Lf may also be related to the ability of this protein to induce apoptosis of cancer cells by activating the Fas signalling pathway in cancerous cells.

Like Lf, Lfc has been shown to exert anti-tumour effects against a number of cancer cell lines. Lfc is a potent inducer of apoptosis in colon and ovarian carcinoma, neuroblastoma and melanoma (Gifford *et al.*, 2005). Lfc has also been reported to exert potent *in vivo* anti-tumour activity in mouse models of cancer. For example, direct injection of Lfc into solid Meth A tumours causes tumour cell lysis and a significant reduction in tumour size (Eliassen *et al.*,

2002). In addition, subcutaneous administration of Lfc inhibits tumour metastasis by highly metastatic murine L5178Y-ML25 lymphoma cells and B16-F10 melanoma cells (Yoo *et al.*, 1997). We therefore hypothesize that using Lf and Lfc as tumour-targeted ligands would improve the overall efficacy of the DAB delivery system.

4.2. Aims and Objectives

In this study, we investigated if the conjugation of the polypropylenimine dendrimer to lactoferrin and lactoferricin, whose receptors are overexpressed on cancer cells, could result in a selective gene delivery to tumours and a subsequently enhanced therapeutic efficacy.

The objectives of this study were:

- 1) Preparation and characterization of lactoferrin- and lactoferricin-bearing DAB dendrimers.
- 2) Evaluation of their targeting and therapeutic efficacy on cancer cells *in vitro* and *in vivo* after intravenous administration.

4.3. Methods

4.3.1. Synthesis and characterization of lactoferrin- and lactoferricin-bearing DAB dendrimers

4.3.1.1. Conjugation of lactoferrin and lactoferricin to DAB

Lactoferrin (Lf) and lactoferricin (Lfc) were conjugated to generation 3-diaminobutyric polypropylenimine dendrimer (DAB) in a similar manner to

that previously reported for the preparation of other conjugates (Koppu *et al.*, 2010; Aldawsari *et al.*, 2011; Al Robaian *et al.*, 2013). DAB (24 mg) was added to lactoferrin or lactoferricin (6 mg) and dimethylsuberimidate (12 mg) in triethanolamine HCl buffer (pH 7.4, 2 mL). The coupling reaction was allowed to take place for 2 h at 25°C whilst stirring. The conjugates were purified by size exclusion chromatography using a Sephadex G75 column and freeze-dried. The grafting of lactoferrin and lactoferricin to DAB was assessed by ¹H NMR spectroscopy using a Jeol Oxford NMR AS 400 spectrometer.

4.3.1.2. Characterization of dendriplex formation

The ability of DNA to form complexes with DAB-Lf and DAB-Lfc dendrimers was assessed by PicoGreen[®] assay, following the protocol provided by the supplier. PicoGreen[®] reagent was diluted 200-fold in Tris-EDTA buffer (10 mM Tris, 1mM EDTA, pH 7.5) on the day of the experiment. One mL PicoGreen[®] solution was added to 1 mL of dendrimer-DNA complexes prepared at various dendrimer : DNA weight ratios (20:1, 10:1, 5:1, 2:1, 1:1, 0.5:1, 0:1). The DNA concentration in the complexes (10 µg/mL) was kept constant during the experiment. The fluorescence intensity of the complexes was analysed at various time points with a Varian Cary Eclipse Fluorescence spectrophotometer (Palo Alto, CA) (λ_{exc} : 480 nm, λ_{em} : 520 nm). Results were represented as percentage of DNA condensation (= 100 - % relative fluorescence to DNA control) and compared with those obtained for DAB-DNA complex (dendrimer: DNA weight ratio 5:1) (n=4).

DNA condensation ability of DAB-Lf and DAB-Lfc was also assessed by agarose gel retardation assay. Dendriplexes were prepared at a final DNA concentration of 20 µg/mL. After mixing with loading buffer, the samples (15 µl) were loaded on a 1X Tris-Borate-EDTA (TBE) (89 mM Tris base, 89 mM boric acid, 2 mM Na₂-EDTA, pH 8.3) buffered 0.8% (w/v) agarose gel containing ethidium bromide (0.4 µg/mL), with 1x TBE as a running buffer and HyperLadder I as a DNA size marker. The gel was run at 50 V for 1 h and then photographed under UV light. Nanoparticles of DAB-Lf and DAB-Lfc complexed with DNA were also visualized by transmission electron microscopy, as previously described (Aldawsari *et al.*, 2011). Formvar/Carbon-coated 200 mesh copper grids were glow discharged and specimens in distilled water were dried down with filter paper to a thin layer onto the hydrophilic support film. Twenty µL of 1% aqueous methylamine vanadate stain (NanoVan) was applied and the mixture dried down immediately using filter paper. Dried specimens were imaged with a LEO 912 energy filtering transmission electron microscope operating at 120 kV. Contrast enhanced, zero-loss energy filtered digital images were recorded with a 14 bit /2K CCD camera.

4.3.1.3. Dendriplex size and zeta potential measurement

Size and zeta potential of DAB-Lf and DAB-Lfc dendriplexes prepared at various dendrimer : DNA weight ratios (20:1, 10:1, 5:1, 2:1, 1:1, 0.5:1, 0:1) were measured by photon correlation spectroscopy and laser Doppler electrophoresis using a Malvern Zetasizer Nano-ZS (Malvern Instruments, Malvern, UK).

4.3.2. *In vitro* biological characterization

4.3.2.1. Cell culture

A431, T98G and B16-F10-luc-G5 cell lines overexpressing Tf receptors were grown as monolayers in DMEM (for A431 and T98G cells) or RPMI-1640 medium (for B16-F10-luc-G5 cells) supplemented with 10% (v/v) foetal bovine serum, 1% (v/v) L-glutamine and 0.5% (v/v) penicillin-streptomycin. Cells were cultured at 37C° in a humid atmosphere of 5% carbon dioxide.

4.3.2.2. *In vitro* transfection

Transfection efficacy of the DNA carried by DAB-Lf and DAB-Lfc dendrimers was assessed by a β -galactosidase transfection assay, using a plasmid DNA encoding β -galactosidase (pCMV β gal). A431, B16-F10 and T98G cells were seeded in quintuplicate at a density of 2 000 cells/well in 96-well plates. After 72h incubation, the cells were treated with the DAB-Lf and DAB-Lfc dendriplexes at the following dendrimer: DNA weight ratios : 20:1, 10:1, 5:1, 2:1, 1:1, 0.5:1, 0:1. DNA concentration (10 μ g/mL) was kept constant for all the formulations tested. Naked DNA served as a negative control, DAB-DNA (dendrimer: DNA weight ratio 5:1) served as a positive control. After 72 h incubation, cells were lysed with 1X passive lysis buffer (PLB) (50 μ L/well) during 20 min. The cell lysates were then analysed for β -galactosidase expression. Briefly, 50 μ L of the assay buffer (2 mM magnesium chloride, 100 mM mercaptoethanol, 1.33 mg/mL o-nitro phenol- β -galactopyranoside, 200 mM sodium phosphate buffer, pH 7.3) were added to each well containing the

lysates. After 2 h incubation at 37°C, the absorbance of the samples was read at 405 nm with a plate reader (Thermo Lab Systems, Multiscan Ascent, and UK).

4.3.2.3. Cellular uptake

Imaging of the cellular uptake of the DNA carried by DAB-Lf and DAB-Lfc was carried out by confocal microscopy. Plasmid DNA encoding β -galactosidase was labelled with the fluorescent probe Cy3 using a Label IT[®] Cy3 Nucleic Acid Labelling kit, as described by the manufacturer. A431, B16-F10 and T98G cells were seeded on coverslips in 6-well plates (10^4 cells/ well) and grown at 37°C for 24 h. They were then incubated for 24 h with Cy3-labeled DNA (2.5 μ g DNA/ well) complexed to DAB-Lf, DAB-Lfc and DAB (dendrimer: DNA weight ratios of 2:1 for DAB-Lf and DAB-Lfc, 5:1 for DAB (Lemarié *et al.*, 2012; Zinselmeyer *et al.*, 2002). Control slides were treated with naked DNA. The cells were then washed three times with PBS and fixed with methanol for 10 min. DAPI was used to stain the nuclei and the cells were examined using a Leica TCS SP5 confocal microscope. DAPI was excited with the 405 nm laser line (bandwidth: 415-491nm), whereas Cy3 was excited with the 543 nm laser line (bandwidth: 550-620 nm).

4.3.2.4. *In vitro* anti-proliferative activity

Anti-proliferative activity of DAB-Lf and DAB-Lfc complexed with a TNF α expression plasmid was assessed in A431, B16-F10 and T98G cancer cell lines. The cells were seeded in quintuplicate at a density of 2 000 cells/well in 96-well plates 72 h before treatment. Following seeding, they were then incubated for 72 h with the DNA formulations at final concentrations of 1.28×10^{-3} to 100

µg/mL. Anti-proliferative activity was evaluated by measurement of the growth inhibitory concentration for 50% of the cell population (IC₅₀) in a MTT assay. Absorbance was measured at 570nm using a plate reader. Dose-response curves were fitted to percentage absorbance values to obtain IC₅₀ values (three independent experiments, with n=5 for each concentration level).

4.3.3. *In vivo* study

The *in vivo* experiments described below were approved by the local ethics committee and performed in accordance with the UK Home Office regulations.

4.3.3.1. Biodistribution of gene expression

A431 cancer cells in exponential growth were subcutaneously implanted to both flanks of female immunodeficient BALB/c mice (1 x 10⁶ cells per flank). When tumours became palpable, vascularized and reached a diameter of 5 mm, the mice were treated with a single intravenous injection of DAB-Lf, DAB-Lfc and DAB dendrimers carrying β-galactosidase expression plasmid (50 µg of DNA). They were sacrificed 24 h after injection and their organs were removed, frozen in liquid nitrogen, before being analysed for their β-galactosidase levels (Zinselmeyer *et al.*, 2003).

4.3.3.2. *In vivo* tumoricidal activity

A431 and B16-F10-luc-G5 cancer cells in exponential growth were subcutaneously implanted to the mice as described above. The mice bearing vascularized, palpable tumours were treated by intravenous tail vein injection of DAB-Lf and DAB-Lfc dendrimers complexed with TNFα expression plasmid,

the non-targeted DAB dendrimer carrying the same plasmid, and naked DNA (50 µg of DNA) once daily for 10 days. The weight of the mice was measured every day as a surrogate marker of toxicity and tumour volume was determined by calliper measurements (volume = $d^3 \times \pi/6$). Results were expressed as relative tumour volume (rel. Vol_{tx} = Vol_{tx} /Vol_{t0}) and responses classified analogous to Response Evaluation Criteria in Solid Tumours (RECIST) (Eisenauer *et al.*, 2009).

4.3.3.3. Statistical Analysis

Results were expressed as means ± standard error of the mean (S.E.M). Statistical significance was assessed by one-way analysis of variance (ANOVA) and Bonferroni multiple comparison post-test (Graph Pad Prism software). Differences were considered statistically significant for P values lower than 0.05.

4.4. Results

4.4.1. Synthesis and characterization of lactoferrin- and lactoferricin-bearing DAB dendrimers

4.4.1.1. Conjugation of lactoferrin and lactoferricin to DAB

The synthesis of DAB-Lf and DAB-Lfc was confirmed by ¹H NMR (Figure 4.1). Spin systems for each moiety were confirmed by ¹H-¹H COSY : ¹H NMR (D₂O) δ: DAB-(H₂N-**CH**₂-CH₂-CH₂-N-) = 3.20-3.45; DAB (-N-**CH**₂-CH₂-**CH**₂-N-) = 2.45-3.00; DAB (O=CHN-**CH**₂-CH₂) = 3.85-4.00; terminal Gly in lactoferrin/lactoferricin (1H) = 3.4; terminal Ala in lactoferrin/lactoferricin (1H) = 3.30; Ala (2H) = 1.65; terminal Val in lactoferrin/lactoferricin (1H) = 2.94; Val (CH₃) = 1.30;

terminal Ile in lactoferrin/lactoferricin (1H) = 2.95; Ile (2H) = 1.65 and 1.41 overlapping with Ala; Ile (2H) = 1.75; Ile (2CH₃) = 1.30 (overlapping). The characteristic triplet peak for the CH₂ adjacent to peripheral primary amino group of DAB at 2.78 was shifted to 3.68 ppm in the NMR spectrum of a conjugated DAB- Lf/Lfc analogue. ¹H NMR spectra showed that 50% of the surface group of dendrimer DAB was bound to 8 units of amino acids as signified by the ratio of the integrals of resonances at ca. 3.69 and 2.78 for methylene units (**d** and **a**) attached to the amide-linked bound amino acid moiety and unbound free amine, respectively.

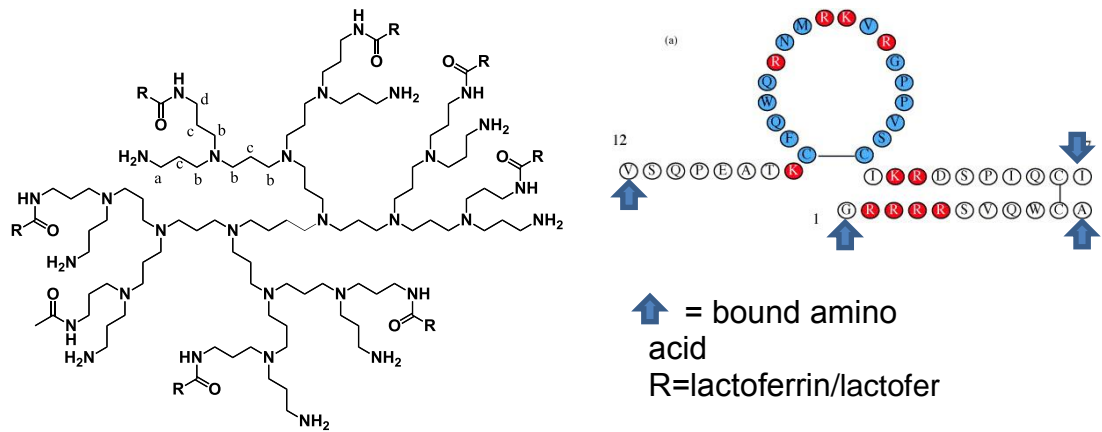
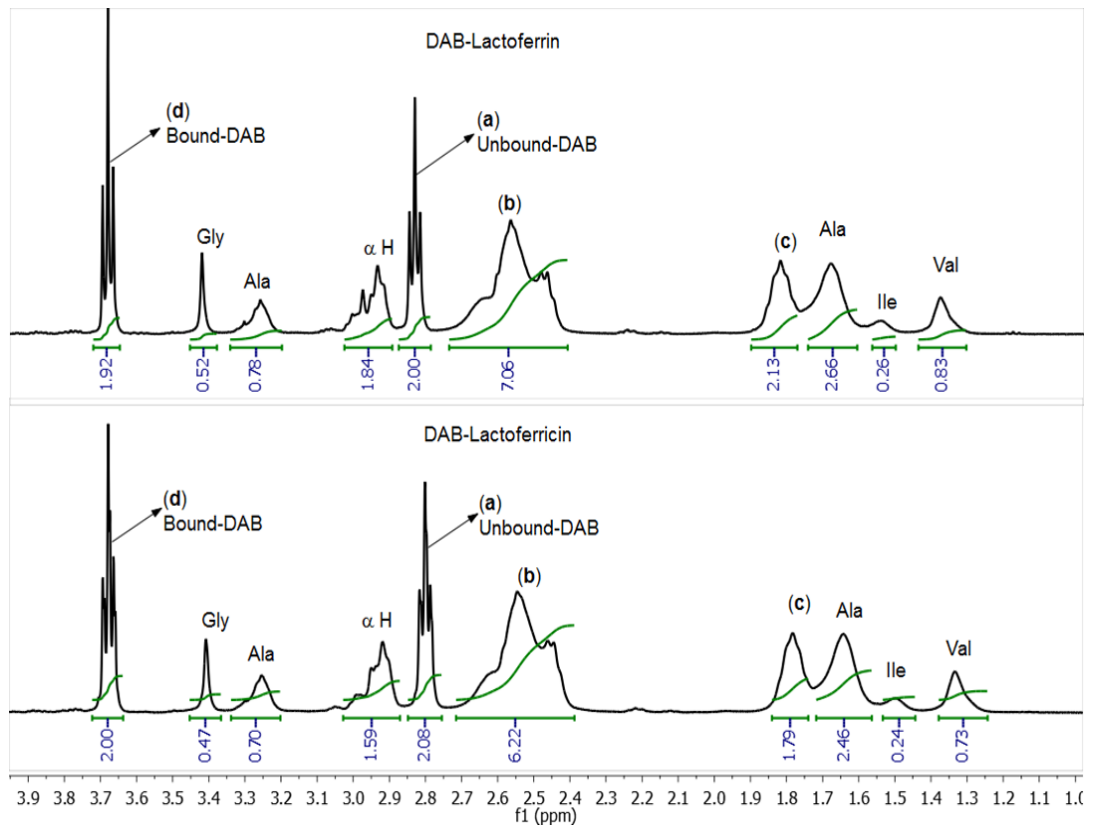


Figure 4.1: ^1H NMR spectra of DAB-Lf (A), DAB-Lfc (B).

4.4.1.2. Characterization of dendriplex formation

DAB-Lf and DAB-Lfc were able to condense more than 80% and 90% of the DNA, respectively, at dendrimer: weight ratios of 2:1 or higher (Figure 4.2). DNA condensation occurred almost instantaneously and was found to be stable over at least 24h. It increased with increasing weight ratios and was almost complete at a dendrimer: DNA weight ratio of 20:1 for DAB-Lfc dendrimer. The DNA condensation observed for dendrimer: DNA weight ratios of 2:1 or higher was much higher than that observed for the unmodified dendrimer, which was of 60% at its best and decreasing with time.

A gel retardation assay confirmed the DNA condensation by DAB-Lf and DAB-Lfc dendrimers (Figure 4.3). At dendrimer: DNA weight ratios ranging from 20:1 to 1:1, DNA appeared to be fully condensed by DAB-Lf and DAB-Lfc, thus preventing ethidium bromide to intercalate with DNA. No free DNA was therefore visible at these ratios.

The formation of spherical nanoparticles of DAB-Lf and DAB-Lfc complexed to DNA was also demonstrated by transmission electron microscopy (Figure 4.4). The results demonstrated that DAB-Lf and DAB-Lfc can condense DNA via electrostatic interactions between the positively charged dendrimer and the negatively charged DNA. An excess of dendrimer was however required to ensure efficient DNA condensation.

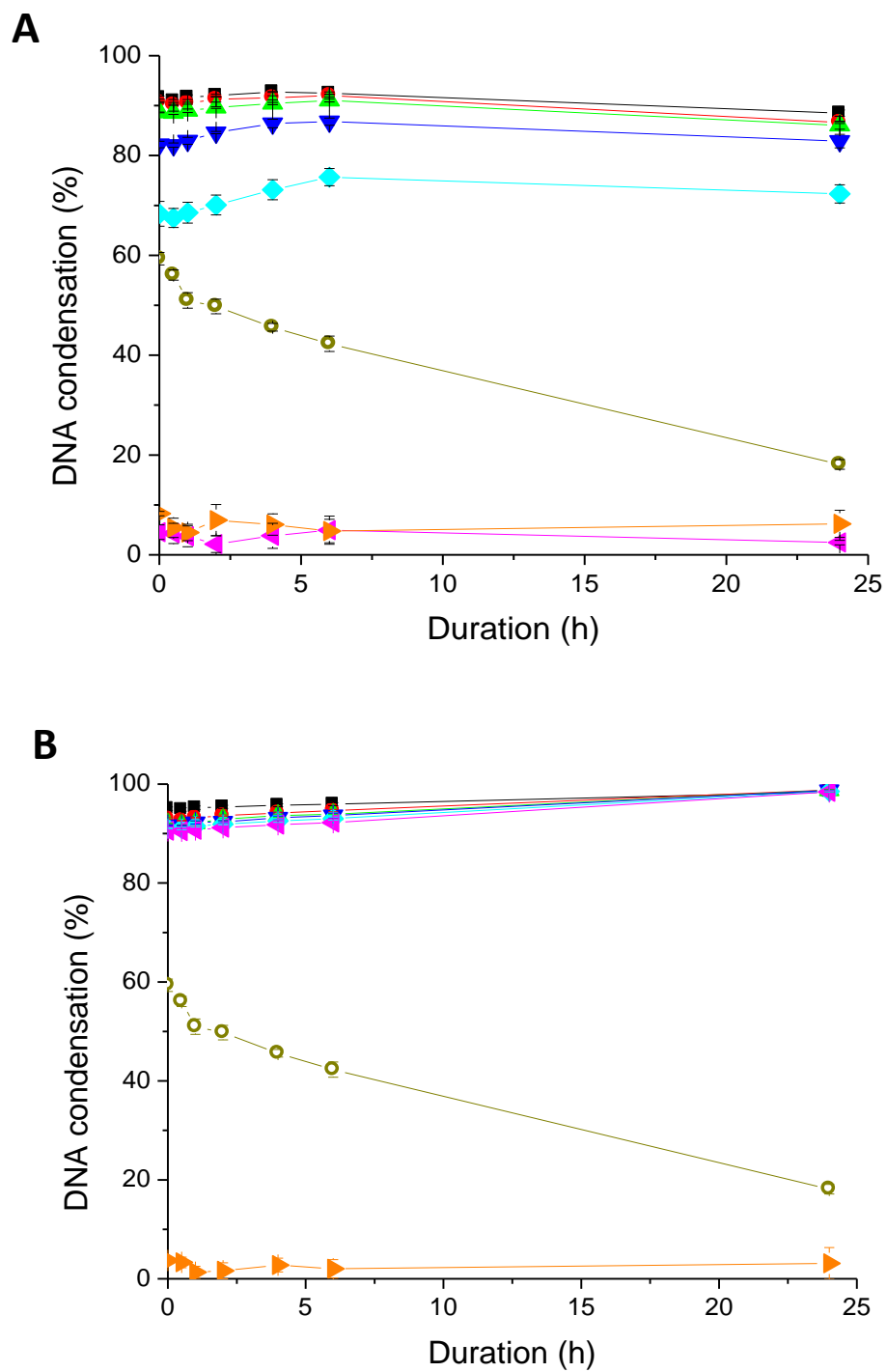


Figure 4.2: DNA condensation of DAB-Lf and DAB-Lfc dendriplexes using PicoGreen® reagent at various durations and dendrimer: DNA weight ratios : 20:1 (■, black), 10:1 (●, red), 5:1 (▲, green), 2:1 (▼, blue), 1:1 (◆, cyan), 0.5:1 (◄, pink), DNA only (▶, orange) (empty symbol, dark yellow : DAB-DNA, dendrimer: DNA weight ratio: 5:1) . Results are expressed as mean \pm SEM (n= 4).

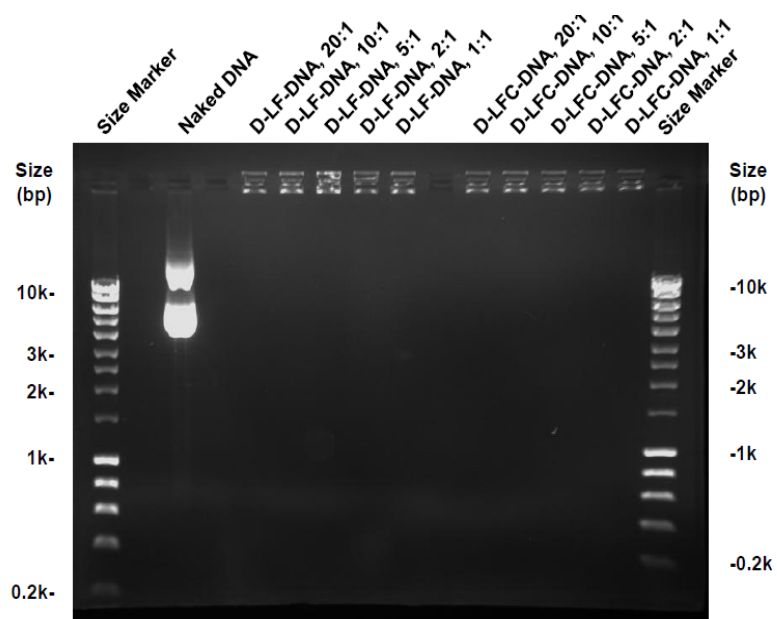


Figure 4.3: Gel retardation assay of DAB-Lf and DAB-Lfc dendriplexes at various dendrimer: DNA weight ratios: 20:1, 10:1, 5:1, 2:1, 1:1, and DNA only.

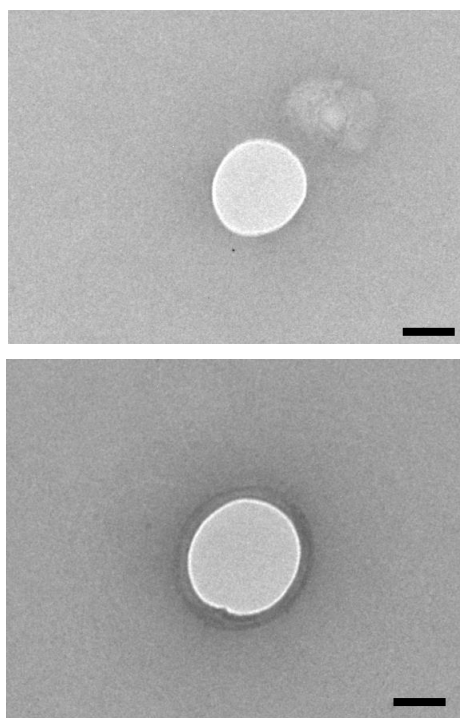


Figure 4.4: Transmission electron micrographs of a) DAB-Lf and b) DAB-Lfc dendriplexes (Bar: 100 nm).

4.4.1.3. Dendriplex size and zeta potential measurement

DAB-Lf and DAB-Lfc dendriplexes displayed average sizes less than 300 nm, at all weight ratios tested (Figure 4.5). The increase of dendrimer: DNA weight ratios did not have a significant impact on the dendriplexes size. Among the two tested targeted dendrimers, DAB-Lf dendriplex at a dendrimer: DNA ratio of 2:1 was found to be the largest, with an average size of 260 ± 18 nm. In contrast, DAB-Lf dendriplex at a dendrimer: DNA ratio of 0.5:1 was the smallest, with an average size of 208 ± 15 nm.

Zeta potential experiments demonstrated that DAB-Lf and DAB-Lfc dendriplexes were bearing a positive surface charge at all dendrimer: DNA weight ratios. The zeta potential values of DAB-Lf dendriplex reached their maximum (35 ± 2 mV) at a weight ratio of 2, before decreasing with increasing weight ratios and finally reaching their minimum (23 ± 1 mV) at a weight ratio of 20. The zeta potential values of DAB-Lfc followed a similar pattern, namely reaching a maximum (33 ± 1 mV) at a weight ratio of 1 and then decreasing with increasing weight ratios to attain the same value as for DAB-Lf dendriplex (23 ± 6 mV at a weight ratio of 20).

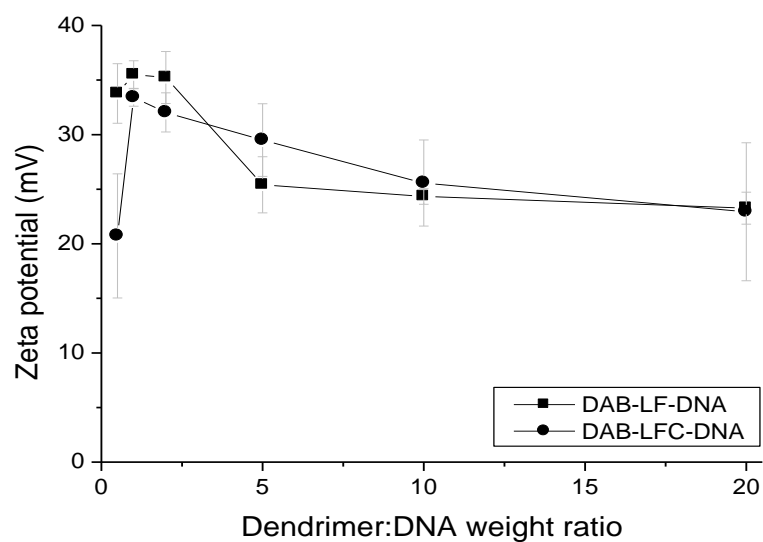
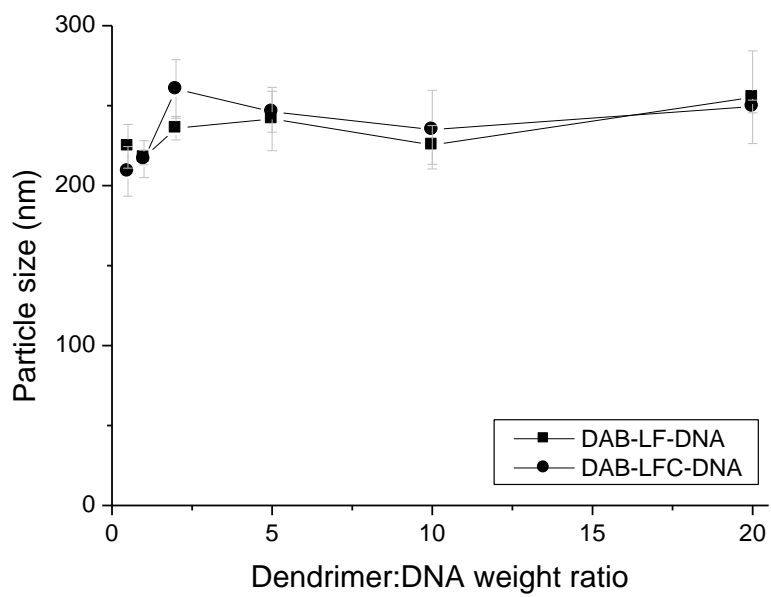


Figure 4.5: Size (A) and Zeta Potential (B) of DAB-Lf and Lfc dendriplexes at various dendrimer:DNA weight ratios: 20:1, 10:1, 5:1, 2:1, 1:1, and 0.5:1. Result are expressed as mean \pm SEM (n=4).

4.4.2. *In vitro* study

4.4.2.1. *In vitro* transfection

The treatment of A431, B16-F10 and T98G cells with DAB-Lf and DAB-Lfc dendriplexes resulted in an increase in gene expression on all the tested cell lines for some dendrimer: DNA ratios.

The highest transfection level after treatment with DAB-Lf and DAB-Lfc dendriplexes was obtained at a dendrimer: DNA weight ratio of 2:1 in A431, B16-F10 and T98G cells (Figure 4.6).

At this ratio, in A431 cells, treatment with DAB-Lfc dendriplex led to the highest transfection ($4.96 \times 10^{-3} \pm 0.19 \times 10^{-3}$ U/mL), which was about 1.4-fold higher than that observed with DAB-Lf dendriplex ($3.45 \times 10^{-3} \pm 0.10 \times 10^{-3}$ U/mL) (Figure 4.6A). By contrast, the highest transfection in B16-F10 cells was obtained after treatment with DAB-Lf dendriplex ($12.07 \times 10^{-3} \pm 0.07 \times 10^{-3}$ U/mL and $11.01 \times 10^{-3} \pm 0.12 \times 10^{-3}$ respectively for DAB-Lf and DAB-Lfc dendriplexes) (Figure 4.6B). In T98G cells as well, the highest transfection resulted from the treatment of the cells with DAB-Lf dendriplex ($5.71 \times 10^{-3} \pm 0.24 \times 10^{-3}$ U/mL), which was about 1.2-fold higher than that of DAB-Lfc dendriplex ($4.67 \times 10^{-3} \pm 0.16 \times 10^{-3}$ U/mL) (figure 4.6C). The conjugation of Lf and Lfc to DAB at their optimal dendrimer: DNA ratio led to an improved transfection compared to unconjugated DAB on all tested cell lines. In T98G cells as well, the highest transfection resulted from the treatment of the cells with DAB-Lf dendriplex ($5.71 \times 10^{-3} \pm 0.24 \times 10^{-3}$ U/mL), which was about 1.2-fold higher than that of DAB-Lfc dendriplex ($4.67 \times 10^{-3} \pm 0.16 \times 10^{-3}$ U/mL). The conjugation of Lf and Lfc

to DAB at their optimal dendrimer: DNA ratio led to an improved transfection compared to unconjugated DAB on all tested cell lines. Gene expression following treatment with DAB-Lf dendriplex was respectively 1.2-fold, 5.6-fold and 1.8-fold higher than following treatment with DAB dendriplex on A431, B16-F10 and T98G cells ($2.83 \times 10^{-3} \pm 0.07 \times 10^{-3}$ U/mL on A431, $2.13 \times 10^{-3} \pm 0.06 \times 10^{-3}$ U/mL on B16-F10, $3.12 \times 10^{-3} \pm 0.17 \times 10^{-3}$ U/mL on T98G cells). Following treatment with DAB-Lfc dendriplex, it was respectively 1.7-fold, 5.1-fold and 1.5-fold higher than that of DAB-DNA on A431, B16-F10 and T98G cells.

In the three prostate cancer cells, the treatment with DAB-Lf and DAB-Lfc also resulted in an increase in gene expression on all the tested cell lines. In PC-3 cells, the highest transfection was obtained after treatment with DAB-Lf dendriplex ($2.75 \times 10^{-3} \pm 1.73 \times 10^{-3}$ U/mL), which was about 1.2-fold higher than that observed with DAB-Lfc dendriplex ($2.22 \times 10^{-3} \pm 1.62 \times 10^{-3}$ U/mL) (Figure 4.7A). In DU145 cells as well, treatment with DAB-Lf dendriplex led to the highest transfection ($5.09 \times 10^{-3} \pm 1.02 \times 10^{-3}$ U/mL), which was around 1.1-fold higher than that obtained after the treatment with DAB-Lfc dendriplex ($4.46 \times 10^{-3} \pm 1.24 \times 10^{-3}$ U/mL) (Figure 4.7B). By contrast, the treatment with DAB-Lf dendriplex in LNCaP was around 1.1-fold higher than that observed with DAB-Lfc dendriplex ($2.74 \times 10^{-3} \pm 1.35 \times 10^{-3}$ U/mL and $2.55 \times 10^{-3} \pm 1.18 \times 10^{-3}$ U/mL respectively for DAB-Lfc and DAB-Lf dendriplexes) (Figure 4.7C).

On all the three prostate cancer cell lines, the conjugation of Lfc to DAB led to an improved transfection compared to unconjugated DAB. Gene expression following treatment with Lfc dendriplex was 1.1-fold higher than following treatment with unconjugated DAB dendriplex on all the three cell lines ($2.01 \times 10^{-3} \pm 1.44 \times 10^{-3}$ U/mL, $4.07 \times 10^{-3} \pm 1.25 \times 10^{-3}$ U/mL and $2.60 \times 10^{-3} \pm 1.45 \times 10^{-3}$ U/mL, for PC3, DU145 and LNCaP, respectively). By contrast, treatment with DAB-Lf dendriplex led to an improved transfection compared to unconjugated DAB on PC-3 and DU145 cell lines only. Gene expression following treatment with Lf dendriplex was respectively 1.4-fold 1.3-fold higher than that of DAB-DNA on PC-3 and DU145, while in LNCaP cell lines, gene expression following treatment with unconjugated DAB dendriplex was slightly higher (about 1.02-fold) than that of DAB-Lf dendriplex.

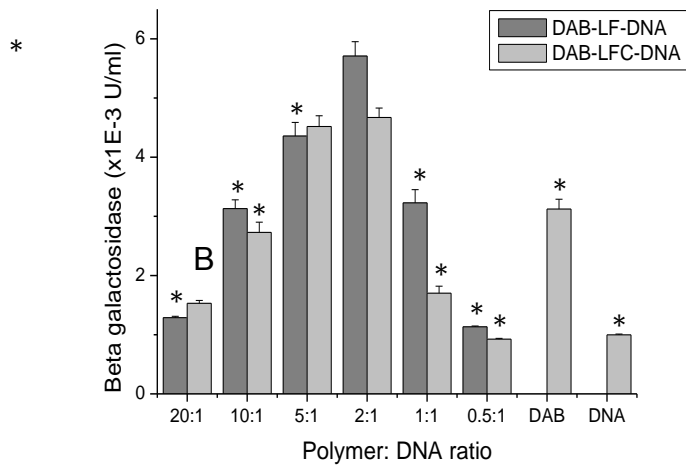
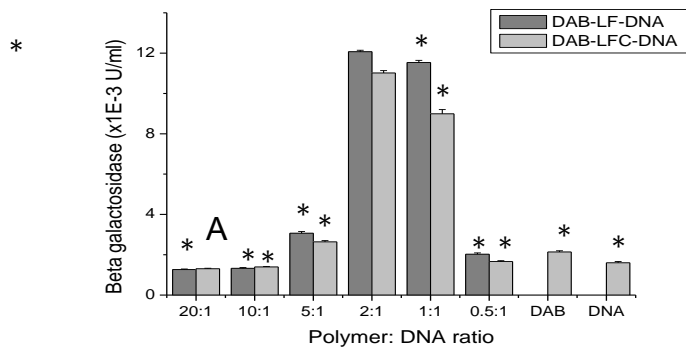
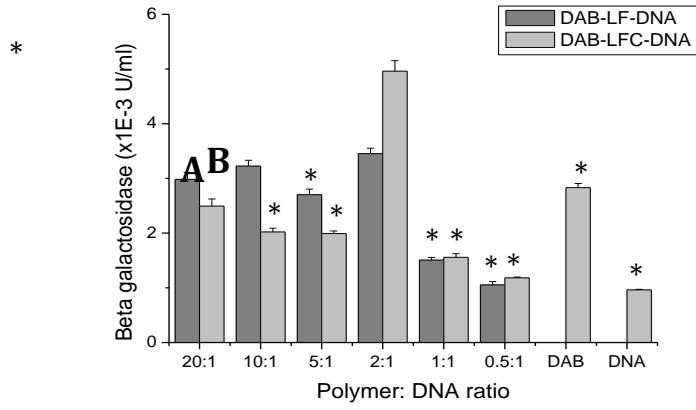


Figure 4.6: Transfection efficacy of DAB-Lf and DAB-Lfc dendriplexes at various dendrimer: DNA weight ratios in A431 (A), B16-F10 (B) and T98G cells (C). DAB-DNA was dosed at its optimal polymer: DNA ratio of 5:1. Results are expressed as the mean \pm SEM of three replicates (n=15). *: P < 0.05 vs. the highest transfection ratio.

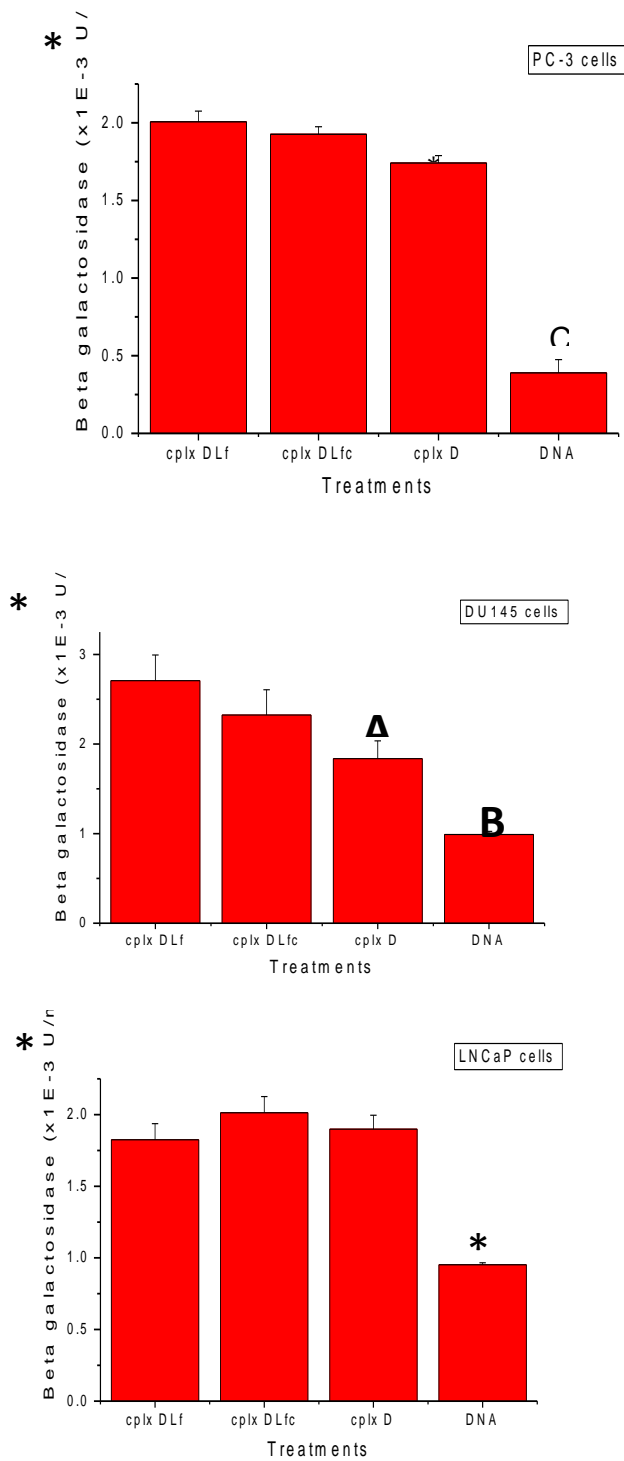


Figure 4.7: Transfection efficacy of DAB-Lf and DAB-Lfc dendriplexes in PC-3 (A), DU145 (B) and LNCaP cells (C). Results are expressed as the mean \pm SEM of three replicates (n=15). *: P <0.05 vs. the highest transfection ratio.

4.4.2.2. Cellular uptake

The cellular uptake of Cy3-labeled DNA carried by DAB-Lf and DAB-Lfc was qualitatively confirmed in the three skin cancer cell lines by confocal microscopy (Figure 4.8). Cy3-labeled DNA was disseminated in the cytoplasm after treatment with all DAB formulations in A431, B16-F10 and T98G cells. However, the DNA uptake appeared to be more pronounced in A431 and T98G cells treated with both DAB-Lf and DAB-Lfc dendriplexes. B16-F10 cells treated with DAB-Lfc dendriplex also appeared to be slightly more fluorescent than the cells treated with other DAB formulations. By contrast, cells treated with naked DNA did not show any Cy3-derived fluorescence.

In contrast, confocal microscopy experiments for prostate cancer cell lines confirmed that Cy3-labelled DNA was taken up by PC-3, DU145 and LNCaP cells (Figure 4.9). The fluorescently-labelled DNA was found to be disseminated in the cytoplasm following treatment with all DAB formulations in the three tested cell lines. However, the DNA uptake appeared to be much more pronounced after treatment with targeted dendriplexes than with the non-targeted dendriplex in PC-3, DU145 and LNCaP cell lines. Both PC-3 and DU145 cell lines appeared to be slightly more fluorescent when treated with Lfc-bearing dendriplex than with Lf-bearing dendriplex.

On prostate cancer cells, no Cy3-derived fluorescence was visible in cells treated with naked DNA. The conjugation of Lf and Lfc to DAB improved the uptake of DNA by PC-3, DU145 and LNCaP prostate cancer cells. However, the

DNA uptake appeared to be much more pronounced in skin cancer cell lines than in prostate cancer cell lines after treatment with both DAB-Lf and DAB-Lfc.

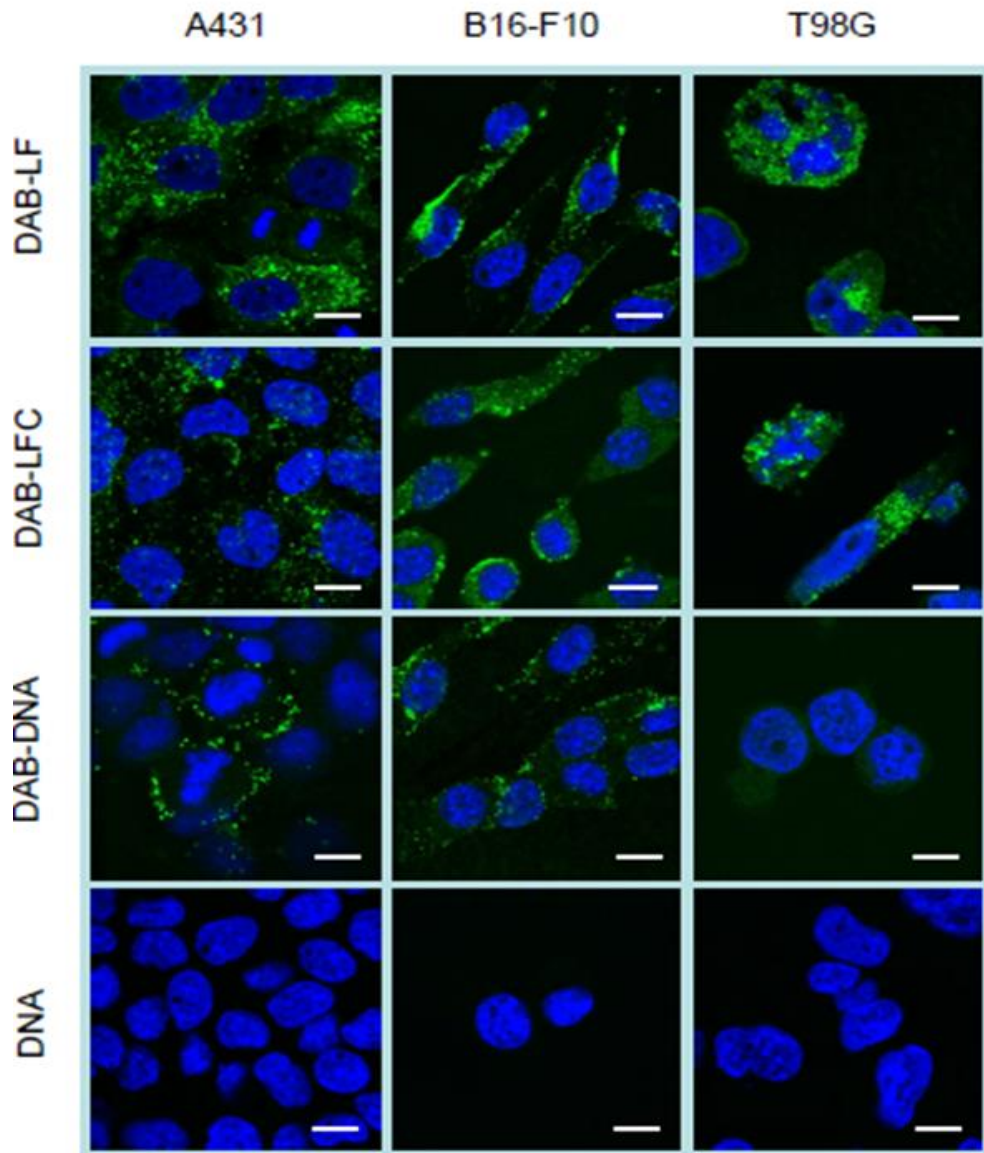


Figure 4.8: Confocal microscopy imaging of the cellular uptake of Cy3- labelled DNA (2.5 μg / well) either complexed with DAB-Lf, DAB-Lfc, DAB or in solution, after incubation for 24 hours with A431 (left) , B16-F10 (middle) and T98G cells (right) (Blue: nuclei stained with DAPI (excitation: 405 nm laser line, bandwidth: 415-491nm), green: Cy3-labeled DNA (excitation: 543 nm laser line, bandwidth: 550-620 nm) (Bar: 10 μm).

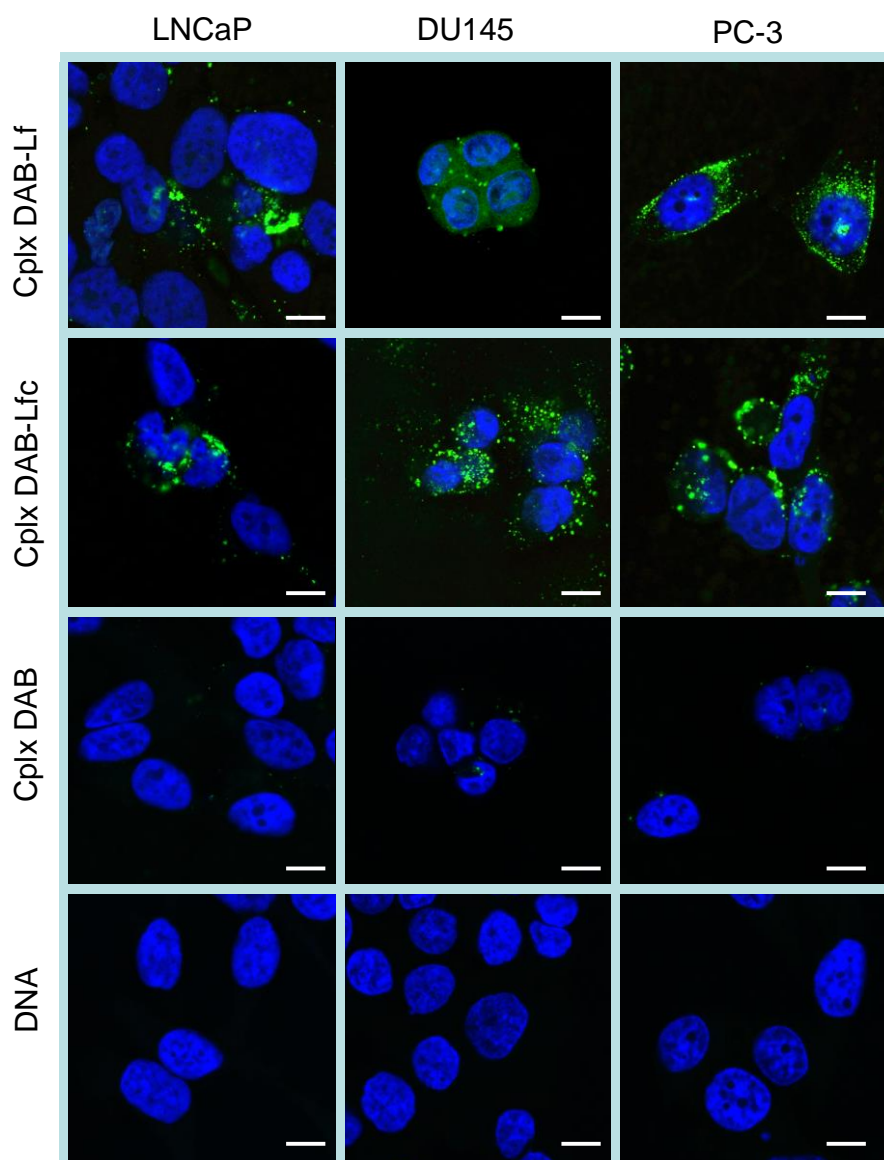


Figure 4.9: Confocal microscopy imaging of the cellular uptake of Cy3- labelled DNA (2.5 μg / well) either complexed with DAB-Lf, DAB-Lfc, DAB or in solution, after incubation for 24 hours with PC-3 (right) , DU145 (middle) and LNCaP cells (left) (Blue: nuclei stained with DAPI (excitation: 405 nm laser line, bandwidth: 415-491nm), green: Cy3-labeled DNA (excitation: 543 nm laser line, bandwidth: 550-620 nm) (Bar: 10 μm).

4.4.2.3. *In vitro* anti-proliferative activity

The conjugation of Lf and Lfc to DAB led to a significant increase of *in vitro* anti-proliferative activity in the three tested cell lines. In A431 cells, the increase

was respectively of 3.5-fold and 2.6-fold for DAB-Lf and DAB-Lfc dendriplexes compared to the unmodified DAB dendriplex (IC_{50} of $2.68 \pm 0.63 \mu\text{g/mL}$, $3.66 \pm 0.22 \mu\text{g/mL}$ respectively for DAB-Lf and DAB-Lfc dendriplexes, $9.47 \pm 1.15 \mu\text{g/mL}$ for unmodified DAB dendriplex (Table 4.1)). In B16-F10 cells, it was of 2.5-fold and 3.3-fold for DAB-Lf and DAB-Lfc dendriplexes compared to the unmodified DAB dendriplex (IC_{50} of $1.88 \pm 0.15 \mu\text{g/mL}$, $1.44 \pm 0.25 \mu\text{g/mL}$ respectively for DAB-Lf and DAB-Lfc dendriplexes, $4.72 \pm 0.32 \mu\text{g/mL}$ for unmodified DAB dendriplex). In T98G cells, however, the increase was at its highest, by 4.8-fold and 5.9-fold for DAB-Lf and DAB-Lfc dendriplexes compared to DAB dendriplex (IC_{50} of $6.20 \pm 0.71 \mu\text{g/mL}$, $5.01 \pm 0.48 \mu\text{g/mL}$ respectively for DAB-Lf and DAB-Lfc dendriplexes, $29.84 \pm 2.79 \mu\text{g/mL}$ for unmodified DAB dendriplex). By contrast, uncomplexed DAB-Lf, DAB-Lfc and naked DNA did not exert any cytotoxicity to the cells at the tested concentrations, thus raising the hypothesis that the conjugation of Lf and Lfc to DAB may hamper their intrinsic anti-cancer activity.

Table 4.1: Anti-proliferative efficacy of encoding DNA complexed with Diaminobutyric polypropylenimine-transferrin and Diaminobutyric polypropylenimine in A431, B16F10 and T98G skin cancer cells.

Cell line	DAB-Lf-DNA	DAB-Lfc-DNA	DAB-DNA	DAB-Lf only	DAB-Lfc only	DAB only	DNA Only
A431	2.68 ± 0.63	3.66 ± 0.22	9.47±1.15	>100	>100	>100	>100
B16F10	1.88 ± 0.15	1.44 ± 0.25	4.72±0.32	>100	>100	>100	>100
T98G	6.20± 0.71	5.01±0.48	29.84±2.79	>100	>100	>100	>100

In all prostate cancer cell lines, the *in vitro* anti-proliferative efficacy of DNA conjugating DAB-Lf and DAB-Lfc experiment did not give IC₅₀ values (Table 4.2). However, a previous treatment with unconjugated DAB-DNA on all three prostate cancer cell lines showed IC₅₀ values (Al Robaian *et al.*, 2013), which indicates that the experiments with DAB-Lf, DAB-Lfc and DAB-DNA will have to be repeated.

Table 4.2: Anti-proliferative efficacy of encoding DNA complexed with DAB-Lf and DAB-Lfc in PC-3, DU145 and LNCaP prostate cancer cells.

IC ₅₀ (µg/mL) (mean ± S.E.M.)					
Formulation					
Cancer cell	Therapeutic DNA	DAB-Lf-DNA	DAB-Lfc-DNA	DAB-DNA	DNA only
PC-3	TNF-alpha	> 100	> 100	>100	>100
	TRAIL	> 100	> 100	>100	>100
	IL-12	> 100	> 100	>100	>100
DU-145	TNF-alpha	> 100	> 100	>100	>100
	TRAIL	> 100	> 100	>100	>100
	IL-12	> 100	> 100	>100	>100
LnCaP	TNF-alpha	> 100	>100	>100	>100
	TRAIL	> 100	> 100	>100	>100
	IL-12	> 100	>100	>100	>100

4.4.3. *In vivo* study

4.4.3.1. Biodistribution of gene expression

The intravenous administration of control DAB dendriplex led to gene expression mainly in the liver (28.6 ± 3.3 mU β -galactosidase per organ) followed by the tumour (23.3 ± 0.5 mU β -galactosidase per organ) (Figure 4.10). By contrast, the conjugation of Lf and Lfc to DAB significantly increased

by more than 1.3-fold the gene expression in the tumour (respectively 31.9 ± 1.2 and 33.9 ± 1.5 mU β -galactosidase in the tumour for DAB-Lf and DAB-Lfc dendriplexes), while decreasing the β -galactosidase amount in the liver by 2.2-fold following treatment with DAB-Lf dendriplex (12.8 ± 2.1 mU β -galactosidase per organ) and by 1.6-fold following treatment with DAB-Lfc dendriplex (17.4 ± 3.7 mU β -galactosidase per organ). The β -galactosidase amounts in the heart were also reduced to less than 5 mU β -galactosidase per organ. In the spleen and the kidneys, gene expression reached similar levels to what was observed following treatment with non-conjugated DAB dendriplex.

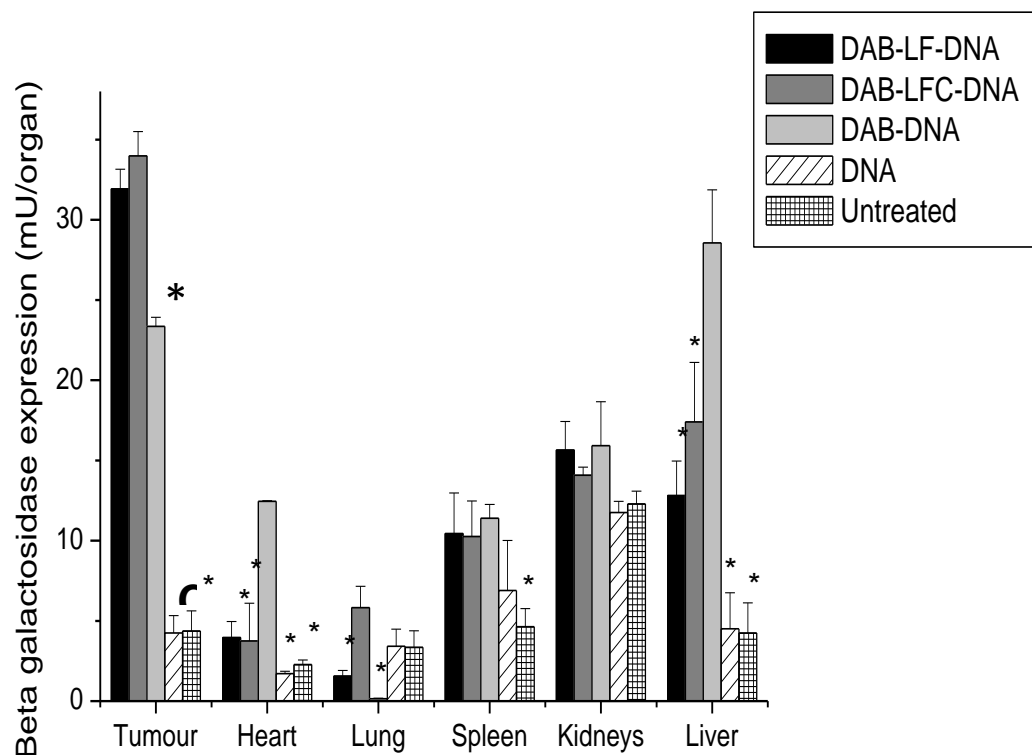


Figure 4.10: Biodistribution of gene expression after a single intravenous administration of DAB-Lf, DAB-Lfc and DAB dendriplexes (50 μ g DNA administered). Results were expressed as

milliunits β -galactosidase per organ (n=5). *: P <0.05 : highest gene expression treatment vs. other treatments for each organ.

4.4.3.2. *In vivo* tumoricidal activity

The intravenous administration of DAB-Lf, DAB-Lfc and DAB complexed to TNF α expression plasmid resulted in tumour regression of A431 tumours (Figure 4.11A). This effect was maintained for the whole duration of the experiment (30 days). By contrast, tumours treated with naked DNA grew steadily at a growth rate close to that observed for untreated tumours.

Treatment of the B16-F10 tumours with the 3 dendriplex formulations led to a different pattern, characterized by a high variability of response to treatment within a same group and an overall slowdown of tumour growth compared to naked DNA treatment (Figure 4.12A).

No apparent signs of toxicity or weight loss were observed during the experiment, thus showing the good tolerability of the treatments by the mice (Figure 4.11B and 4.12B).

On the last day of the experiment, 60% of A431 tumours treated with DAB-Lf and DAB-Lfc dendriplexes had completely disappeared, which is an improvement compared to the 40% of A431 tumours disappearing following treatment with DAB dendriplex (Figure 4.11C). The remaining A431 tumours treated by these 3 dendriplexes formulations showed a partial response.

Treatment of B16-F10 tumours with DAB-Lf dendriplex led to 40% tumour disappearance and 20 % tumour regression (Figure 4.12C). Replacing

DAB-Lf dendriplex by DAB-Lfc dendriplex led to enhanced results, with 50% tumour disappearance and 20% tumour regression. These results were better compared to those obtained with control DAB dendriplex, which resulted in 20% tumour disappearance and 40% tumour regression. By contrast, all tumours treated with naked DNA or left untreated were progressive for both tumour types.

This improved therapeutic effect resulted in an extended survival of 22 days compared to untreated mice, for all A431-bearing mice treated with targeted or control dendriplexes (Figure 4.11D). Sixty percents of B16-F10-bearing mice treated with DAB-Lf and DAB-dendriplexes had their life extended by 24 days compared to untreated mice. This enhanced survival is similar that observed following treatment with DAB-Lfc dendriplex, but the percentage of surviving animals in that case increased to 80% (Figure 4.12D). On the other hand, treatment with naked DNA did not extend the survival of the animals compared to untreated mice.

End
of

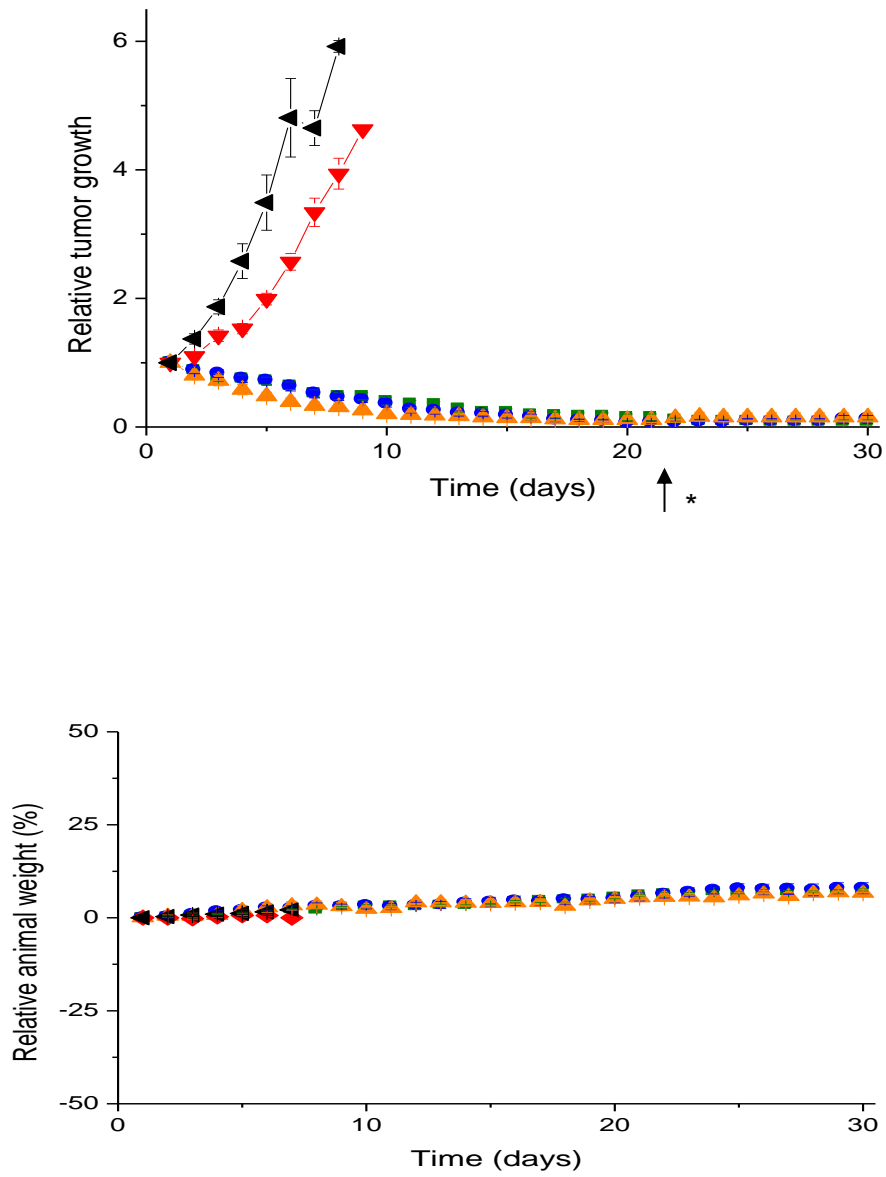


Figure 4.11: A) Tumour growth studies in a mouse A431 xenograft model after intravenous administration of DAB-Lf dendriplex carrying plasmid DNA encoding TNF α (50 μ g/injection) (green), DAB-Lfc dendriplex (blue), DAB dendriplex (orange), naked DNA (red) and untreated tumours (back) (n=10). B) Variations of the animal body weight throughout the treatment (Colour coding as in A).

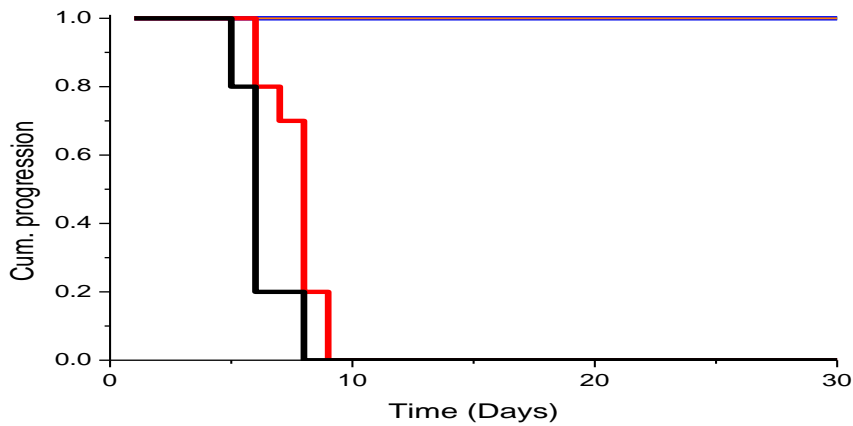
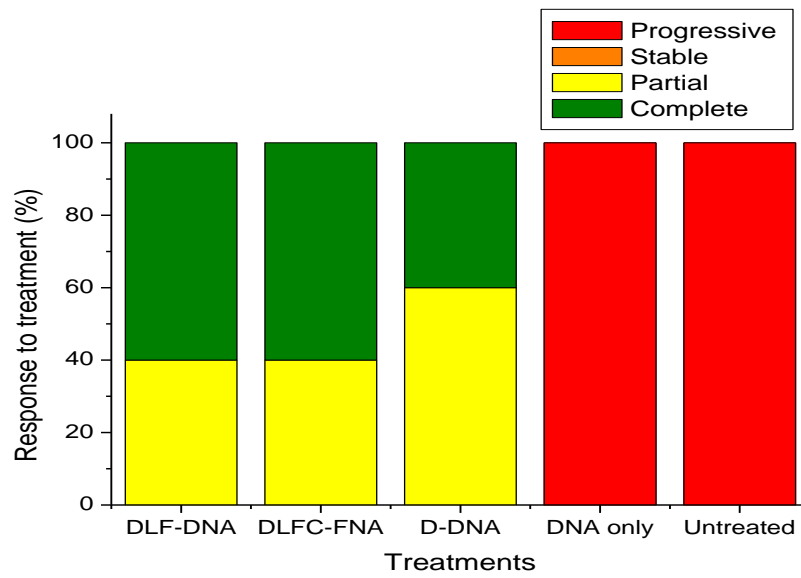


Figure 4.11 (continued): C) Overall tumour response to treatments at the end of the study. D) Time to disease progression. The Y axis gives the proportion of surviving animals over time. Animals were removed from the study once their tumour reached 11 mm diameter (Colour coding as in A).

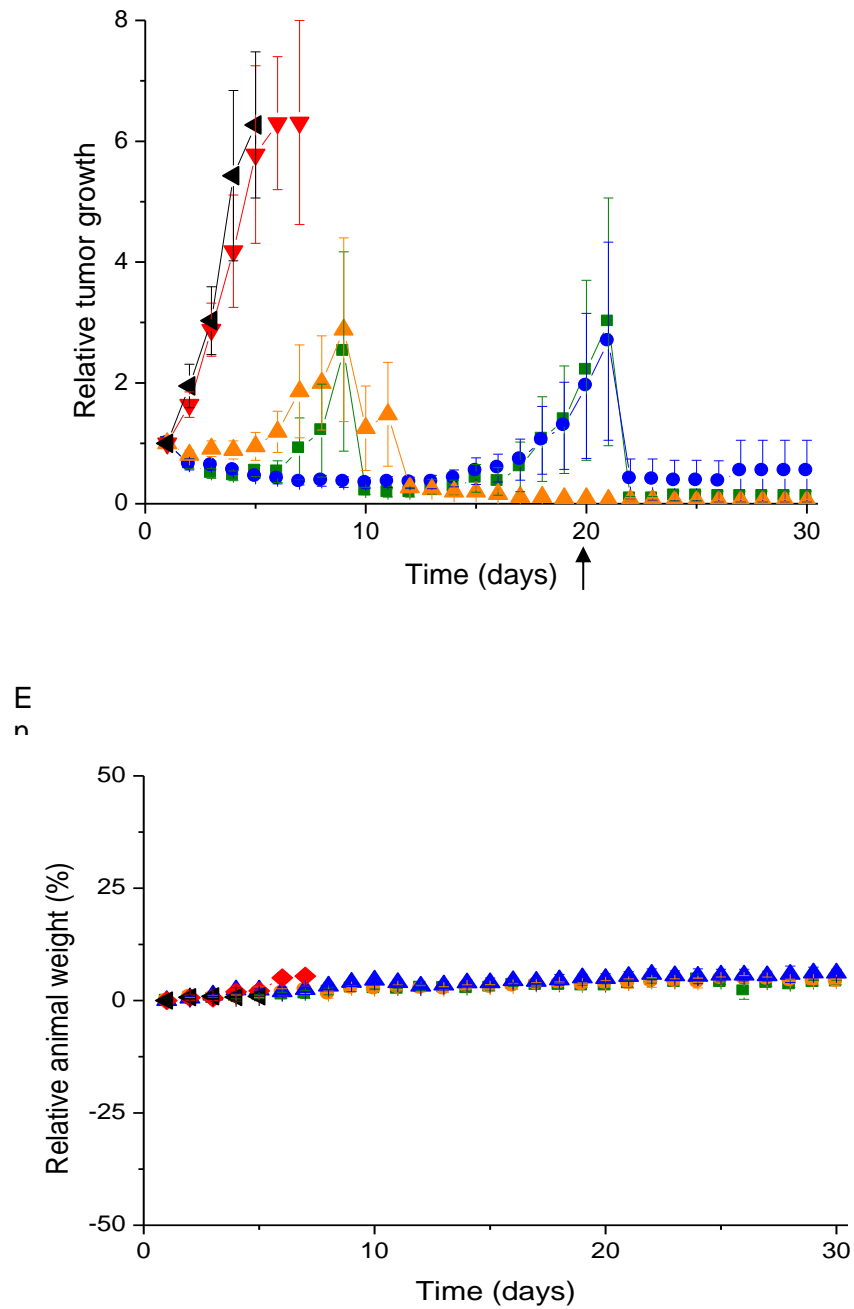


Figure 4.12: A) Tumour growth studies in a mouse B16-F10 model after intravenous administration of DAB-Lf dendriplex carrying plasmid DNA encoding TNF α (50 μ g/injection) (green), DAB-Lfc dendriplex (blue), DAB dendriplex (orange), naked DNA (red) and untreated tumours (back) (n=10). B) Variations of the animal body weight throughout the treatment (Colour coding as in A).

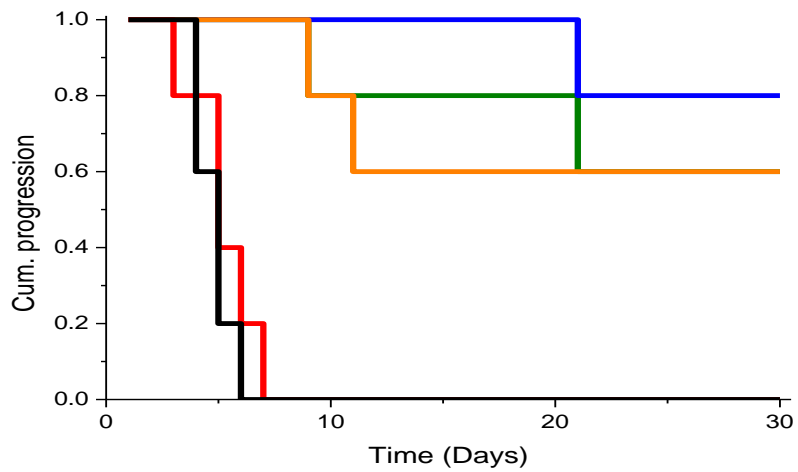
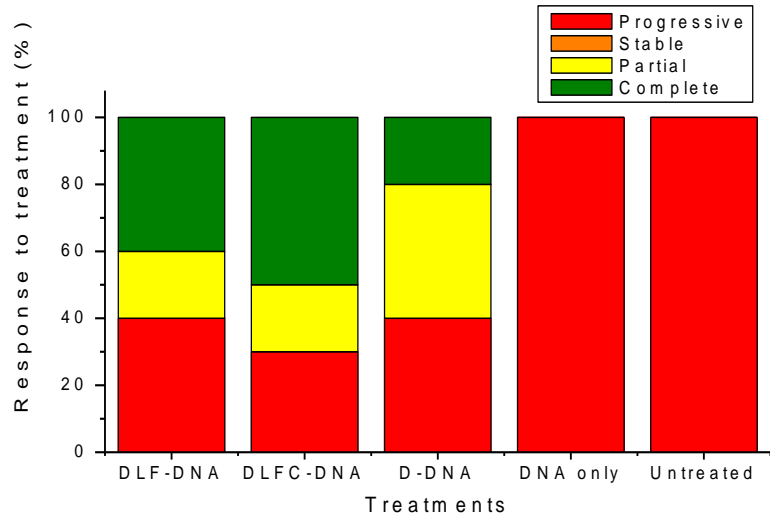


Figure 4.12 (continued): C) Overall tumour response to treatments at the end of the study. D) Time to disease progression. The Y axis gives the proportion of surviving animals over time. Animals were removed from the study once their tumour reached 11 mm diameter (Colour coding as in A).

4.5. Discussion

The possibility of using gene therapy for the treatment of cancer is currently limited by the lack of safe, intravenously administered delivery systems able to selectively deliver therapeutic genes to tumours. However, several delivery systems have been investigated to circumvent this problem. Among these delivery systems, generation 3 diaminobutyric polypropylenimine dendrimer (DAB) appears to be particularly promising. Moreover, recent advances in nanomaterial have shown that the combination of active targeting, based on the use of ligands, and passive targeting, based on the accumulation of particulate delivery systems due to the enhanced permeability and retention (EPR) (Maeda *et al.*, 1992), resulted in a tumour-selective targeting strategy. In the previous chapter, we have demonstrated that the intravenous administration of this dendrimer conjugated to transferrin (Tf), whose receptors are overexpressed on cancer cells, resulted in gene expression mainly in the tumours after intravenous administration.

Building on the promising results already obtained, in this study we hypothesized that the conjugation of a generation 3- diaminobutyric polypropylenimine (DAB) dendrimer to lactoferrin and lactoferricin, promising tumour-targeting ligands of the transferrin family that have intrinsic anti-tumoural activity and whose receptors are abundantly expressed on cancer cells, would improve the delivery of therapeutic DNA to cancer cells, resulting in better therapeutic efficacy *in vitro* and *in vivo*.

The NMR results demonstrated that DAB has been successfully conjugated with the respective ligands. Percentage conjugation of the amino acids with the dendrimer was found to be 50% for both lactoferrin and lactoferricin, as previously observed when preparing amino acid- and transferrin -bearing DAB using the same simple one-step synthesis (Koppu *et al.*, 2010; Aldawsari *et al.*, 2011).

The conjugation of Lf and Lfc to DAB did not destabilized DNA condensation. However, an excess of DAB was required for an efficient DNA condensation. The ability of DAB-Lf and DAB-Lfc dendriplexes to condense DNA was measured using Picogreen® reagent and the gel retardation assay at various durations and dendrimer: DNA weight ratios. It was obvious that stability of DNA is directly related to the increase in the dendrimer: DNA weight ratio. In addition, variations in the sensitivity of the nucleic acid stains used in these assays could be responsible of the condensation discrepancy observed in these two assays for the dendriplexes at a dendrimer: DNA weight ratio of 1:1.

The conjugation of Lf and Lfc to the periphery of the DAB dendrimer led to an increase in the size of both DAB-Lf and DAB-Lfc dendriplexes compared to the unmodified DAB dendriplex, which had an average size of 196 nm (polydispersity index: 0,683) (Aldawsari *et al.*, 2011). As the cut-off size for extravasation across tumour vasculature has been found to be 400 nm for most tumours (Yuan *et al.*, 1995), DAB-Lf and DAB-Lfc dendriplexes have therefore

the size needed for being able to efficiently deliver therapeutic DNA to the tumours.

Moreover, the conjugation of Lf and Lfc to DAB increased the overall positive charge of the dendriplexes compared to non-targeted DAB-DNA (6 mV) (Aldawsari *et al.*, 2011) for weight ratios over 2:1. This zeta potential increase is most likely due to the presence of the positively charged amino acids of Lf and Lfc. It would eventually lead to an increase of the electrostatic interactions of the dendriplexes with negatively charged cellular membranes, resulting in an improved cellular uptake through internalization mechanisms (Mahato *et al.*, 1999).

In vitro treatment of A431, B16-F10 and T98G cells with DAB-Lf and DAB-Lfc dendriplexes resulted in an enhanced transfection compared to the unconjugated DAB on all the tested cell lines. The improved β -gal expression following treatment with DAB-Lf and DAB-Lfc at a dendrimer: DNA ratio of 2 most likely resulted from the higher zeta potential of these dendriplexes at this ratio, as there is a strong correlation between cellular uptake and positive charge density of dendriplexes (Futaki *et al.*, 2001). Our transfection results are in accordance with those obtained by Elfinger and colleagues in an experiment done with polyethylenimine (PEI) conjugated to Lf (Elfinger *et al.*, 2007). They demonstrated that Lf-PEI polyplexes exhibited a luciferase gene expression 5-fold higher than that of PEI polyplexes in cells overexpressing Lf receptors. Furthermore, we could not find any studies describing the transfection efficacy

of Lf-and Lfc-bearing gene delivery systems in cancer cells to allow a comparison with our results. Lf has been previously used as part of a gene therapeutic system against cancer, but as therapeutic Lf cDNA instead of cancer-targeting moiety (Wang *et al.*, 2011).

Confocal microscopy imaging in our study showed efficient cellular uptake of Cy3-labeled DNA treated with both DAB-Lf and DAB-Lfc dendriplexes compared to cells treated with naked DNA. Our results were in line with previous data obtained by Wei and colleagues (Wei *et al.*, 2012), who demonstrated that the uptake of Lf-conjugated, coumarin- and DiR-loaded liposomes was much higher than that of unconjugated liposomes in HepG2 human hepatoma cells. This outcome was also confirmed by Chen *et al.* (2011), who revealed that doxorubicin encapsulated in Lf-bearing liposomes was more efficiently taken up by C6 glioma cells compared to other formulations. These results therefore demonstrated that DAB-Lf and DAB-Lfc have the required physicochemical properties for being efficient gene delivery systems.

In vitro, the conjugation of Lf and Lfc to DAB increased the anti-proliferative activity of the dendriplex in the three tested cell lines. These results may be attributed to the improved transfection efficacy when treated with Lf- and Lfc-bearing DAB dendriplexes. DAB-Lf and DAB-Lfc dendriplexes were the most efficacious treatments on B16-F10 cells, which may be a result of their highest transfection efficacy on the same cell line. However, the lack of

studies describing the anti-proliferative efficacy of Lf-and Lfc-bearing gene delivery systems in cancer cells prevented comparison with our results.

In vivo, the conjugation of lactoferrin and lactoferricin to the dendrimer significantly increased the gene expression in subcutaneous tumours, while decreasing the non-specific gene expression in the liver and the heart. Similar improvements have been obtained by (Wei *et al.*, 2012) when using Lf-bearing PEGylated liposomes for hepatocellular carcinoma targeting. The authors demonstrated that the accumulation of DiR in tumours was significantly increased after the conjugation of Lf to the PEGylated liposomes, whereas expression in the lungs and the other organs was reduced compared to the non-targeted liposomes.

The predominant gene expression in the tumour compared to the other organs is comparable to the gene expression pattern previously reported following intravenous administration of DAB-Tf dendriplex (Koppu *et al.*, 2010). However, when using Tf instead of Lf and Lfc as tumour targeting moieties, gene expression in the tumour was slightly higher (more than 35 mU/organ) than with Lf or Lfc. In addition, the β -galactosidase amounts in spleen, kidneys and liver were further decreased compared to what observed when using Lf and Lfc. Lf and Lfc therefore appear to be slightly less efficacious than Tf as tumour targeting moieties.

The *in vivo* tumoricidal activity experiments proof the improvement in the therapeutic efficacy by the intravenous administration of DAB-Lf, DAB-Lfc

and DAB complexed to TNF α expression plasmid which resulted in tumour regression. This effect was maintained for the whole duration of the experiment (30 days) compared to tumours treated with naked DNA that grew steadily at a growth rate close to that observed for untreated tumours.

The intravenously administered DAB-Lf and DAB-Lfc complexed to TNF α expression plasmid led to tumour regression and even complete tumour suppression in some cases. Other researchers have already reported the ability of Lf to target tumours *in vivo* (Wei *et al.*, 2012), but did not assess the therapeutic efficacy of their delivery system yet. As far as we know, Lf and Lfc have been widely studied for their intrinsic anti-cancer properties, but have not been used so far as targeting moieties on a gene therapeutic system. In this study, the intravenous administration of the targeted dendriplexes encoding TNF α led to the complete suppression of 60% of A431 tumours and up to 50% of B16-F10 tumours over one month. The treatment was well tolerated by the animals, with no apparent signs of toxicity. Consequently, the therapeutic effect of DAB-Lf and DAB-Lfc dendriplexes encoding TNF α was more pronounced in the A431 xenograft model than that obtained with B16-F10 tumours, contrarily to what was observed in our anti-proliferative assay *in vitro*. This could be explained by the fact that TNF α exerts its potent cytotoxic effects on tumours *in vivo* via the death receptor-dependent apoptotic pathway, but also via its anti-angiogenic effects, believed to be critical for its anti-cancer activity (Mocellin *et al.*, 2005). It actually highlights the limitation of *in vitro* experiments for predicting the anti-cancer outcome of novel therapeutic systems *in vivo*. In

addition, these tumour-targeted systems are intravenously delivered, thereby allowing them in theory to reach metastases as well as primary tumours, which is particularly important for the treatment of cancer.

Our previous study, carried out with DAB-Tf as a tumour-targeting dendrimer, led to a more pronounced therapeutic effect than that observed when using DAB-Lf and DAB-Lfc. This appears to be the consequence of the enhanced tumour targeting ability of this dendrimer compared to DAB-Lf and DAB-Lfc. Nevertheless, DAB-Lf and DAB-Lfc have been shown in this study to be able to increase the level of gene expression in tumours and the therapeutic efficacy compared to DAB dendriplex, resulting in complete tumour suppression of 40% of the A431 tumours and up to 50% of the B16-F10 tumours.

These results suggest that lactoferrin- and lactoferricin-bearing dendrimers should be further explored as a promising therapeutic strategy for cancer therapy.

CHAPTER 5.

CONCLUSION AND FUTURE WORK

Earlier stages of prostate cancer can be treated using conventional therapies such as radiation, chemotherapy and radical prostatectomy. However, the prognosis is dismal for patients with recurrent or metastatic disease. (Fujita *et al.*, 2007; Lu., 2009). For effective prostate cancer therapy, it is necessary to improve the knowledge of cancer physiopathology, discover new anti-cancer therapies, taking into consideration, developing novel biomedical technologies (Byrne *et al.*, 2008). Thus, gene therapy offers interesting alternative to conventional therapies.

During the past decades, intensive research has been carried out to establish viral and non-viral methods for delivering therapeutic genes into cancer cells. Viral vectors are currently the efficient transporters being used for transfecting therapeutic genes into cancer cells (Xiao *et al.*, 2012). Despite their high transfection efficacy, the use of viral vectors is limited by the size of the genetic material they can deliver, their immunogenicity and the lack of safety. In contrast, non-viral vectors are less toxic and associated with low immunogenic response than viruses. While the transfection efficiency of non-viral vectors is still low viral vectors than that for their viral counterparts, the current research is focused on improving the transfection efficiency of this category of carriers which are believed to be the most promising of gene delivery systems (Morille *et al.*, 2008).

Nanotechnology offers several solutions for enhanced delivery systems through the use of nanoparticles carriers. Due to the small size of these carriers,

they exhibit better passive targeting by the EPR effect. Moreover, reports have shown that particle size between 10-100 nm is non-toxic to mammalian cells (Singh, 2013).

Recently, polymer-based nanocarriers that include the use of polymer-DNA complexes (polyplexes) have received more attention for its ability to improve the efficacy of cancer therapeutics. Due to their small size, these nanosized polymer therapeutic agents can circulate in the bloodstream for long time, allowing them to reach the target tumour tissues (Park *et al.*, 2008). However, the delivery of nano-sized agents into cancer tissue is challenging because it mostly relies on the enhanced permeability and retention (EPR) effect that depends on the leaky nature of the tumour vasculature and the prolonged circulation of nano-sized agents, allowing slow but uneven accumulation in the tumour bed. Delivery of nano-sized agents is dependent on several factors that influence the EPR effect which include regional blood flow to the tumour, permeability of the tumour vasculature, structural barriers imposed by perivascular tumour cells and extracellular matrix and finally, intratumoural pressure (Kobayashi *et al.*, 2013). Therefore, attempts have been made to improve polymeric gene delivery efficacy through rational design of vehicles capable of overcoming the various extra- and intracellular barriers that restrain their performance.

Recent advances in nanomaterial have shown that the combination of active targeting, based on the use of ligands, and passive targeting, based on the

accumulation of nanoparticles encapsulating therapeutic genes due to the enhanced permeability and retention (EPR) (Maeda *et al.*, 1992), resulted in a tumour-selective targeting strategy and improved the therapeutic efficacy at lower doses.

On the basis of this, the objectives of this research have been the preparation and characterization of novel non-viral delivery systems by the conjugation of a generation 3- diaminobutyric polypropylenimine (DAB) dendrimer to the iron-carriers transferrin (Tf), lactoferrin (Lf) and lactoferricin (Lfc), promising tumour-targeting ligands of the transferrin family that have intrinsic anti-tumoural activity and whose receptors are abundantly expressed on cancer cells. This study also aimed to evaluate *in vitro* and *in vivo* the therapeutic and targeting efficacies of these therapeutic systems.

In this study, we have demonstrated for the first time that a tumour-targeting, dendrimer-based gene delivery system complexed to a plasmid DNA encoding TNF α and TRAIL can lead to eradication of some prostate tumours after intravenous administration. *In vitro*, DAB-Tf complexed to TNF α , TRAIL and IL-12 expression plasmids significantly enhanced the anti-proliferative efficacy on PC-3, DU145 and LNCaP prostate cancer cells when compared to the unconjugated dendriplex, by up to 100-fold in LNCaP cells. *In vivo*, the intravenous administration of DAB-Tf dendriplex encoding TNF α resulted in tumour suppression for 60% of PC-3 and 50% of DU145 tumours. Treatment with of DAB-Tf dendriplex encoding TRAIL led to tumour suppression of 10%

of PC-3 tumours. IL-12 mediated gene therapy resulted in tumour regression of 20% of both types of prostate tumours. By contrast, all the tumours treated with DAB-Tf, naked DNA or left untreated were progressive for both tumour types. The animals did not show any signs of toxicity. Transferrin-bearing DAB dendriplexes encoding TNF α , TRAIL and IL-12 therefore hold great potential as a novel approach for the gene therapy of prostate cancer and should be further investigated to optimize their therapeutic potential.

We have also demonstrated that a tumour-targeting, lactoferrin- and lactoferricin-bearing DAB dendriplexes can lead to eradication of some skin tumours after intravenous administration. *In vitro*, the conjugation of Lf and Lfc to DAB increased the anti-proliferative activity of the dendriplex in the three tested cell lines. These results may be attributed to the improved transfection efficacy when treated with Lf- and Lfc-bearing DAB dendriplexes. DAB-Lf and DAB-Lfc dendriplexes were the most efficacious treatments on B16-F10 cells, which may be a result of their highest transfection efficacy on the same cell line. However, the lack of studies describing the anti-proliferative efficacy of Lf- and Lfc-bearing gene delivery systems in cancer cells prevented comparison with our results. *In vivo*, an intravenously administered lactoferrin- and lactoferricin-bearing DAB dendriplexes resulted in an improved tumour gene expression, while decreasing non-specific gene expression in the liver. Consequently, the intravenous administration of Lf- and Lfc-bearing, TNF α -encoding dendriplexes led to a sustained inhibition of tumour growth and even tumour suppression for 40% of the A431 tumours and up to 50% of the B16-

F10 tumours, with long-term survival of the animals. In contrast, 100% of the tumours treated with naked DNA or left untreated were progressive. The animals did not show any signs of toxicity.

The promising results presented in this thesis offer different opportunities for research which could be pursued in the future. In particular, it is likely that researchers will continue to develop novel TfR-targeted delivery systems and to increase the specificity of their targeting to cancer cells. In our study, the *in vivo* studies showed that the gene expression was significantly increased in the tumours for both Lf- and Lfc-bearing DAB dendriplexes compared to the non-conjugated DAB. However, in both systems, gene expression in the spleen and the kidneys reached similar levels to what was observed following treatment with non-conjugated DAB dendriplex. Despite the decreased levels of gene expression in the liver compared to the non-conjugated DAB, these levels along with the levels in the spleen and the kidneys highlight the need for further experiments to improve gene expression specificity to tumour cells.

TfR-targeted systems in this study have demonstrated promising *in vitro* and *in vivo* therapeutic effects against cancer cells. However, in our *in vivo* experiments, we had to use immunodeficient BALB/c mice unable to produce T cells in order for them to grow tumours from human origin. Therefore, the therapeutic effect observed could be further investigated using fully immunocompetent mouse bearing a murine tumour model (Heinzerling *et al.*, 2002).

These therapeutic effects observed in this study, together with the lack of toxicity, potentially make transferrin-, lactoferrin- and lactoferricin- bearing DAB dendrimers promising gene delivery systems for intravenous prostate cancer therapy and should be further investigated to optimize their therapeutic potential.

References

- Abbott, A. 1992. Gene therapy. Italians first to use stem cells. *Nature*, 356(6369): 465.
- Adlerova, L., Bartoskova, A., and Faldyna, M. 2008. Lactoferrin: a review. *Veterinari Medicina*, 53(9): 457-468.
- Akitt, J., and Mann, B. 2000. NMR and chemistry: an introduction to modern NMR spectroscopy, 4th ed, *Cheltenham: Stanley Thornes*.
- Al Robaian, M., Chiam, K., Blatchford, D., and Dufès, C. 2013. Therapeutic efficacy of intravenously administered transferrin-conjugated dendriplexes on prostate carcinomas. *Nanomedicine*, (2014)9(4): 421-434
- Aldawsari, H., Edrada-Ebel R., Blatchford, D., Tate, R., Dufès, C. 2011. Enhanced gene expression in tumours after intravenous administration of arginine-, lysine- and leucine-bearing polypropylenimine polyplex. *Biomaterials*, 32:5889-5899.
- Aldawsari, H., Sundara, Raj B., Edrada-Ebel R., Blatchford, D., Tate, R., Tetley, L. 2011. Enhanced gene expression in tumours after intravenous administration of arginine-lysine and leucine-bearing polyethylenimine polyplex. *Nanomedicine*, 7:815-823.
- Alimirah, F., Chen, J., Basrawala, Z., Xin, H., and Choubey, D. 2006. DU-145 and PC-3 human prostate cancer lines express androgen receptor: implications for the androgen receptor functions and regulation. *Febs Letters*, 580(9):2294-300.
- Al-Jamal, K., Sakthivel, T., and Florence, A. 2003. Dendrisomes: cationic lipidic dendron vesicular assemblies. *International Journal of Pharmaceutics*, 254(1): 33-36.
- Anand, P., Kunnumakara, A. Sundaram, C., Harikumar, K., Tharakan, S., Lai, O., and Aggarwal, B. 2008. Cancer is a Preventable Disease that Requires Major Lifestyle Changes. *Pharmaceutical Research*, 25(9): 2097-211.
- Anderson, W. 1995. Gene therapy. *Scientific American*, 273:124-8.
- Balazs, D., and Godbey, W. 2011. Liposomes for Use in Gene Delivery. *Journal of Drug Delivery*, 2011:32649.

- Berridge, M., Herst, P., and Tan, A. 2005. Tetrazolium dyes as tools in cell biology: new insights into their cellular reduction. *Biotechnology Annual Review*, 11: 127-152.
- Bezault, J., Bhimani, R., Wiprovnick, J., and Furmanski, P. 1994. Human lactoferrin inhibits growth of solid tumours and development of experimental metastases in mice. *Cancer Research*, 54(9): 2310-2312.
- Bianco J., Scardino, T., and Eastham, A. 2005. Radical prostatectomy: long-term cancer control and recovery of sexual and urinary function ("trifecta"). *Urology*, 66(5): 83-94.
- Brooks, D., Wolf, A., Smith, R., Dash, C., and Guessous, I. 2010. Prostate cancer screening: updated recommendations from the American Cancer Society. *Journal of National Medicine Association*, 102(5): 423-429.
- Brown, B., Venneri, M., Zingale, A., Sergi, L., and Naldini, L. 2006. Endogenous microRNA regulation suppresses transgene expression in hematopoietic lineages and enables stable gene transfer. *Nature Medicine*, 12(5): 585-591.
- Brown, D., Gray, A., Tetley, L., Santovena, A., Rene, J., Schätzlein, G., and Uchegbu, F. 2003. *In vitro* and *in vivo* gene transfer with poly (amino acid) vesicles. *Journal of Controlled Release*, 93:193-211.
- Brown, M., Schätzlein, A., and Uchegbu, I. 2001. Gene delivery with synthetic (non-viral) carrier. *International Journal of Pharmaceutics*, 229:1-21.
- Campbell, R. 2008. Gene Therapy and Cancer Research Focus. *Nova Publishers*, Page 24-26.
- Cavazzana-Calvo, M., Lagresle, C., Hacein-Bey-Abina, S., and Fischer, A. 2005. Gene therapy for severe combined immunodeficiency. *Annual Review of Medicine*, 56:585- 602.
- Chen, H., Qin, Y., Zhang, Q., Jiang, W., Tang, L., and Liu, J. 2011. Lactoferrin modified doxorubicin-loaded procationic liposomes for the treatment of glioma. *European Journal of Pharmaceutical Sciences*, 44:164-173.
- Chilkoti, A., Dreher, M., Meyer, D., and Raucher, D. 2002. Targeted drug delivery by thermally responsive polymers. *Advanced Drug Delivery Reviews*, 54(5): 613-630.
- Christian, D., Cai, S., Bowen, D., Kim, Y., Pajerowski, D., and Discher, D. 2009. Polymersomes carriers: From self-assembly to siRNA and protein therapeutics. *European Journal of Pharmaceutics and Biopharmaceutics*, 71(3): 463-474.

- Claxton, N., Fellers, T., and Davidson, M. 2006. Laser scanning confocal microscopy Olympus. Available online at. Olympus confocal Com/theory/LSCMIntro.
- Conchello, J. and Lichtman, J. 2005. Optical sectioning microscopy. *Nature methods*, 2(12): 920-931.
- Connors, K., 2002. A textbook of pharmaceutical analysis. *John Wiley & Sons, Singapore*
- Cotten, M., Wagner, E., and Birnstiel, M. 1993. Receptor-mediated transport of DNA into eukaryotic cells. *Methods Enzymology Journal*, 217: 618-644.
- Dabbs, D., and Silverman, J. 2001. Immunohistochemical workup of metastatic carcinoma of unknown primary. *Pathology Case Reviews*, 6(4): 146-153.
- Damez, J., and Clerjon, S. 2008. Meat quality assessment using biophysical methods related to meat structure. *Meat Science*, 80(1): 132-149.
- Danhier, F., Feron, O., and Pr eat, V. 2010. To exploit the tumour microenvironment: Passive and active tumour targeting of Nan carriers for anti-cancer drug delivery. *Journal of Controlled Release*, 148(2): 135-146.
- Dass, C., 2002. Biochemical and biophysical characteristics of lipoplexes pertinent to solid tumour gene therapy. *International Journal of Pharmaceutics*, 241(1): 1-25.
- Delgado, A., Gonzalez-Caballero, R., Hunter, L., Koopal, and Lyklema. 2007. Measurement and interpretation of electrokinetic phenomena. *Journal of Colloid and Interface Science*, 309:194-224.
- Discher, D., and Ahmed, F. 2006. Polymersomes. *Annual Review of Biomedical Engineering*, 8: 323-341.
- Dougan, M., and Dranoff, G. 2009. Immune therapy for cancer. *Annual Review of Immunology*, 27: 83-117.
- Dragan, A., Casas-Finet, J., Bishop, E., Strouse, R., Schenerman, M., and Geddes, C. 2010. Characterization of PicoGreen interaction with dsDNA and the origin of its fluorescence enhancement upon binding. *Biophysical Journal*, 99(9): 3010-3019.
- Duf es, C. 2011. Delivery of the vitamin E compound tocotrienol to cancer cells. *Therapeutic Delivery*, 2(11): 1385-1389.
- Duf es, C. 2011. Research Spotlight: Delivery of the vitamin E compound tocotrienol to cancer cells. *Therapeutic Delivery*, 2(11): 1385-1389.

- Dufès, C., Al Robaian, M., and Somani, S. 2013. Transferrin and the transferrin receptor for the targeted delivery of therapeutic agents to the brain and cancer cells. *Therapeutic Delivery*, 4(5): 629-640.
- Dufès, C., Muller, J., Couet, W., Olivier, J., Uchegbu, I., and Schätzlein, A. 2004. Anticancer drug delivery with transferrin targeted polymeric chitosan vesicles. *Pharmaceutical Research*, 21(1): 101-107.
- Dufès, C., Uchegbu, I. and Schätzlein, A., 2005. Dendrimers in gene delivery. *Advanced Drug Delivery Reviews*, 57(15): 2177-2202.
- Eisenauer, E., Therasse, P., Bogaerts, J., Schwartz, L., Sargent, D., Ford, R. 2009. New response evaluation criteria in solid tumours: revised RECIST guideline. *European Journal of Cancer*, 45:228-247.
- Elfinger, M., Maucksch, C., Rudolph, C. 2007. Characterization of lactoferrin as a targeting ligand for nonviral gene delivery to airway epithelial cells. *Biomaterials*, 28:3448-3455.
- Eliassen, L., Berge, G., Sveinbjørnsson, B., Svendsen, J., Vorland, L., and Rekdal, Ø. 2002. Evidence for a direct antitumour mechanism of action of bovine lactoferricin. *Anticancer Research*, 22:2703-2710.
- Elsabahy, M., Nazarali, A., and Foldvari, M. 2011. Non-viral nucleic acid delivery: key challenges and future directions. *Current Drug Delivery*, 8(3): 235-244.
- Escors, D., and Breckpot, K. 2010. Lentiviral vectors in gene therapy: their current status and future potential. *Archivum Immunologiae et Therapiae Experimentalis*, 58(2):107-119.
- Feinbaum, R. 1998. Vectors derived from plasmids. *Current Protocols in Molecular Biology*. *John Wiley & sons incorporated*. 1.5.1-1.5.17.
- Feinbaum, R. 2001. Introduction to Plasmid Biology. *Current Protocols in Molecular Biology*, 41:1.5.1-1.5.17.
- Fessenden, R., and Fessenden, J., 1990. Fundamentals of organic chemistry: Harper and Row, 4th ed, 307-420.
- Fifth Report on the Statistics on the Number of Animals used for Experimental and other Scientific Purposes in the Member States of the European Union. 2007. *Commission of the European Communities*.
- Freshney, R. 2000. Culture of Animal Cells: A Manual of Basic Technique. A John Wiley and Sons Incorporated, 4th ed, 96-114.

- Fu, J., Blatchford, D., Tetley, L., and Dufès, C. 2009. Tumour regression after systemic administration of tocotrienol entrapped in tumour-targeted vesicles. *Journal of Controlled Release*, 140(2): 95-99.
- Fu, J., Zhang, W., Blatchford, D., Tetley, L., McConnell, G., and Dufès, C. 2011. Novel tocotrienol-entrapping vesicles can eradicate solid tumours after intravenous administration. *Journal of Controlled Release*, 154(1): 20-26.
- Fujita, T., Timme, T., Tabata, K., Naruishi, K., Kusaka, N., Watanabe, M., and Thompson, T., 2007. Cooperative effects of adenoviral vector-mediated interleukin 12 gene therapy with radiotherapy in a preclinical model of metastatic prostate cancer. *Gene therapy*, 14(3): 227-236.
- Furmanski, P., Li, Z., Fortuna, M., Swamy, C., and Das, M. 1989. Multiple molecular forms of human Lactoferrin. *Journal of Experimental Medicine*, 170: 415-428.
- Futaki, S., Ohashi, W., Suzuki, T., Niwa, M., Tanaka, S., and Ueda, K., 2001. Stearylated arginine-rich peptides: a new class of transfection systems. *Bioconjugate Chemistry*, 12:1005-1011.
- Gao, X., and L. Huang. 1995. Cationic liposome-mediated gene transfer. *Gene Therapy*, 2:710-722.
- Gayther, S., de Foy, K., Harrington, P., Pharoah, P., Dunsmuir, W., Edwards, S., and Eeles, R. 2000. The frequency of germ-line mutations in the breast cancer predisposition genes BRCA1 and BRCA2 in familial prostate cancer. The Cancer Research Campaign/British Prostate Group United Kingdom Familial Prostate Cancer Study Collaborators. *Cancer Research*, 60(16):4513-4518.
- Gebhart, C., and Kabanov, A. 2001. Evaluation of polyplexes as gene transfer agents. *Journal of Controlled Release*, 73(2-3): 401-416.
- Gifford, J., Hunter, H., and Vogel, H. 2005. Lactoferricin: a lactoferrin-derived peptide with antimicrobial, antiviral, antitumour and immunological properties. *Cellular and Molecular Life Sciences*, 62:2588-2598.
- Gohel, M. 2009. Dendrimer, dendrimer structure, dendrimer drug delivery and amp; Applications of the dendrimer. From <http://www.pharmainfo.net/reviews/dendrimer-overview>.
- Goindi, S., and Maheshwari, M. 2009. Dendrimers: The Novel Pharmaceutical Drug Carriers. *International Journal of Pharmaceutical Sciences and Nanotechnology*, 2(2): 493-502.
- Gómez-Navarro, J., Curiel, D., and Douglas, J. 1999. Gene therapy for cancer. *European Journal of Cancer*, 35(14): 2039-2057.

- Gomme, P., McCann, K., and Bertolini, J. 2005. Transferrin: structure, function and potential therapeutic actions. *Drug Discovery Today*, 10(4): 267-273.
- González-Chávez, S., Arévalo-Gallegos, S., and Rascón-Cruz, Q. 2009. Lactoferrin: structure, function and applications. *International journal of antimicrobial agents*, 33(4):301-e1.
- Gorman, C., Moffatt, L. and Howard, B., 1982. Recombinant genomes which express chloramphenicol acetyltransferase in mammalian cells. *Molecular and Cellular Biology*, 2: 1044–1051.
- Goverdhana, S., Puntel, M., Xiong, W., Zirger, J., Barcia, C., Curtin, J., and Castro, M. 2005. Regulatable gene expression systems for gene therapy applications: progress and future challenges. *Molecular Therapy*, 12 (2): 189-211.
- Gu, F., Karnik, R., Wang, A., Alexis, F., Levy-Nissenbaum, E., Hong, S., and Farokhzad, O. 2007. Targeted nanoparticles for cancer therapy. *Nano Today*, 2(3): 14-21.
- Habermacher, G., Chason, J., and Schaeffer, A. 2006. Prostatitis/chronic pelvic pain syndrome. *Annual Review of Medicine*, 57: 195-206.
- Han, L., Huang, R., Li, J., Liu, S., Huang, S., and Jiang, C. 2011. Plasmid pORF-hTRAIL and doxorubicin co-delivery targeting to tumour using peptide-conjugated polyamidoamine dendrimer. *Biomaterials*, 32(4): 1242-1252.
- Harlan, S., Cooperberg, M., Elkin, E., Lubeck, D., Meng, M., Mehta, S., and Carroll, P., 2003. Time trends and characteristics of men choosing watchful waiting for initial treatment of localized prostate cancer: results from CaPSURE. *The Journal of Urology*, 170(5): 1804-1807.
- Hawkey, M. 1998. The origins and molecular basis of antibiotic resistance. *Bmj*, 317(7159): 657-660.
- Head, J. F., Wang, F., and Elliott, R. L. 1997. Antineoplastic drugs that interfere with iron metabolism in cancer cells. *Advances in Enzyme Regulation*, 37: 147-169.
- Hellman, L., and Fried, M. 2007. Electrophoretic mobility shift assay (EMSA) for detecting protein–nucleic acid interactions. *Nature protocols*, 2(8): 1849-1861.
- Heinzerling, L., Dummer, R., Pavlovic, J., Schultz, J., Burg, G., and Moelling, K. (2002). Tumour regression of human and murine melanoma after intratumoural injection of IL-12-encoding plasmid DNA in mice. *Experimental dermatology*, 11(3), 232-240.

- Hopkins, R. 1983. Intracellular routing of transferrin and transferrin receptors in epidermoid carcinoma A431 cells. *Cell*, 35(1): 321-330.
- Horoszewicz, J., Leong, S., Kawinski, E., Karr, J., Rosenthal, H., Chu, T., and Murphy, G. 1983. LNCaP model of human prostatic carcinoma. *Cancer research*, 43(4):1809-1818.)
- Hughes, C., Murphy, A., Martin, C., Sheils, O., and O'Leary, J. 2005. Molecular pathology of prostate cancer. *Journal of Clinical Pathology*, 58(7): 673-684.
- Hu-Lieskovan, S., Heidel, J., Bartlett, D., Davis, M., and Triche, T. 2005. Sequence-specific knockdown of EWS-FLI1 by targeted, nonviral delivery of small interfering RNA inhibits tumour growth in a murine model of metastatic Ewing's sarcoma. *Cancer Research*, 65(19):8984-8992.
- Jarrard, D., Kinoshita, H., Shi, Y., Sandefur, C., Hoff, D., Meisner, L., and Nassif, N. 1998. Methylation of the androgen receptor promoter CpG Island is associated with loss of androgen receptor expression in prostate cancer cells. *Cancer Research*, 58(23):5310-5314.
- Jin, X., Yang, Y., and Li, Y. 2008. Gene therapy: regulations, ethics and its practicalities in liver disease. *World Journal of Gastroenterology*, 14(15): 2303-2307.
- Kaighn, M., Narayan, K., Ohnuki, Y., Lechner, J., and Jones, L. 1979. Establishment and characterization of a human prostatic carcinoma cell line (PC-3). *Investigative urology*, 17:16-23.
- Kamimura, K., Suda, T., Zhang, G., and Liu, D, 2011. Advances in gene delivery systems. *Pharmaceutical medicine*, 25(5): 293-306.
- Karatas, H., Aktas, Y., Gursoy-Ozdemir, Y., Bodur, E., Yemisci, M., Caban, S., and Dalkara, T. 2009. A nanomedicine transports a peptide caspase-3 inhibitor across the blood-brain barrier and provides neuroprotection. *The Journal of Neuroscience*, 29(44): 13761-13769.
- Keer, H., Kozlowski, J., Tsai, Y., CHUNG, L., McEwan, R., and Grayhack, J. 1990. Elevated transferrin receptor content in human prostate cancer cell lines assessed *in vitro* and *in vivo*. *The Journal of urology*, 143(2): 381-385.
- Kelland, L. 2004. Of mice and men: values and liabilities of the athymic nude mouse model in anticancer drug development. *European Journal of Cancer*, 40:827-836.
- Khalil, I., Kogure, K., Akita, H., and Harashima, H. 2006. Uptake pathways and subsequent intracellular trafficking in nonviral gene delivery. *Pharmacological reviews*, 58(1):32-45.

- Kim, E., Lee, E., Lee, W., Son, E., Seo, K., Li, J., and Lee, J. 2011. Isorhamnetin suppresses skin cancer through direct inhibition of MEK1 and PI3-K. *Cancer Prevention Research*, 4(4): 582-591.
- Kimura, T., Yamaoka, T., Iwase, R., and Murakami, A. 2001. Structure/function relationship in the polyplexes containing cationic polypeptides for gene delivery. *Nucleic Acids Research Supplement*, 1: 203-204.
- Kircheis, R., Ostermann, E., Wolschek, M., Lichtenberger, C., Magin-Lachmann, C., Wightman, L., and Wagner, E. 2002. Tumour-targeted gene delivery of tumour necrosis factor-alpha induces tumour necrosis and tumour regression without systemic toxicity. *Cancer Gene Therapy*, 98: 673-680.
- Kobayashi, H., Watanabe, R., and Choyke, P. 2013. Improving Conventional Enhanced Permeability and Retention (EPR) Effects; What Is the Appropriate Target? *Theranostics*, 4(1): 81
- Komáromy, A., Alexander, J., Rowlan, J., Garcia, M., Chiodo, V., Kaya, A., and Aguirre, G. 2010. Gene therapy rescues cone function in congenital achromatopsia. *Human Molecular Genetics*, 19(13): 2581-2593.
- Koppu, S., Oh, Y., Edrada-Ebel, R., Blatchford, D., Tetley, L., Tate, R., and Dufès, C. 2010. Tumour regression after systemic administration of a novel tumour-targeted gene delivery system carrying a therapeutic plasmid DNA. *Journal of Controlled Release*, 143(2): 215-221.
- Kursa, M., Walker, G., Roessler, V., Ogris, M., Roedl, W., Kircheis, R., and Wagner, E. 2003. Novel shielded transferrin-polyethylene glycol-polyethylenimine/DNA complexes for systemic tumour-targeted gene transfer. *Bioconjugate Chemistry*, 14(1): 222-231.
- Labat-Moleur, F., Steffan, A. M., Brisson, C., Perron, H., Feugeas, O., Furstenberger, P., and Behr, J. 1996. An electron microscopy study into the mechanism of gene transfer with lipopolyamines. *Gene Therapy*, 3(11): 1010-1017.
- Lai, B., Gao, J., and Lanks, K. 1998. Mechanism of action and spectrum of cell lines sensitive to a doxorubicin-transferrin conjugate. *Cancer Chemotherapy and Pharmacology*, 41(2): 155-160.
- Laniel, A., Béliveau, A., and Guérin, S. 2001. Electrophoretic mobility shift assays for the analysis of DNA-protein interactions. In *DNA-Protein Interactions*, 13-30.
- Ledley, F. 1995. Nonviral gene therapy: the promise of genes as pharmaceutical products. *Human Gene Therapy*, 6(9): 1129-1144.

- Lemarié, F., Chang, C., Blatchford, D., Amor, R., Norris, G., Tetley, L., and Dufès, C. 2013. Antitumour activity of the tea polyphenol epigallocatechin-3-gallate encapsulated in targeted vesicles after intravenous administration. *Nanomedicine*, 8(2): 181-192.
- Lemarié, F., Croft, D., Tate, R., Ryan, K., and Dufès, C. 2012. Tumour regression following intravenous administration of a tumour-targeted p73 gene delivery system. *Biomaterials*, 33:2701-2709.
- Lemoine, R. 1999. Understanding Gene Therapy. First Ed. BIOS Scientific Publishers Ltd. 172.
- LePecq, J., and Paoletti, C. 1967. A fluorescent complex between ethidium bromide and nucleic acids: physical—chemical characterization. *Journal of molecular biology*, 27(1):87-106.
- Levine, B., Humeau, L., Boyer, J., MacGregor, R., Rebello, T., Lu, X., and June, C., 2006. Gene transfer in humans using a conditionally replicating lentiviral vector. *Proceedings of the National Academy of Sciences of the United States of America*, 103(46): 17372-17377.
- Levine, D., Ghoroghchian, P., Freudenberg, J., Zhang, G., Therien, M., Greene, M., and Murali, R. 2008. Polymersomes: A new multi-functional tool for cancer diagnosis and therapy. *Methods*, 46(1): 25-32.
- Li, S., and Huang, L. 2007. Non-viral is superior to viral gene delivery. *Journal of Controlled Release*, 123:181-183.
- Li, X., Ding, L., Xu, Y., Wang, Y., and Ping, Q. 2009. Targeted delivery of doxorubicin using stealth liposomes modified with transferrin. *International Journal of Pharmaceutics*, 373(1-2): 116-123.
- Liu, A. (2000). Differential expression of cell surface molecules in prostate cancer cells. *Cancer research*, 60(13):3429-3434.
- Łubgan, D., Józwiak, Z., Grabenbauer, G., and Distel, L., 2009. Doxorubicin-transferrin conjugate selectively overcomes multidrug resistance in leukaemia cells. *Cellular and Molecular Biology Letters*, 14(1):113-127.
- Lungwitz, U., Breunig, M., Blunk, T., and Gopferich, A. 2005. Polyethylenimine-based non-viral gene delivery systems. *European Journal of Pharmaceutics and Biopharmaceutics*, 60(2): 247-266.
- Luo, D., and Saltzman, W., 2000. Synthetic DNA delivery systems. *Nature Biotechnology*, 18:33-37.
- Lu, Y. 2009. Transcriptionally regulated, prostate-targeted gene therapy for prostate cancer. *Advanced drug delivery reviews*, 61(7):572-588

- Maeda, H. 1992. The tumour blood vessel as an ideal target for macromolecular anticancer agents. *Journal of Controlled Release*, 19:315-324.
- Maguire, A., Simonelli, F., Pierce, E., Pugh, E., Mingozzi, F., Bennicelli, J., and Bennett, J. 2008. Safety and efficacy of gene transfer for Leber's congenital amaurosis. *New England Journal of Medicine*, 358(21):2240-2248.
- Mahale, S., Dani, N., Ansari, S., and Kale, T. 2009. Gene therapy and its implications in Periodontics. *Journal of Indian Society of Periodontology*, 13(1):1-5.
- Mahato, R., Smith, L., and Rolland, A. 1999. Pharmaceutical perspectives of nonviral gene therapy. *Advances in Genetics*, 41:95-156.
- Majka, G., Śpiewak, K., Kurpiewska, K., Heczko, P., Stochel, G., Strus, M., and Brindell, M. 2013. A high-throughput method for the quantification of iron saturation in lactoferrin preparations. *Analytical and Bioanalytical Chemistry*, 405(5191):1-10.
- Mann, M. 1999. Pressure-mediated oligonucleotide transfection of rat and human cardiovascular tissues. *Proceedings of the National Academy of Sciences of the United State of America*, 96: 6411-6416
- Marcum, J., 2005. From the molecular genetics revolution to gene therapy: translating basic research into medicine. *Journal of Laboratory and Clinical Medicine*, 146(6): 312-316.
- Marko, J., 1997. Stretched, Twisted, Supercoiled and Braided DNA. *In Materials Research Society Symposium Proceedings Vol. 463*, pp. 31-42.
- Medina-Kauwe, L., Xie, J., and Hamm-Alvarez, S. 2005. Intracellular trafficking of nonviral vectors. *Gene Therapy*, 12(24):1734-51.
- Mercer, E., Shields, T., Amin, M., Sauvé, J., Appella, E., Romano, W., and Ullrich, J. 1990. Negative growth regulation in a glioblastoma tumour cell line that conditionally expresses human wild-type p53. *Proceedings of the National Academy of Sciences*, 87(16): 6166-6170.
- Mickey, D., Stone, K., Wunderli, H., Mickey, G., Vollmer, R., and Paulson, D., 1977. Heterotransplantation of a human prostatic adenocarcinoma cell line in nude mice. *Cancer Research*, 37: 4049-58.
- Miller, N. 2012. Glybera and the future of gene therapy in the European Union. *Nature Reviews Drug Discovery*, 11(5): 419-419.
- Mocellin, S., Rossi, C., Pilati, P., and Nitti, D. 2005. Tumour necrosis factor, cancer and anticancer therapy. *Cytokine and Growth Factor Reviews*, 16:35-53.

- Morgan, R., Dudley, M., Wunderlich, J., Hughes, M., Yang, J., Sherry, R., and Rosenberg, S. 2006. Cancer regression in patients after transfer of genetically engineered lymphocytes. *Science*, 314(5796):126-9.
- Morille, M., Passirani, C., Vonarbourg, A., Clavreul, A., and Benoit, J.P. 2008. Progress in developing cationic vectors for non-viral systemic gene therapy against cancer. *Biomaterials*, 29(24): 3477-3496.
- Mossman, T. 1983. Rapid colorimetric assay for cellular growth and survival: application to proliferation and cytotoxicity assays. *Journal of immunological methods*, 65(1): 55-63.
- Mosquito, S., Ochoa, T., Cok, J., and Cleary, T. 2010. Effect of bovine lactoferrin in Salmonella ser. Typhimurium infection in mice. *Biometals*, 23(3): 515-521.
- Munoz, F., Franco, P., Ciammella, P., Clerico, M., Giudici, M., Filippi, A., and Ricardi, U. 2007. Squamous cell carcinoma of the prostate: long-term survival after combined chemo-radiation. *Radiation Oncology*, 2:15.
- Nickel, J. 1991. Prostatitis Syndromes: A continuing enigma for the family physician. *Canadian Family Physician*, 37: 921.
- Nishida, K., Suzuki, T., Kakutani, K., Yurube, T., Maeno, K., Kurosaka, M., and Doita, M. 2008. Gene therapy approach for disc degeneration and associated spinal disorders. *European Spine Journal*, 4: 459-466.
- Nishikawa, M., and Huang, L. 2001. Nonviral vectors in the new millennium: delivery barriers in gene transfer. *Human Gene Therapy*, 12(8): 861-870.
- Oberaigner, W., Horninger, W., Klocker, H., Schönitzer, D., Stühlinger, W., and Bartsch, G. 2006. Reduction of prostate cancer mortality in Tyrol, Austria, after introduction of prostate-specific antigen testing. *The American Journal of Epidemiology*, 164(4): 376-384.
- Ogris, M., Brunner, S., Schuller, S., Kircheis, R., and Wagner, E. 1999. PEGylated DNA/transferrin-PEI complexes: reduced interaction with blood components, extended circulation in blood and potential for systemic gene delivery. *Gene Therapy*, 6:595-605.
- Okajima, E., Yoshikawa, M., Masuda, Y., Shimizu, K., Tanaka, N., Hirayama, A., and Hirao, Y. 2012. Improvement of the surgical curability of locally confined prostate cancer including non-organ-confined high-risk disease through retropubic radical prostatectomy with intentional wide resection. *World Journal of Surgical Oncology*, 10: 249.
- Ott, M., Schmidt, M., Schwarzwaelder, K., Stein, S., Siler, U., Koehl, U., and Grez, M. 2006. Correction of X-linked chronic granulomatous disease by gene

- therapy, augmented by insertional activation of MDS1-EVI1, PRDM16 or SETBP1. *Nature Medicine*, 12(4): 401-409.
- Panno, J. 2004. *Cancer: The Role of Genes, Lifestyle, and Environment*, 1st ed, New York: Facts on File, P 14-16.
- Park, T., Jeong, J., and Kim, S. 2006. Current status of polymeric gene delivery systems. *Advanced Drug Delivery Reviews*, 58(4): 467-486.
- Pata, V., and Dan, N. 2003. The effect of chain length on protein solubilisation in polymer-based vesicles (polymersomes). *Biophysical Journal*, 85(4): 2111-2118.
- Peng, Z. 2005. Current status of Gendicine in China: recombinant human Ad-p53 agent for treatment of cancers. *Human Gene Therapy*, 16(9): 1016-1027.
- Perner, S., Hofer, M., Kim, R., Shah, R., Li, H., Möller, P., and Rubin, M. 2007. Prostate-specific membrane antigen expression as a predictor of prostate cancer progression. *Human pathology*, 38(5):696-701.
- Picard, J., Golshayan, A., Marshall, D., Opfermann, K., and Keane, T. (2012, February). The multi-disciplinary management of high-risk prostate cancer. In *Urologic Oncology: seminars and original investigations* (Vol. 30, No. 1, P 3-15
- Plumb, A. 2004. Cell sensitivity assays: the MTT assay. In *Cancer Cell Culture*, pp. 165-169.
- Porteus, M., Connelly, J., and Pruett, S. M. 2006. A look to future directions in gene therapy research for monogenic diseases. *Plos Genetics*, 2(9): e133.
- Pulkkinen, M., Pikkarainen, J., Wirth, T., Tarvainen, T., Haapa-aho, V., Korhonen, H., and Järvinen, K. 2008. Three-step tumour targeting of paclitaxel using biotinylated PLA-PEG nanoparticles and avidin-biotin technology: Formulation development and *in vitro* anticancer activity. *European Journal of Pharmaceutics and Biopharmaceutics*, 70(1): 66-74.
- Pulukuri, S., Gondi, C., Lakka, S., Jutla, A., Estes, N., Gujrati, M., and Rao, J. 2005. RNA interference-directed knockdown of urokinase plasminogen activator and urokinase plasminogen activator receptor inhibits prostate cancer cell invasion, survival, and tumourigenicity *in vivo*. *Journal of Biological Chemistry*, 280(43): 36529-36540.
- Qian, Z., Li, H., Sun, H., and Ho, K. 2002. Targeted drug delivery via the transferrin receptor-mediated endocytosis pathway. *Pharmacology Review*, 54(4): 561-587.

- Rogers, S., Lowenthal, A., Terheggen, H., and Columbo, J. 1973. Induction of arginase activity with the Shope papilloma virus in tissue culture cells from an argininemic patient. *Journal of Experimental Medicine*, 137: 1091-1096.
- Sakthivel, K., and Florence, A. 2005. Solubilisation and transformation of amphipathic lipidic dendron vesicles (dendrisomes) into mixed micelles. *Colloids and Surfaces a-Physicochemical and Engineering Aspects*, 268(1): 52-59.
- Sakthivel, T., and Florence, A. 2003. Dendrimers and Dendrons: Facets of Pharmaceutical Nanotechnology. *Drug Delivery Technology*, 3(5): 73-78.
- Sanchez, L., Calvo, M., and Brock, J. 1992. Biological role of lactoferrin. *Archives of disease in childhood*, 67(5): 657.
- Saraswat, P., Soni, R., Bhandari, A., and Nagori, B. 2009. DNA as therapeutics; an update. *Indian Journal of Pharmaceutical Sciences*, 71(5): 488-498.
- Sato, A., B. Klaunberg, and R. Tolwani. 2004. *In vivo* bioluminescence imaging. *Complementary Medicine*, 54:631-634.
- Schaefer, S. 2010. A comparative study of Gemini surfactants 16-3-16 and 16-7NH-16 as possible microbubble gene carriers. University of Waterloo, Canada. Retrieved from <http://hdl.handle.net/10012/5723>.
- Schäfer, J., Höbel, S., Bakowsky, U., and Aigner, A. 2010. Liposome-polyethylenimine complexes for enhanced DNA and siRNA delivery. *Biomaterials*, 31(26):6892-6900.
- Scheller, E., and Krebsbach, P. 2009. Gene therapy: design and prospects for craniofacial regeneration. *Journal of Dental Research*, 88(7): 585-596.
- Schenborn, E., Groskreutz, D. Reporter Gene Vectors and Assays, 1999. *Molecular Biotechnology*, 13(1):29-44.
- Scollay, R. 2001. Gene Therapy. *Annals of the New York Academy of Sciences*, 953(1): 26-30.
- Semwogerere, D., and Weeks, E. 2005. Confocal microscopy. In *Encyclopedia of Biomaterials and Biomedical Engineering* (G. E. Wnek, and G. L. Bowlin, Eds.). Marcel Dekker, New York.
- Seow, Y., and Wood, M. 2009. Biological gene delivery vehicles: beyond viral vectors. *Molecular Therapy*, 17(5): 767-777.
- Shah, N., Chaudhari, K., Dantuluri, P., Murthy, R. and Das, S. 2009. Paclitaxel-loaded PLGA nanoparticles surface modified with transferrin and Plutonic

- ((R)) P85, an *in vitro* cell line and *in vivo* biodistribution studies on rat model. *Journal of Drug Targeting*, 17(7): 533-542.
- Sharma, S., Sinha, M., Kaushik, S., Kaur, S., and Singh, T. 2013. *Biochemistry Research International*, 20(13):271641.
- Shaw, D. J., and Costello, B. 1993. Introduction to colloid and surface chemistry: *Butterworth-Heinemann*, 26 (3): 222.
- Shcharbin, D., Pedziwiatr, E., Blasiak, J., and Bryszewska, M. 2010. How to study dendriplexes II: Transfection and cytotoxicity. *Journal of Controlled Release*, 141:110-127.
- Sheppard, A., and Pearlman, A. 1997. Abnormal reorganization of preplate neurons and their associated extracellular matrix: an early manifestation of altered neocortical development in the reeler mutant mouse. *Journal of Comparative Neurology*, 378(2): 173-179.
- Singh, M., Atwal, H., and Micetich, R. 1998. Transferrin directed delivery of Adriamycin to human cells. *Anticancer Research*, 18(3A): 1423-1427.
- Singh, S. (2013). Nanomaterials as non-viral siRNA delivery agents for cancer therapy. *BioImpacts: BI*, 3(2):53.
- Sleigh, M. 1986. A nonchromatographic assay for expression of the chloramphenicol acetyltransferase gene in eukaryotic cells, *Analytical Biochemistry*, 156 (1):251-256.
- Stevermer, J., and Easley, S. 2000. Treatment of prostatitis. *American Family Physician*, 61(10):3015-3034.
- Stolberg, S. 1999. The biotech death of Jesse Gelsinger. *The New York Times Magazine*, 136-140: 149-150.
- Suzuki, S., Inoue, K., Hongoh, A., Hashimoto, Y., and Yamazoe, Y. 1997. Modulation of doxorubicin resistance in a doxorubicin-resistant human leukaemia cell by an immunoliposome targeting transferring receptor. *British Journal of Cancer*, 76(1): 83-89.
- Tai, S., Sun, Y., Squires, J., Zhang, H., Oh, W., Liang, C., Huang, J. 2011. PC-3 is a cell line characteristic of prostatic small cell carcinoma. *The Prostate*, 71(15): 1668-1679.
- Taylor, B., Schultz, N., Hieronymus, H., Gopalan, A., Xiao, Y., Carver, B., and Gerald, W. 2010. Integrative genomic profiling of human prostate cancer. *Cancer Cell*, 18(1): 11-22.

- Thorpe, A., and Neal, D. 2003. Benign prostatic hyperplasia. *The Lancet*, 361(9366): 1359-1367.
- Tilley, W., Wilson, C., Marcelli, M., and McPhaul, M. 1990. Androgen receptor gene expression in human prostate carcinoma cell lines. *Cancer Research*, 50(17):5382-5386.
- Tomita, M., Wakabayashi, H., Shin, K., Yamauchi, K., Yaeshima, T., and Iwatsuki, K. 2009. Twenty-five years of research on bovine lactoferrin applications. *Biochimie*, 91(1): 52-57.
- Torchilin, P. 2006. Multifunctional nanocarriers. *Advanced Drug Delivery Reviews*, 58: 1532-1555.
- van Sande, M., and Van Camp, K. 1981. Lactoferrin in human prostate tissue. *Urological Research*, 9(5):241-244.
- Vinogradov, S., Batrakova, E., Li, S., and Kabanov, A. 1999. Polyion complex micelles with protein-modified corona for receptor-mediated delivery of oligonucleotides into cells. *Bioconjugate Chemistry*, 10(5): 851-860.
- Wang, F., Jiang, X., Yang, D., Elliott, R., and Head, J., 2000. Doxorubicin-gallium-transferrin conjugate overcomes multidrug resistance: evidence for drug accumulation in the nucleus of drug resistant MCF-7/ADR cells. *Anticancer Research*, 20(2): 799-808.
- Wang, J., Li, Q., Li, K., Ou, Y., Han, Z., and Gao, D. 2011. Effects of adenovirus vectors mediated human lactoferrin cDNA on mice bearing EMT6 breast carcinoma. *Pharmazie*, 66:704-709.
- Wang, J., Li, Q., Ou, Y., Han, Z., Li, K., and Wang, P. 2011. Inhibition of tumour growth by recombinant adenovirus containing human lactoferrin through inducing tumour cell apoptosis in mice bearing EMT6 breast cancer. *Archives of Pharmacal Research*, 34(6):987-95.
- Wang, J., Li, Q., Ou, Y., Li, K., Han, Z., and Wang, P. 2012. Recombination adenovirus-mediated human lactoferrin cDNA inhibits the growth of human MCF-7 breast cancer cells. *Journal of Pharmacy and Pharmacology*, 64:457-463.
- Wei, M., Xu, Y., Zou, Q., Tu, L., Tang, C., and Xu, T. 2012. Hepatocellular carcinoma targeting effect of PEGylated liposomes modified with lactoferrin. *The European Journal of Pharmaceutical Sciences*, 46:131-141.
- Welsh, D., and Kay, S. 2005. Bioluminescence imaging in living organisms. *Current opinion in biotechnology*, 16(1):73-78.

- Wenz, G., Han, B., and Müller, A. 2006. Cyclodextrin rotaxanes and polyrotaxanes. *Chemical Review*, 106(3): 782-817.
- Wilfinger, W., Mackey, K., and Chomczynski, P. 1997. Effect of pH and ionic strength on the spectrophotometric assessment of nucleic acid purity. *Biotechniques*. 22:474-476, 478-481.
- Williams, D., and Fleming, I. 1995. *Spectroscopic Methods in Organic Chemistry*, 5th ed, London: McGraw-Hill.
- Wirth, T., and Ylä-Herttuala, S. 2013. History of gene therapy. *Gene*, 525(2):162-9.
- Wolff, J. A., Malone, R. W., Williams, P., Chong, W., Acsadi, G., Jani, A., and Felgner, P. L. 1990. Direct Gene-Transfer into mouse muscle *in vivo*. *Science*, 247(4949): 1465-1468.
- Wong, H., Bendayan, R., Rauth, A., Li, Y., and Wu, X. 2007. Chemotherapy with anticancer drugs encapsulated in solid lipid nanoparticles. *Advanced Drug Delivery Reviews*, 59(6): 491-504.
- Workman, P., Aboagye, E., Balkwill, F., Balmain, A., Bruder, G., Chaplin, D., Double, J., Everitt, J., Farningham, D., Glennie, M., Kelland, L., Robinson, V., Stratford, I., Tozer, G., Watson, S., Wedge, S., and Eccles, S. 2010. Guidelines for the welfare and use of animals in cancer research, *British Journal of Cancer*. 102: 1555 – 1577.
- Xin, H. 2006. Chinese gene therapy Gendicine's efficacy: hard to translate. *Science*, 314: 1233.
- Xu, L., Frederik, P., Pirollo, K., Tang, W., Rait, A., Xiang, L., and Chang, E. 2002. Self-assembly of a virus-mimicking nanostructure system for efficient tumour-targeted gene delivery. *Human Gene Therapy*, 13(3): 469-481.
- Yanasarn, N., Sloat, B., and Cui, Z. 2011. Negatively charged liposomes show potent adjuvant activity when simply admixed with protein antigens. *Molecular pharmaceutics*, 8(4):1174-85.
- Yao, V., and Bacich, D. 2006. Prostate specific membrane antigen (PSMA) expression gives prostate cancer cells a growth advantage in a physiologically relevant folate environment *in vitro*. *The Prostate*, 66(8): 867-875.
- Yoo, Y.C., Watanabe, S., Watanabe, R., Hata, K., Shimazaki, K., and Azuma, I., 1997. Bovine lactoferrin and lactoferricin, a peptide derived from bovine lactoferrin, inhibit tumour metastasis in mice. *Japanese Journal of Cancer Research*, 88:184-190.

- Yuan, F., Dellian, M., Fukumura, D., Leunig, M., Berk, D., and Torchilin, V. 1995.
- Zhou, Y., Zeng, Z., Zhang, W., Xiong, W., Wu, M., and Tan, Y. 2008. Lactotransferrin: a candidate tumour suppressor- Deficient expression in human nasopharyngeal carcinoma and inhibition of NPC cell proliferation by modulating the mitogen-activated protein kinase pathway. *International Journal of Cancer*, 123:2065-72.
- Zinselmeyer, B., Mackay, S., Schätzlein, A., and Uchegbu, I., 2002. The lower-generation polypropylenimine dendrimers are effective gene-transfer agents. *Pharmaceutical Research*. 19:960-967.
- Zinselmeyer, B., Beggbie, N., Uchegbu, I., and Schätzlein, A. 2003. Quantification of beta-galactosidase activity after non-viral transfection *in vivo*. *Journal of Controlled Release*, 91:201-208.
- Zuckerman, S., and Groome, J., 2005. The ætiology of benign enlargement of the prostate in the dog. *The Journal of Pathology and Bacteriology*, 44(1): 113-124.

Appendix I: Publications

- 1- Al Robaian, M., Chiam, K., Blatchford, D., and Dufès, C. 2013. Therapeutic efficacy of intravenously administered transferrin-conjugated dendriplexes on prostate carcinomas. *Nanomedicine*, (2014)9(4): 421-434
- 2- Dufès, C., Al Robaian, M., and Somani, S. 2013. Transferrin and the transferrin receptor for the targeted delivery of therapeutic agents to the brain and cancer cells. *Therapeutic Delivery*, 4(5): 629-640

Appendix II: Conference abstracts

- 1- *Poster presentation at the Pharmaceutical Sciences Research Group Research Day (May 2012).*
- 2- *Poster presentation at the University of Strathclyde Research Day (June 2012).*
- 3- *Poster presentation at the 6th Saudi Student Scientific International Conference (October 2012)*
- 4- *Poster presentation at the Annual Symposium of the United Kingdom and Ireland Controlled Release Society (April 2013)*
- 5- *Poster presentation at the 7th Saudi Scientific International Conference (February 2014).*

Others:

- 1- *One of a top 20 Best posters at the University of Strathclyde Research Day (June 2012)*
- 2- *Certificate of the valuable contribution in the 7th Saudi Student Conference (February 2014).*
- 3- *Mention on the Distinction Board of the UK Saudi Cultural Bureau, which highlights the achievements of the top Saudi students in the UK.*